
Marine Conditions 2008–2019

Report Series: Phytoplankton



December 2022



King County

Department of Natural Resources and Parks
Water and Land Resources Division
Science and Technical Support Section
King Street Center, KSC-NR-5600
201 South Jackson Street, Suite 5600
Seattle, WA 98104
206-477-4800 TTY Relay: 711
www.kingcounty.gov/EnvironmentalScience

Alternate Formats Available
206-477-4800 TTY Relay: 711

Marine Conditions 2008–2019 Report Series: Phytoplankton

Submitted by:

Gabriela Hannach

King County Water and Land Resources Division
Department of Natural Resources and Parks



King County

Department of
Natural Resources and Parks

Water and Land Resources Division

Acknowledgements

The author would like to thank the King County Environmental Laboratory Field Science Unit for sample collection and Lyndsey Swanson for sample analysis. Katherine Bourbonais and Erin McCabe provided laboratory project management.

Citation

King County. 2022. Marine Conditions 2008–2019 Report Series: Phytoplankton. Prepared by Gabriela Hannach, Water and Land Resources Division, Seattle, Washington.

Table of Contents

1.0	Introduction	1
2.0	Methods	4
2.1	Sampling Locations	4
2.2	Sampling Methods	7
2.3	Analysis Methods	9
2.3.1	Sample Processing	9
2.3.2	Sample Analysis	10
2.3.3	Data Analysis	13
3.0	Qualitative and Semi-Quantitative Data Results	15
3.1	Seasonality	15
3.2	Dominant Diatom Species	21
3.3	Inter-Annual Patterns in Species Composition	24
3.4	Harmful Algal Bloom (HAB) Species	24
4.0	Quantitative Data Results	30
4.1	Biovolumes and Seasonality	30
4.2	Growth and Water Column Stratification	34
4.3	Seasonal Succession	38
4.4	Diatom Biovolume	40
4.5	Flagellate Abundance and Biovolume	43
4.6	<i>Noctiluca</i>	46
4.7	Community Analysis	47
4.8	Size Class Distribution	50
4.9	Trends by Mode of Nutrition	51
4.10	Microzooplankton	52
4.11	Cumulative Biovolume	53
4.12	Chlorophyll- <i>a</i> and Biovolume	55
4.13	Dockton: Growth and Species Composition	56
4.14	Dockton: Trends by Mode of Nutrition	61
4.15	Dockton: Microzooplankton	62

5.0	POC Study Results: Relationship Between Particulate Organic Carbon and Microplankton Biovolume Measured by FlowCAM.....	63
5.1	Data Overview.....	63
5.2	Relationship Between POC, PON and FlowCAM Biovolume	65
5.3	Carbon Density.....	67
5.4	Measured Carbon Biomass Compared to Calculated Values.....	68
5.5	Relationship Between POC, PON and Chlorophyll- <i>a</i>	69
5.6	Seasonal Trends.....	71
6.0	Phytoplankton Summary	74
6.1	Qualitative and Semi-Quantitative Results	74
6.2	Quantitative Results.....	74
6.3	POC Study.....	76
7.0	References	77

Figures

Figure 1.	Marine Monitoring Program phytoplankton sampling locations.....	6
Figure 2.	Seasonality of 50 most common taxa at Pt. Jefferson (KSBP01) in surface samples (2008 - 2019).....	16
Figure 3.	Seasonality of 50 most common taxa in East Passage (NSEX01) surface samples (2008 - 2019).....	17
Figure 4.	Seasonal and annual differences in relative abundance at Pt. Jefferson (KSBP01) (2008 - 2014), based on semi-quantitative and qualitative assessments.	19
Figure 5.	Seasonal and annual differences in relative abundance at East Passage (NSEX01) (2008 - 2014), based on semi-quantitative and qualitative assessments.	20
Figure 6.	Seasonal and year to year differences in relative abundance at Dockton (NSAJ02) (2009 - 2014), based on semi-quantitative and qualitative assessments.	21
Figure 7.	<i>Chaetoceros</i> species and their relative proportions (frequency), 2008 - 2019.	22
Figure 8.	<i>Thalassiosira</i> species and their relative proportions (frequency), 2008 - 2019.	23
Figure 9.	Relative proportions (frequency) of <i>Dinophysis</i> at ten stations, 2008 - 2019.....	25

Figure 10.	Relative proportions (frequency) of <i>Alexandrium</i> at ten stations, 2008 – 2019	26
Figure 11.	Relative proportions (frequency) of <i>Heterosigma akashiwo</i> at ten stations, 2008 - 2019	27
Figure 12.	Relative proportions (frequency) of small-celled <i>Pseudo-nitzschia</i> observations at ten stations, 2008 - 2019	28
Figure 13.	Relative proportions (frequency) of <i>Akashiwo</i> , <i>Protoceratium</i> , and <i>Mesodinium</i> at ten stations, 2008 - 2019	29
Figure 14.	Seasonal changes in biovolume of diatoms, dinoflagellates and total microplankton (100-300 µm) for all stations, 2014 - 2019.	32
Figure 15.	Seasonal changes in mean biovolume of diatoms, dinoflagellates and total microplankton (100-300 µm) for 7 stations sampled 2014 - 2019 (Dockton excluded).....	33
Figure 16.	Comparison of seasonal changes in diatom biovolume at Pt. Jefferson and East Passage (2014 - 2019).	34
Figure 17.	Total biovolume as a function of maximum density gradient at time of sampling for three ambient stations, showing seasonal and geographic differences (2014 - 2019, n=120-121).	36
Figure 18.	Total biovolume as a function of maximum density gradient at time of sampling at three outfall stations (2014 - 2019, n=120-122), showing seasonal and geographic differences.	37
Figure 19.	Seasonal pattern of total biovolume and maximum density gradient at time of sampling at Pt. Wells (JSUR01) and East Passage (NSEX01) (2014 - 2019; only mid-March-October samples).	38
Figure 20.	Seasonal succession in mean biovolumes for 6 top taxa (based on biovolume) for each year	39
Figure 21.	Relative biovolumes of the 25 diatom taxonomic categories.	41
Figure 22.	Seasonal and interannual changes in biovolume for 8 top diatom taxa (2014-2019).....	42
Figure 23.	Relative mean abundances.....	44
Figure 24.	Seasonal and interannual changes in biovolume for 8 top flagellate taxa (2014 - 2019).....	45
Figure 25.	Cell concentrations of the large heterotrophic dinoflagellate <i>Noctiluca scintillans</i>	46
Figure 26.	Non-metric multidimensional scaling (nMDS) of microplankton community composition, highlighted by season (top panel), and cluster analysis by season (bottom panel).	47

Figure 27.	Non-metric multidimensional scaling (nMDS) of microplankton community composition, showing separation by sample week consistent with seasonal succession (clockwise).	48
Figure 28.	Non-metric multidimensional scaling (nMDS) of microplankton community composition, highlighted by locator and year (top panel), and cluster analyses by locator and year (bottom panels).	49
Figure 29.	Species richness (as number of taxonomic categories) and Shannon's diversity index at 8 stations sampled 2015 - 2019.....	50
Figure 30.	Seasonal changes in particle size structure quantified for 7 (2014 - 2015) or 9 (2016 - 2019) stations, expressed as relative biovolume (top panel) and relative abundance (bottom panel).	51
Figure 31.	Abundance of autotrophic, mixotrophic and heterotrophic microplankton.	52
Figure 32.	Abundance of ciliates and other microzooplankton.	53
Figure 33.	Twelve-month cumulative phytoplankton biovolumes by station and year (left panel) and geographic distribution (right panel).....	54
Figure 34.	Relationship between chlorophyll- <i>a</i> ($\mu\text{g/L}$) and biovolume (mm^3/L) for surface data collected at all stations (2014 - 2019) ($n = 1116$).....	55
Figure 35.	Seasonal changes in chlorophyll- <i>a</i> to biovolume ratio for surface data (2014 - 2019) at all stations ($n = 1112$).....	56
Figure 36.	Monthly surface temperatures (<2 m) at Dockton (NSAJ02) (2014 - 2019).....	58
Figure 37.	Biovolumes of top 12 taxonomic categories at Dockton (NSAJ02) (2014 - 2019).	59
Figure 38.	Seasonal and interannual changes in biovolume for 4 top diatoms (top panels) and abundance for 4 top flagellate taxa (bottom panels) at Dockton...60	
Figure 39.	Abundances (top panel) and proportions (center panel) of autotrophic, mixotrophic and heterotrophic microplankton at Dockton.....	61
Figure 40.	Abundance of ciliates and other microzooplankton at Dockton (NSAJ02).	62
Figure 41.	Seasonal variation in FlowCam based biovolumes for major taxonomic groups (2015 and 2016).	64
Figure 42.	Regressions of POC and PON vs. FlowCAM based biovolume for A) Fraction A (<100 μm) and B) Fraction B (100-300 μm), showing best fit regression lines.	66
Figure 43.	Predicted carbon density for two particle size fractions.....	67
Figure 44.	Measured vs. expected POC, as calculated from published cell sizes, carbon density and taxonomic composition of each sample.	68
Figure 45.	Variation in ratio of measured/calculated carbon biomass (2015-2016).	69
Figure 46.	POC and PON as a function of chlorophyll- <i>a</i>	70

Figure 47. POC:Chl- <i>a</i> and PON:Chl- <i>a</i> seasonal variation (weight/weight ratios).....	72
Figure 48. C:N seasonal variation for two particle size fractions (weight/weight ratios).....	73

Tables

Table 1. Phytoplankton monitoring stations, depths, and first year of data collection.....	5
Table 2. Phytoplankton sampling stations, sampling depths and analysis methods 2008 - 2019.....	8
Table 3. Taxa identified using light microscopy (2008 – 2019).	11
Table 4. Timing of spring diatom bloom at all stations, based on biovolume, 2015 - 2019.	33
Table 5. Regression analysis results of POC and PON vs FlowCAM based sample biovolume.	65
Table 6. Fitted relationships between carbon and chlorophyll using linear least squares regression on log-transformed data for this and other studies.....	71
Table 7. Ratios of POC and PON to biovolume and chlorophyll- <i>a</i>	73

Appendices

Appendix A: Species List
Appendix B: POC Study

1.0 INTRODUCTION

For over 50 years, King County has conducted extensive water quality monitoring to assess conditions in the Puget Sound Central Basin (King County waters). The King County Marine Monitoring Program is managed by scientists in the Water and Land Resources Division within the Department of Natural Resources. The program includes two types of monitoring (1) baseline monitoring to assess background conditions (ambient monitoring) and (2) monitoring to assess conditions near King County’s wastewater treatment plant (TP), wet weather treatment station (TS), and combined sewer overflow (CSO) marine outfalls (outfall monitoring).

The goals of the Marine Monitoring Program are to characterize water quality and food web (phytoplankton and zooplankton) conditions in King County receiving waters, provide information for management decisions, and evaluate the status and trends of marine waters within King County. These data provide insight into both short- and long-term variations and form a baseline from which water quality conditions can be assessed on multiple temporal and spatial scales. Please see *Marine Conditions Report Series 2008–2019: Marine Monitoring Program Overview* (King County, 2022a) for a more detailed description of the background and purpose of the Marine Monitoring Program.

This report presents results for the phytoplankton component of the Marine Monitoring Program collected since its inception (2008 – 2019). Results of a special study conducted in 2015 and 2016 to examine particulate organic carbon (POC) and particulate organic nitrogen (PON) in surface samples are also presented here. This special study was conducted to better understand the relationship between POC/PON and phytoplankton biovolume since carbon and nitrogen content are key parameters for food web modeling.

The phytoplankton data collected by the Marine Monitoring Program are used to:

- Assess potential water quality impacts following TP upset discharges by comparing against historical data.
- Assist in special studies such as siting new wastewater treatment plant outfalls (King County, 2001).
- Assess influences of large-scale and regional climate patterns on riverine and freshwater inputs and nutrient concentrations.
- Evaluate how primary producers respond to nutrients and potential effects to the Puget Sound food web.
- Support regional efforts and collaborations such as the Puget Sound Ecosystem Monitoring Program (PSEMP) Marine Waters Workgroup marine conditions monthly update meetings, Puget Sound Marine Waters Annual Report (PSEMP Marine Waters Workgroup, 2019), Washington Department of Ecology’s (Ecology) Nutrient Reduction Effort, and regional modeling efforts.

Marine phytoplankton are a group of diverse, single-celled or colonial algae that form the base of marine food webs as the dominant primary producers. They range in size from around 1 μm to over 300 μm . Phytoplankton are generally photosynthetic (autotrophic), meaning they use solar energy to incorporate carbon dioxide into energy-storing carbon molecules, which can then be used (via respiration) for growth and reproduction. However, there are many species of mixotrophic phytoplankton which can take up dissolved organic matter or ingest other organisms for energy in addition to photosynthesizing. Some types of algae often grouped with the phytoplankton are fully heterotrophic (non-photosynthetic), ingesting other organisms as their sole source of energy and carbon. Some phytoplankton species are of particular interest for monitoring because they produce toxins and form blooms that can be harmful to humans and/or wildlife.

The diversity in size, physiology, toxicity, and nutritional modes within the phytoplankton community corresponds to a variety of complex and specific ecological roles played by the different taxa. Thus, detailed information on community composition is necessary for understanding marine food webs. Phytoplankton community composition and biomass at any one point in time is a product of various interacting bottom-up (e.g., nutrient concentration, temperature, light intensity, physical mixing) and top-down (i.e., consumption by microzooplankton) controls. This makes phytoplankton community composition both a valuable metric of biological response to environmental change and a key explanatory variable for the dynamics of higher trophic levels in the marine food web.

Phytoplankton biovolume calculations are often used to estimate carbon biomass. Currently biovolume is measured quantitatively using an imaging particle analyzer (FlowCAM) with software that estimates biovolume from stored particle images. However, the suitability of using particle biovolume values generated by this quantitative method as a surrogate for biomass required further validation. Conversion of plankton biovolume to carbon biomass is essential to use these data to understand and model carbon flow and trophic structure. In 2015 and 2016 a special study was conducted to examine particulate organic carbon (POC) and particulate organic nitrogen (PON) in surface samples, and more specifically, to evaluate the relationship between carbon biomass and FlowCAM generated biovolume values.

The overall goal of the POC special study was to assess feasibility of using FlowCAM-generated biovolumes to estimate POC in microplankton samples. Additional objectives were to assess seasonal changes in POC and PON content, their relationship with chlorophyll-*a* (Chl-*a*), and to compare measured carbon density values with calculations based on published values.

The extensive literature on carbon content in phytoplankton indicates that it is dependent on both cell type and volume. Various equations have been developed that describe the relationship between carbon content and cell volume (Montagnes *et al.*, 1994; Menden-Deuer and Lessard, 2000) both in natural samples and cultures. In general, diatoms contain less carbon per cell than dinoflagellates and other flagellates due to the presence of a large cell vacuole, and smaller cells are more carbon dense than larger cells. This implies that

taxonomic composition, which is both spatially and seasonally dependent, is a critically important factor for predictions of carbon content in marine phytoplankton.

The Marine Monitoring Program monitors multiple physical and chemical parameters concurrently at each sampling location. A summary of all data collected at each station is provided in *Marine Conditions Report Series 2008–2019: Marine Monitoring Program Overview* (King County, 2022a). Results for other Marine Monitoring Program components monitored between 2008–2019, (except pH), are provided in separate reports with hyperlinks (click on titles to access reports) below and include the following topics:

- [Marine Monitoring Program overview](#)
- [Nutrients in offshore waters](#)
- [Nutrients in beach waters](#)
- [Dissolved oxygen in offshore waters](#)
- [Temperature, salinity, and density in offshore waters](#)
- [Temperature and salinity in beach waters](#)
- [Water clarity in offshore waters](#)
- [Fecal indicator bacteria in beach and offshore waters](#)
- [Chlorophyll in offshore waters](#)
- [Zooplankton](#)
- [Chemical and physical parameters and benthic infauna in beach \(intertidal\) and offshore \(subtidal\) sediments](#)
- [Chemical parameters in clam tissues.](#)

2.0 METHODS

The following sections provide an overview of the sampling and analysis methods used to assess phytoplankton. A more detailed description of these methods can be found in the Sampling and Analysis Plan (SAP) (King County 2016b) for the phytoplankton monitoring component of the program. Also summarized here are the sampling and analysis methods used for the special study to assess POC/PON.

2.1 Sampling Locations

Phytoplankton sampling locations are located within the Puget Sound Central Basin, extending south to Dumas Bay and north to Edwards Point. Elliott Bay, a large urban embayment, which includes the City of Seattle waterfront, is located within the monitoring area. The eastern shoreline of Vashon Island and Quartermaster Harbor, an embayment between Vashon and Maury Islands, are also included in the sampling area.

Throughout this report the term ‘mainstem’ is used to refer to all sampling areas except Elliott Bay and Quartermaster Harbor, while the term ‘offshore’ refers to all locations. Stations are designated as either “outfall” or “ambient”. Outfall stations are located at/near the end of a TP, TS, or CSO discharge point. Table 1 provides station information and Figure 1 shows station locations.

Samples were collected for qualitative, as well as semi-quantitative and quantitative analysis. Samples for semi-quantitative phytoplankton abundance and community structure (qualitative data) analysis were collected from 2008 - 2014 at three ambient locations: Point Jefferson (KSBP01) (surface and chlorophyll [chl] max), East Passage (NSEX01) (surface and chl max), and inner Quartermaster Harbor (MSWH01) or outer Quartermaster Harbor (NSAJ02) (Figure 1). A modification to the phytoplankton monitoring program in 2009 included a site change from the inner Quartermaster Harbor Station (MSWH01) to the outer station (NSAJ02). In May of 2014, a quantitative analysis method was implemented, and two additional ambient stations at Point Williams (LSNT01) and Inner Elliott Bay (LTED04) were added to the program (Table 1, Figure 1).

Three outfall locations (Brightwater [JSUR01], West Point [KSSK02], and South Plant [LSEP01]) were monitored for quantitative phytoplankton abundance and community structure starting in May of 2014. Two additional outfall stations (Alki TS [LSKQ06] and Vashon TP [MSJN02]) were added to the program in March 2016 (Table 1, Figure 1). Starting in March of 2016, only surface samples were collected from all stations.

Samples for the POC special study were collected along with routine phytoplankton monitoring samples from eight stations (Pt. Wells [JSUR01], Pt. Jefferson, [KSBP01], West Point [KSSK02], Elliott Bay [LTED04], South Plant [LSEP01], Pt Williams [LSNT01], East Passage [NSEX01] and Dockton in Outer Quartermaster Harbor [NSAJ02]).

Table 1. Phytoplankton monitoring stations, depths, and first year of data collection.

Station	Central Basin Region	Station Rationale	Station Type	First Year of Record	Average Station Depth (m)
JSUR01	North	Brightwater TP - outfall diffuser	outfall	2014	178
KSBP01	North	Point Jefferson - represents conditions in the northern Central Basin	ambient	2008	262
KSSK02	North	West Point TP - outfall diffuser	outfall	2014	65
LTED04	Middle – Elliott Bay	Inner Elliott Bay - represents Elliott Bay conditions	ambient	2014	85
LSEP01	Middle	South Plant TP - north outfall diffuser	outfall	2014	185
LSKQ06	Middle	Alki Wet Weather TS - outfall	outfall	2016	43
LSNT01	Middle	Point Williams - represents conditions in mid Central Basin	ambient	2014	205
MSJN02	South	Vashon TP - outfall	outfall	2016	63
MSWH01	Quartermaster Harbor	Inner Quartermaster Harbor - shallow embayment	ambient	2008*	5.5
NSAJ02	Quartermaster Harbor	Dockton in Outer Quartermaster Harbor - shallow embayment	ambient	2009	9
NSEX01	South	East Passage - represents conditions in southern Central Basin	ambient	2008	173

* one year only

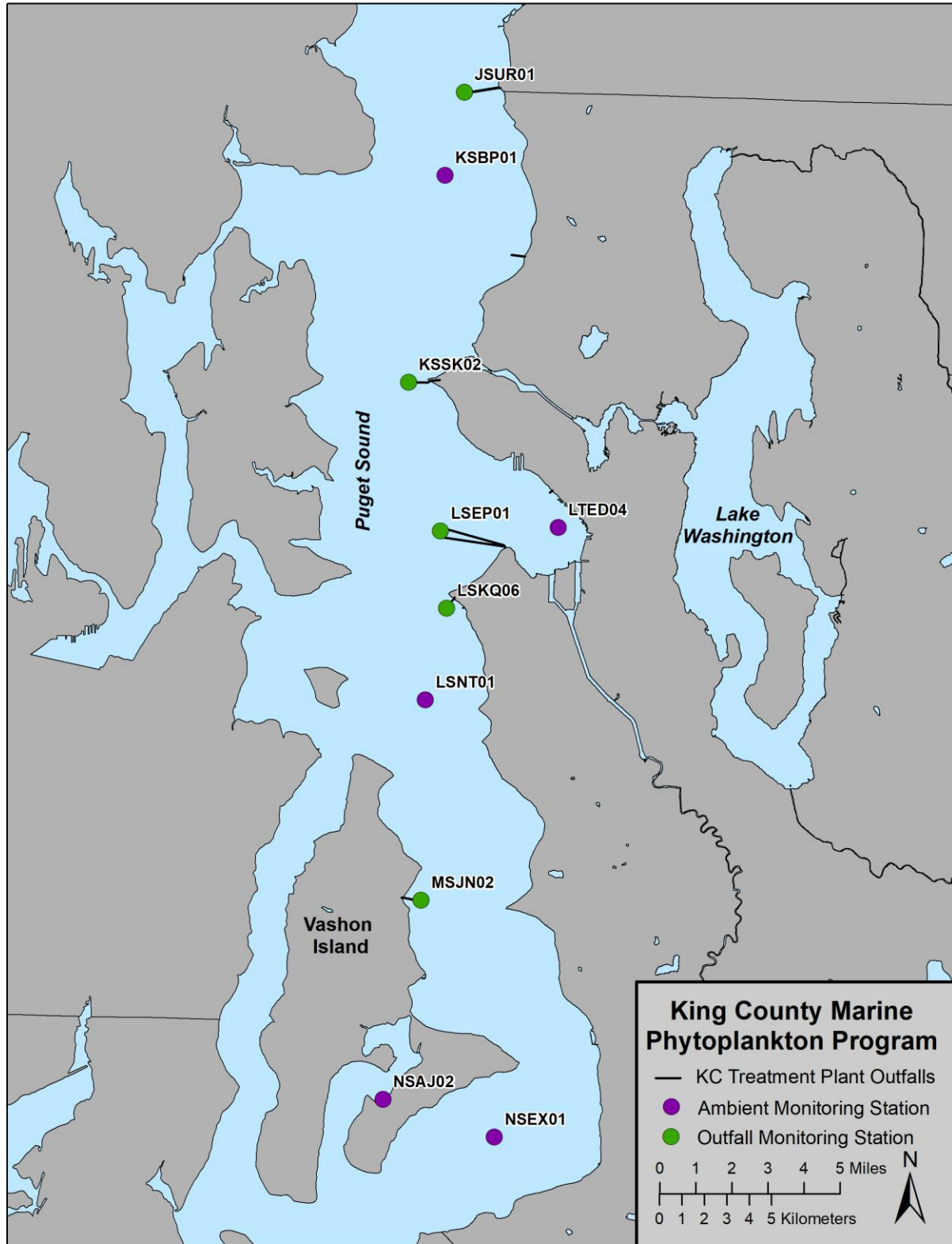


Figure 1. Marine Monitoring Program phytoplankton sampling locations.

2.2 Sampling Methods

All phytoplankton samples were collected concurrently with other samples for laboratory parameters using five-liter Niskin bottles mounted to a rosette, except in Quartermaster Harbor, where samples were collected with a four-liter Scott bottle. Samples were placed into 1 L appropriate sample containers and held on ice until and during transport to the laboratory for analysis.

From 2008 to April 2014 samples were collected twice monthly April - October except in 2009 -2010 when samples were not collected in October (Table 2). Samples were collected from both the 1 m and chlorophyll maximum depths at KSBP01 and NSEX01.

From May 2014 to 2019 samples were collected twice monthly through most of the year and monthly in January and December (Table 2). Samples were collected from both the 1 m and chlorophyll maximum depths at Point Jefferson (KSBP01) and East Passage (NSEX01) until February of 2016. A duplicate sample was collected during each sampling event on a rotating station schedule.

One-liter surface samples for the POC special study were collected twice a month from June 15 to November 19, 2015, once in December 2015, and twice a month from March 21 to September 21, 2016 (n = 200). Samples were collected concurrently with routine phytoplankton samples. Quality control (QC) samples were collected twice a month from Pt. Williams for whole water analysis (i.e., no fractionation) of plankton, and a duplicate sample was collected monthly based on a rotating station schedule.

Table 2. Phytoplankton sampling stations, sampling depths and analysis methods 2008 - 2019. All stations in mainstem Central Basin except LTED04, MSWH01 and NSAJ02. Greyed- out cells indicate no sampling.

Station	Depth (m)	2008	2009	2010	2011	2012	2013	2014 Jan-Apr	2014 May-Dec	2015	2016 Jan-Feb	2016 Mar-Dec	2017	2018	2019
JSUR01	1								M, F	M, F	M, F	M, F	M, F	M, F	M, F
KSBP01	1	M, S	M, S	M, S	M, S	M, S	M, S	M, S	M, F	M, F	M, F	M, F	M, F	M, F	M, F
	Chl max	M, S	M, S	M, S	M, S	M, S	M, S	M, S	M, F	M, F	M, F				
KSSK02	1								M, F	M, F	M, F	M, F	M, F	M, F	M, F
LTED04	1								M, F	M, F	M, F	M, F	M, F	M, F	M, F
LSEP01	1								M, F	M, F	M, F	M, F	M, F	M, F	M, F
LSKQ06	1											M, F	M, F	M, F	M, F
LSNT01	1								M, F	M, F	M, F	M, F	M, F	M, F	M, F
MSJN02	1											M, F	M, F	M, F	M, F
MSWH01	1	M, S													
NSAJ02	1		M, S	M, S	M, S	M, S	M, S	M, S	M, F	M, F	M, F	M, F	M, F	M, F	M, F
NSEX01	1	M, S	M, S	M, S	M, S	M, S	M, S	M, S	M, F	M, F	M, F	M, F	M, F	M, F	M, F
	Chl max	M, S	M, S	M, S	M, S	M, S	M, S	M, S	M, F	M, F	M, F				

M = microscope, live sample, qualitative method

S = microscope, preserved sample, semi-quantitative method

F = Flowcam, live sample, quantitative method

2.3 Analysis Methods

All routine phytoplankton analysis was conducted by the King County Environmental Lab (KCEL). The POC and PON elemental analysis was conducted by the University of California (UC) at Davis.

Routine monitoring program samples were analyzed using qualitative, semi quantitative, and quantitative methods (King County 2011, 2015, 2016a). Phytoplankton samples for the POC study were analyzed according to the Sampling and Analysis Plan (SAP) guidelines (King County, 2016b) with additional details described below.

2.3.1 Sample Processing

Routine Monitoring Samples

For qualitative microscopy, a 400 mL live subsample was concentrated by reverse filtration (Dodson and Thomas 1978) using filter assemblies made with 5 µm nitex mesh sealed to the end of acrylic tubes. Samples were concentrated to about 40 mL, mounted on a PhycoTech nanoplankton chamber (0.06 mL) and examined immediately.

For semi-quantitative microscopy samples were transferred to 500 mL conical centrifuge tubes, preserved by addition of 5 mL formaldehyde (final concentration 0.4% v/v) and allowed to settle at room temperature for at least 48 h. The overlying water was removed and the concentrated sample (ca. 10 mL) transferred to a glass scintillation vial.

For FlowCAM analysis, a 200 mL live subsample was separated into two fractions using nitex mesh: a <100 µm particle size-fraction and a 100-300 µm particle size-fraction for imaging with 10x and 4x objectives, respectively. The >300 µm fraction was saved for qualitative observation under a dissecting microscope and *Noctiluca* counts.

POC Special Study Samples

Samples collected for the POC special study were processed within 24 h of collection. Samples were fractionated with 300 µm and 100 µm Sefar nylon mesh filters following the routine procedure developed for FlowCAM analysis (KCEL, 2016). The >300 µm fraction was discarded and the remaining sample was separated into Fractions A (<100 µm) and B (100-300 µm). Note that particle sizes are nominal; many particles <100 µm are present in Fraction B, and particles >100 µm may be present in Fraction A. Sample fractions were then slowly passed through 25 mm glass fiber filters (Whatman 934-AH, 1.5 µm particle retention) using a filtering manifold fitted with 200 mL filter funnels attached to a vacuum pump. The full 1-L sample was processed, except during bloom conditions with very high particle concentrations. For dense samples a smaller volume was processed, judged by the color on the filter. Samples collected concurrently for routine monitoring FlowCAM analysis were processed and analyzed in parallel.

Two QC samples were also processed. A blank sample, consisting of 0.45 µm filtered seawater, and a duplicate plankton sample were processed concurrently on the second sampling event of the month. A whole (unfractionated) sample from the Pt. Williams

station was processed with every sampling event. Due to concerns about background levels of carbon in the clean, non-combusted filters used for sample filtration, 20 blank dry filters were also analyzed for POC and PON. Ten of these filters were pre-combusted at 450 °C for 4 hours.

The filters were packed immediately for POC/PON analysis (except for a few samples frozen at -23 °C prior to packing). Filters were blotted, folded, and rolled with forceps to fit inside a 11 x 8 mm tin capsule (Elemental Microanalysis D1103). The capsules, lightly crimped and compressed to 8 x 8 mm using a crimper plate and metal dowel, were transferred to a 48 well plate (Falcon 353230), dried overnight at 60 °C and then sealed and stored in a desiccator at room temperature prior to shipping for elemental analysis.

2.3.2 Sample Analysis

Qualitative Phytoplankton Analysis

Qualitative plankton (community structure) data for all routine samples (2008 - 2019) were obtained via direct observation using a Nikon 80i compound microscope with 10x ocular and 10x – 60x objectives (Table 2). One duplicate sample was analyzed with each batch on a rotating basis.

Observations were limited to presence/absence of an organism in the live, concentrated sample, with identifications to the lowest possible taxonomic level. Taxonomic identification was based primarily on Horner (2002), Tomas (1997) and Hoppenrath *et al.* (2009). Some taxonomic names were added to the database later in the program, especially in 2012, 2014 and 2015, leading to inconsistencies in some taxonomic categories across years. As of 2019 the list included 149 categories: 74 diatoms, 64 flagellates and 11 ciliates/zooplankton (Table 3).

Table 3. Taxa identified using light microscopy (2008 – 2019). Some taxa were added at different times after the start of the program.

Diatoms		Dinoflagellates	Other Microplankton
Centric	Centric (contd)	<i>Akashiwo sanguinea</i>	Ebrideans
<i>Actinoptychus senarius</i>	<i>Odontella longicruris</i>	<i>Alexandrium catenella</i>	<i>Ebria tripartita</i>
<i>Asteromphalus heptactis</i>	<i>Paralia sulcata</i>	<i>Alexandrium</i> sp.	
<i>Aulacodiscus kittonii</i>	<i>Rhizosolenia setigera</i>	<i>Amylax triacantha</i>	Prymnesiophytes
<i>Bacteriastrium delicatulum</i>	<i>Skeletonema costatum</i>	<i>Ceratium lineatum</i>	<i>Chrysochromulina</i>
<i>Cerataulina pelagica</i>	<i>Stephanopyxis nipponica</i>	<i>Ceratium furca</i>	<i>Phaeocystis</i> sp.
<i>Chaetoceros (Hyalochaete)</i> sp.	<i>Stephanopyxis palmeriana</i>	<i>Ceratium fusus</i>	
<i>Chaetoceros (Phaeoceros)</i> sp.	<i>Thalassiosira angustelineata</i>	<i>Ceratium</i> sp.	Raphidophytes
<i>Chaetoceros affinis</i>	<i>Thalassiosira eccentrica</i>	<i>Dinophysis acuminata</i>	<i>Heterosigma akashiwo</i>
<i>Chaetoceros concavicornis</i>	<i>Thalassiosira nordenskiöldii</i>	<i>Dinophysis acuta/norvegica</i>	
<i>Chaetoceros contortus</i>	<i>Thalassiosira pacifica/aestivalis</i>	<i>Dinophysis fortii</i>	Chrysophytes
<i>Chaetoceros convolutus</i>	<i>Thalassiosira punctigera</i>	<i>Dinophysis rotundata</i>	<i>Apedinella spinifera</i>
<i>Chaetoceros curvisetus</i>	<i>Thalassiosira rotula</i>	<i>Dinophysis</i> sp.	<i>Dinobryon</i> sp.
<i>Chaetoceros danicus</i>	<i>Thalassiosira</i> sp.	<i>Dinophysis parva</i>	<i>Meringosphaera mediterranea</i>
<i>Chaetoceros debilis</i>	unidentified centric	<i>Dissodinium pseudolunula</i>	
<i>Chaetoceros decipiens</i>		<i>Gonyaulax digitale</i>	Silicoflagellates
<i>Chaetoceros diadema</i>		<i>Gonyaulax</i> sp.	<i>Dictyocha fibula</i>
<i>Chaetoceros didymus</i>		<i>Gymnodinium gracile</i>	<i>Dictyocha speculum</i>
<i>Chaetoceros eibonii</i>		<i>Gymnodinium rubrum</i>	
<i>Chaetoceros laciniosus</i>		<i>Gymnodinium</i> sp.	Other flagellates
<i>Chaetoceros lorenzianus</i>		<i>Gyrodinium</i> sp.	cryptomonad
<i>Chaetoceros radicans</i>	Pennate	<i>Gyrodinium spirale</i>	euglenoid
<i>Chaetoceros similis</i>	<i>Asterionellopsis glacialis</i>	<i>Heterocapsa triquetra</i>	unidentified nanoflagellates
<i>Chaetoceros socialis</i>	<i>Cylindrotheca closterium</i>	<i>Minuscula bipes</i>	
<i>Chaetoceros teres</i>	<i>Navicula</i> sp.	<i>Nematodinium armatum</i>	Ciliates
<i>Chaetoceros vanheurckii</i>	<i>Nitzschia acicularis</i>	<i>Noctiluca scintillans</i>	<i>Mesodinium rubrum</i>
<i>Corethron hystrix</i>	<i>Pleurosigma</i> sp.	<i>Oxyphysis oxytoxoides</i>	<i>Strobilidium</i> sp.
<i>Coscinodiscus centralis</i>	<i>Pseudo-nitzschia americana</i>	<i>Oxytoxum</i> sp.	<i>Tiarina fusus</i>
<i>Coscinodiscus concinnus</i>	<i>Pseudo-nitzschia</i> sp. (large)	<i>Polykrikos schwartzii</i>	<i>Favella</i> sp.

Diatoms		Dinoflagellates	Other Microplankton
Centric (contd)	Pennate	<i>Prorocentrum gracile</i>	Ciliates (contd)
<i>Coscinodiscus curvatulus</i>	<i>Pseudo-nitzschia</i> sp. (small)	<i>Prorocentrum micans</i>	<i>Helicostomella</i> sp.
<i>Coscinodiscus granii</i>	<i>Striatella unipunctata</i>	<i>Protoceratium reticulatum</i>	<i>Parafavella</i> sp.
<i>Coscinodiscus marginatus</i>	<i>Thalassionema nitzschioides</i>	<i>Protoperidinium brevipes</i>	unidentified ciliate
<i>Coscinodiscus oculus-iridis</i>	<i>Thalassionema frauenfeldii</i>	<i>Protoperidinium conicum</i>	unidentified tintinnid
<i>Coscinodiscus</i> sp.	<i>Tropidoneis antarctica</i>	<i>Protoperidinium depressum</i>	
<i>Coscinodiscus wailesii</i>	unidentified pennate	<i>Protoperidinium excentricum</i>	Other Zooplankton
<i>Dactyliosolen fragilissimus</i>		<i>Protoperidinium leonis</i>	nauplius
<i>Detonula pumila</i>		<i>Protoperidinium oblongum</i>	copepod
<i>Ditylum brightwellii</i>		<i>Protoperidinium oceanicum</i>	unid. zooplankton
<i>Eucampia zodiacus</i>		<i>Protoperidinium pellucidum</i>	
<i>Guinardia delicatula</i>		<i>Protoperidinium</i> sp.	
<i>Guinardia striata</i>		<i>Protoperidinium steinii</i>	
<i>Hemiaulus hauckii</i>		<i>Pyrophacus horologium</i>	
<i>Lauderia annulata</i>		<i>Scrippsiella trochoidea</i>	
<i>Leptocylindrus danicus</i>		diplopsalid	
<i>Leptocylindrus minimus</i>		gymnodinioid dinoflagellate	
<i>Melosira moniliformis</i>		unid. dinoflagellate (<25 um)	
		unid. dinoflagellate (>25 um)	

Semi-quantitative Phytoplankton Analysis

Microscopy-based semi-quantitative analysis was conducted on preserved samples collected from 2008 – 2014 from 3 stations (Point Jefferson [KSBP01 at 2 depths], East Passage [NSEX01 at 2 depths] and Outer Quartermaster Harbor [NSAJ02 at 1 depth] (Table 2).

Genera were assigned a relative abundance category based on a quantitative assessment and a subjective assessment. Each genus was categorized as “dominant” when cell counts were dominant in >50% of nine or more microscope fields, “subdominant” when counts were dominant in less than 50% but more than 25% of the fields, or “present” if observed but not dominant or subdominant. Starting in 2019 taxa were also categorized as “present and common” if they were considered abundant in the live sample (qualitative analysis) but did not qualify as dominant or subdominant in the preserved sample.

Quantitative Analysis

In May 2014 use of a bench-top FlowCAM system was initiated to conduct quantitative phytoplankton analysis on samples collected at 6 mainstem stations, and in Elliott Bay and Dockton in Quartermaster Harbor (Figure 1, 0). In March 2016 quantitative phytoplankton analysis was initiated in samples collected at two additional stations (Alki TS [LSKQ06], Vashon WP [MSJN02]).

The FlowCAM is a semi-automated system that combines elements of flow cytometry and microscopy to image, count, and analyze particle images in the 10-300 μm size range. Each sample was separated into two particle size fractions for analysis (<100 μm and 100-300 μm for imaging with 10x and 4x objectives, respectively). The >300 μm fraction was retained for observation under a dissecting microscope and enumeration of the large dinoflagellate *Noctiluca scintillans*. Using FlowCAM software phytoplankton and other microplankton were identified to the lowest practical taxonomic level (typically genus) or grouped into various broader, unidentified categories. Some microzooplankton, such as ciliates and crustaceans, were also quantified to the extent feasible. Image analysis endpoints included particle abundance and area-based biovolume.

Elemental sample analysis for POC/PON

Samples were analyzed by combustion for POC and PON content at the University of California Davis Stable Isotope Facility using an elemental analyzer interfaced to a continuous flow isotope ratio mass spectrometer (IRMS). The particulates were analyzed using an Elementar Vario EL Cube or Micro Cube elemental analyzer (Elementar Analysensysteme GmbH, Hanau, Germany) interfaced to a PDZ Europa 20-20 isotope ratio mass spectrometer (Sercon Ltd., Cheshire, UK). In this analysis, samples are combusted at 1080°C in a reactor packed with copper oxide and tungsten (VI) oxide. Following combustion, oxides are removed in a reduction reactor (reduced copper at 650°C). The helium carrier then flows through a water trap (magnesium perchlorate). N_2 and CO_2 are separated using a molecular sieve adsorption trap before entering the IRMS ([Stable Isotope Facility \(ucdavis.edu\)](https://www.stableisotopefacility.ucdavis.edu)). POC and PON concentrations are calculated from linear regressions of glutamic acid standards, which contain 40.81% C and 9.52% N. Standard concentrations varied from run to run, ranging from approximately 20 to 800 μg C and 5 to 200 μg N.

2.3.3 Data Analysis

Community analyses by non-metric multidimensional scaling (nMDS), cluster analysis and diversity indices were performed using Primer-e v7, a software package for non-parametric analysis of multivariate data tailored for marine communities (Clarke *et al.* 2014). The nMDS analyses were performed on standardized and transformed abundance values for each taxonomic category at the eight stations sampled 2015-2019 ($n=872$). The complete linkage cluster analysis by season was performed on standardized and transformed seasonal means of abundance for each taxonomic category, after combining abundance data for the eight stations. Likewise, cluster analyses by station and year were performed on standardized and transformed station and year means of abundance for each taxonomic category, after combining abundance data for all years and stations, respectively.

Diversity indices were calculated on total abundance for each taxonomic category after combining abundance data for each year and station and plotted as five-year means. Unidentified particle categories (e.g., misc 10-25 µm, misc 25-100 µm, misc diatoms) were omitted from these analyses.

POC Special Study Data Analysis - Comparison of measured carbon biomass with literature values

One objective of the POC study was to compare empirically obtained carbon values from the POC analysis with carbon values calculated using literature-based carbon content equations. Carbon content was calculated for 58 of the 59 FlowCAM taxonomic categories using equations established by Menden-Deuer and Lessard (2000) for small diatoms, large diatoms, dinoflagellates, other protist flagellates, and ciliates (Table A-3.). These power equations express carbon content as a function of cell volume:

$$y = a \text{ vol}^b, \text{ or} \\ \log y = b \log \text{ vol} + \log a,$$

where y = pg C cell⁻¹, vol = cell volume, b = slope, and a is derived from the y -intercept of the log-log regression equation.

Most cell volumes were taken from median values published by Harrison *et al.* (2015), based on an extensive survey of cell volumes for Salish Sea phytoplankton. In a few instances, when species names did not match the species identified by these authors, cell volumes for a closely related species were used instead (Table A-3). For taxa not included by Harrison *et al.* (2015), morphometric data in Horner (2002) were used, or in some cases images from in-house FlowCAM libraries were used to determine ABD (area based diameter) median volumes (Table A-3). Carbon density (C µm⁻³) was then calculated for each FlowCAM taxonomic category as carbon content (C cell⁻¹) divided by cell volume (µm³ cell⁻¹). For zooplankton, we assumed a density of 1 g/mL (wet), 10% dry/wet weight ratio, and 40% C/dry weight. These taxon-specific carbon density values allow us to express FlowCAM biovolume values as carbon biomass if the taxonomic composition of the sample is known. The carbon biomass in a sample (mg C L⁻¹) can thus be calculated as the sum of the (biovolume x carbon density) values for each taxonomic category. These calculations were performed in Primer 7 and the results exported as carbon biomass for higher level groupings: diatoms, dinoflagellates, other phytoplankton, ciliates, other zooplankton, and unidentified.

3.0 QUALITATIVE AND SEMI-QUANTITATIVE DATA RESULTS

3.1 Seasonality

Seasonal changes in taxonomic composition of phytoplankton at Pt. Jefferson (KSBP01; northern station) and East Passage (NSEX01; southern station) (2008 - 2019) show a basin-wide diatom-dominated community that peaks in April–August (Figure 2, Figure 3). During the winter months, *Skeletonema costatum* (filamentous colonial diatom), small dinoflagellates, cryptomonads and unidentified nanoflagellates occurred frequently at both Pt. Jefferson and East Passage sites. *Coscinodiscus* spp. (large non-colonial diatom), unidentified pennate diatoms (often benthic freshwater types), and *Dictyocha speculum* were also frequent at Pt. Jefferson, whereas *Mesodinium rubrum* (mixotrophic ciliate) and other ciliates were frequent in East Passage during the winter months. The *Thalassiosira*-dominated early spring bloom typically appeared in March at Pt. Jefferson, and April at the East Passage station, and was dominated primarily by *T. nordenskioldii* and *T. pacifica/aestivalis*, but also included *T. anguste-lineata* at East Passage. The diatoms *Cylindrotheca closterium*, *Paralia sulcata*, *Thalassionema nitzschioides* and *Skeletonema costatum* were often also observed in the early spring bloom. The *Chaetoceros* bloom usually started in April with *C. debilis* and *C. socialis* and continued at both stations through the summer with a number of different *Chaetoceros* species. *Chaetoceros debilis*, a species that forms spiraling chains with profuse setae (hairs)—a morphology that presumably increases their buoyancy—remained abundant until October. Other notable spring and summer taxa were *Ditylum brightwellii*, *Eucampia zodiacus*, *Pseudo-nitzschia* spp. (large forms), *Rhizosolenia setigera*, and small dinoflagellates. Some large mixotrophic flagellates were more predominant in summer/fall, e.g., *Akashiwo sanguinea* (especially at Pt. Jefferson), *Ceratium fusus* (especially at East Passage), and *Prorocentrum gracile*.

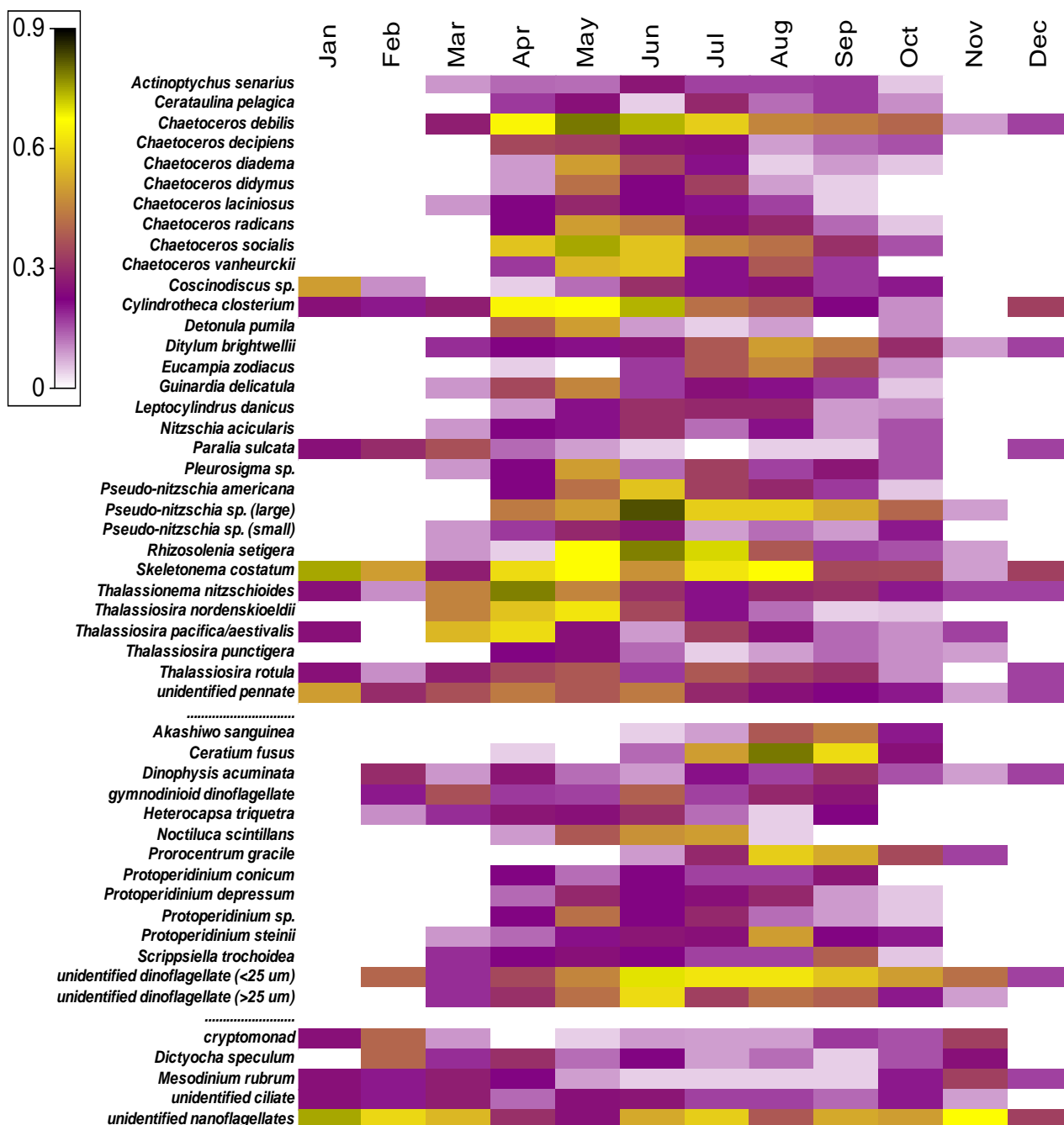


Figure 2. Seasonality of 50 most common taxa at Pt. Jefferson (KSBP01) in surface samples (2008 - 2019). Taxa ordered by group, top to bottom: diatoms, dinoflagellates, and misc. others. Values represent the relative proportion (number of qualitative observations / number of samples) a taxon was recorded by month. A qualitative observation refers to the presence of a particular taxon in a sample and does not reflect abundance. 5 - 12 samples/month for November–March, and 20 - 24 samples/month for April–October, all years combined.

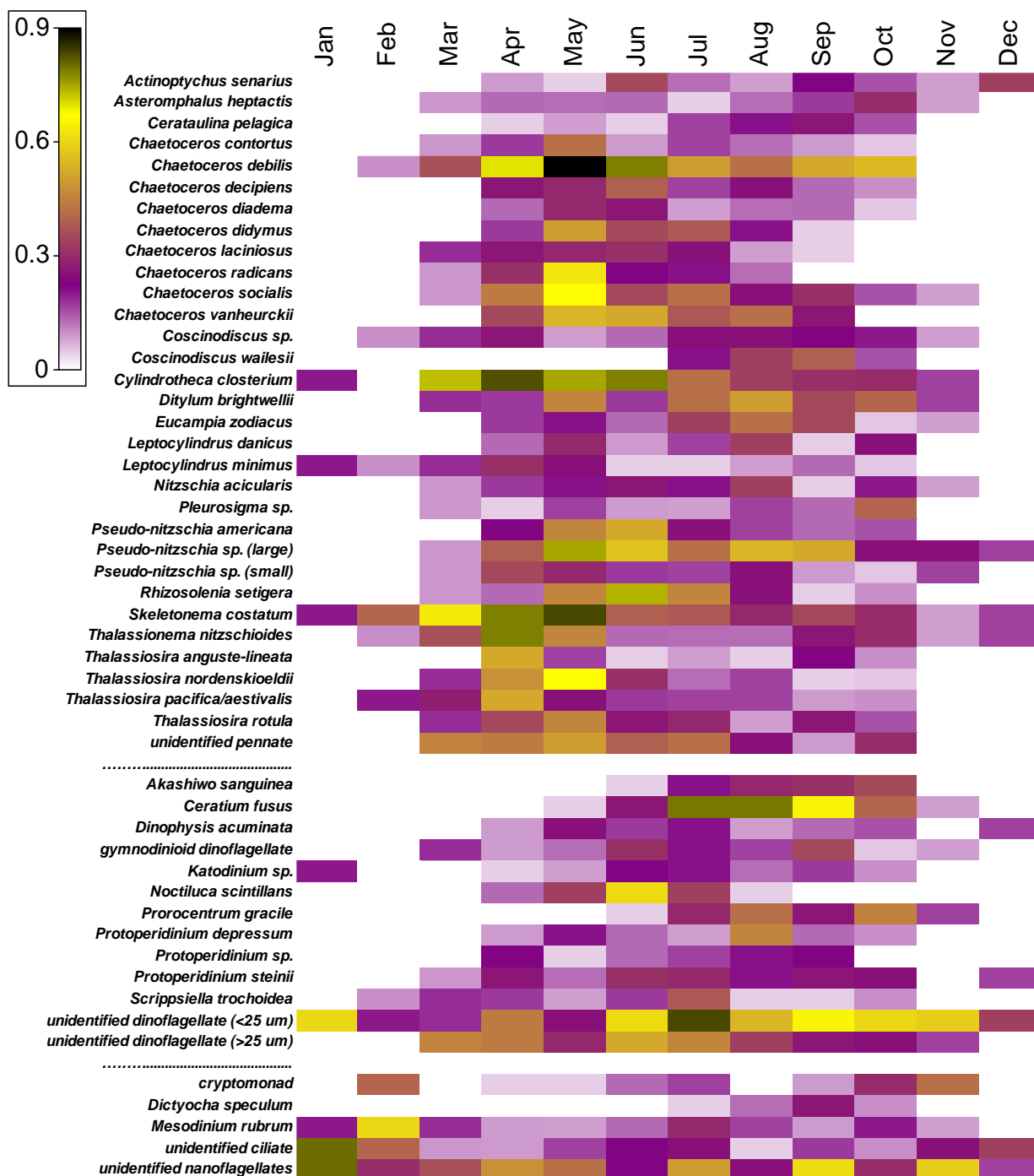


Figure 3. Seasonality of 50 most common taxa in East Passage (NSEX01) surface samples (2008 - 2019). Taxa ordered by group, top to bottom: diatoms, dinoflagellates and misc. others. Values represent the relative proportion (number of qualitative observations / number of samples) a taxon was recorded by month. A qualitative observation refers to the presence of a particular taxon in a sample and does not reflect abundance. 5 - 12 samples/month for November–March, and 20 - 24 samples/month for April–October, all years combined.

Semi-quantitative data (Subdominant, Dominant, Present+Common, Present) (2008 – 2014) indicate seasonal and year-to-year changes in relative abundance of major taxa at the mainstem stations Pt. Jefferson and East Passage (Figure 4 and Figure 5). Because sampling was limited to April–October, it is possible that early season (March) blooms of *Thalassiosira* spp. or late fall/winter blooms of *Coscinodiscus* spp. were missed.

Thalassiosira, *Chaetoceros* and *Ceratium* patterns were similar for the two stations, but relative abundance of *Pseudo-nitzschia* was higher at Pt. Jefferson. *Rhizosolenia* and *Detonula* became dominant more often at Pt. Jefferson, as did *Eucampia* and *Heterosigma* at East Passage, indicating that certain blooms are not evenly distributed through the Central Basin or that their timing is different, such that they can easily be missed during a sampling event.

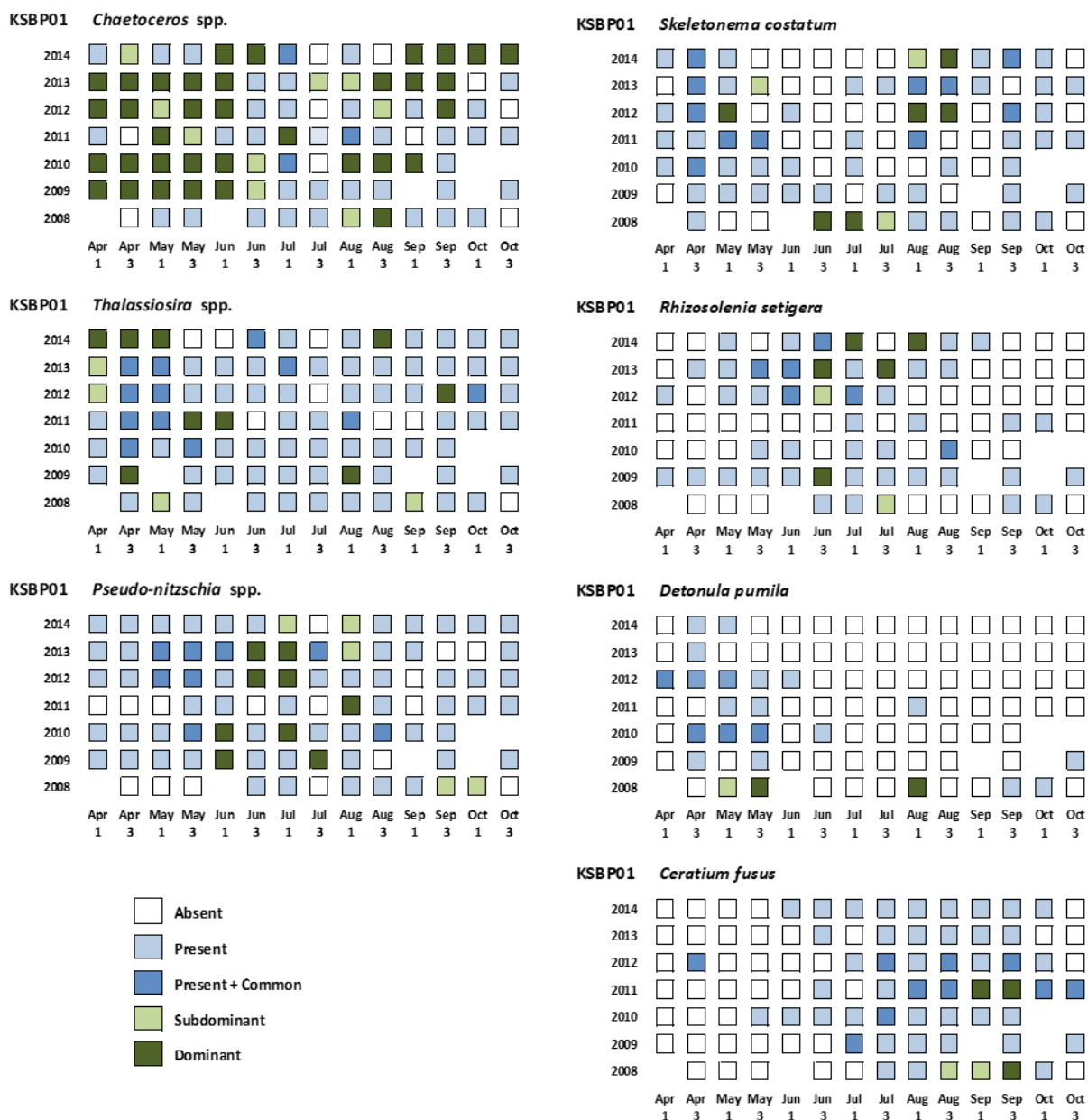


Figure 4. Seasonal and annual differences in relative abundance at Pt. Jefferson (KSBP01) (2008 - 2014), based on semi-quantitative and qualitative assessments. Data for seven taxa that were dominant at least twice are presented, surface and depth samples combined. Numbers below months indicate first or third week of the month.

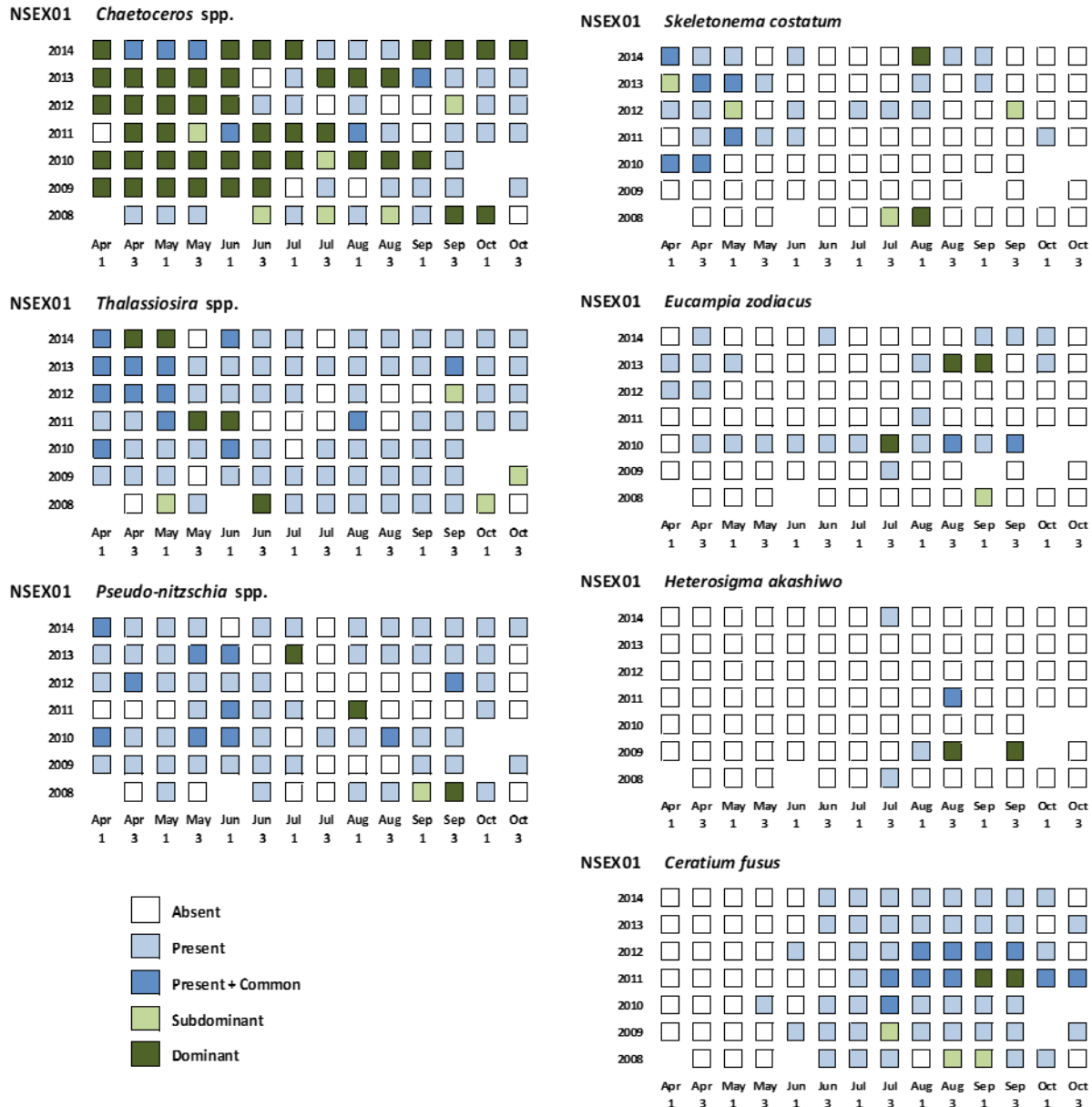


Figure 5. Seasonal and annual differences in relative abundance at East Passage (NSEX01) (2008 - 2014), based on semi-quantitative and qualitative assessments. Data for seven taxa that were dominant at least twice are presented, surface and depth samples combined. Numbers below months indicate first or third week of the month.

Semi-quantitative data (2009 - 2014) at Dockton (NSAJ02) indicate seasonal and year-to-year changes in relative abundance of major taxa (Figure 6). Species composition at Dockton differs somewhat from mainstem stations (see Section 4.7), yet there are many similarities. *Chaetoceros* was also a major component of the Dockton phytoplankton community, often becoming dominant or abundant in spring and summer, and *Thalassiosira* species were dominant early in the season in 2011 and 2014, mirroring these events at the mainstem stations. As elsewhere, *Skeletonema* was most abundant at the beginning and end of the season. Mid-summer blooms of *Heterosigma* at Dockton were

short and while the 2009 bloom was also detected at nearby East Passage, the 2013 and 2014 blooms were not observed outside the Dockton area. *Ceratium* and *Akashiwo* were both late season bloomers. Cells of the mixotroph *Akashiwo* are likewise typically observed late in the season at mainstem stations (Figure 2 and Figure 3). At Dockton, dense *Akashiwo* blooms were recorded in fall of 2012 and of 2014.

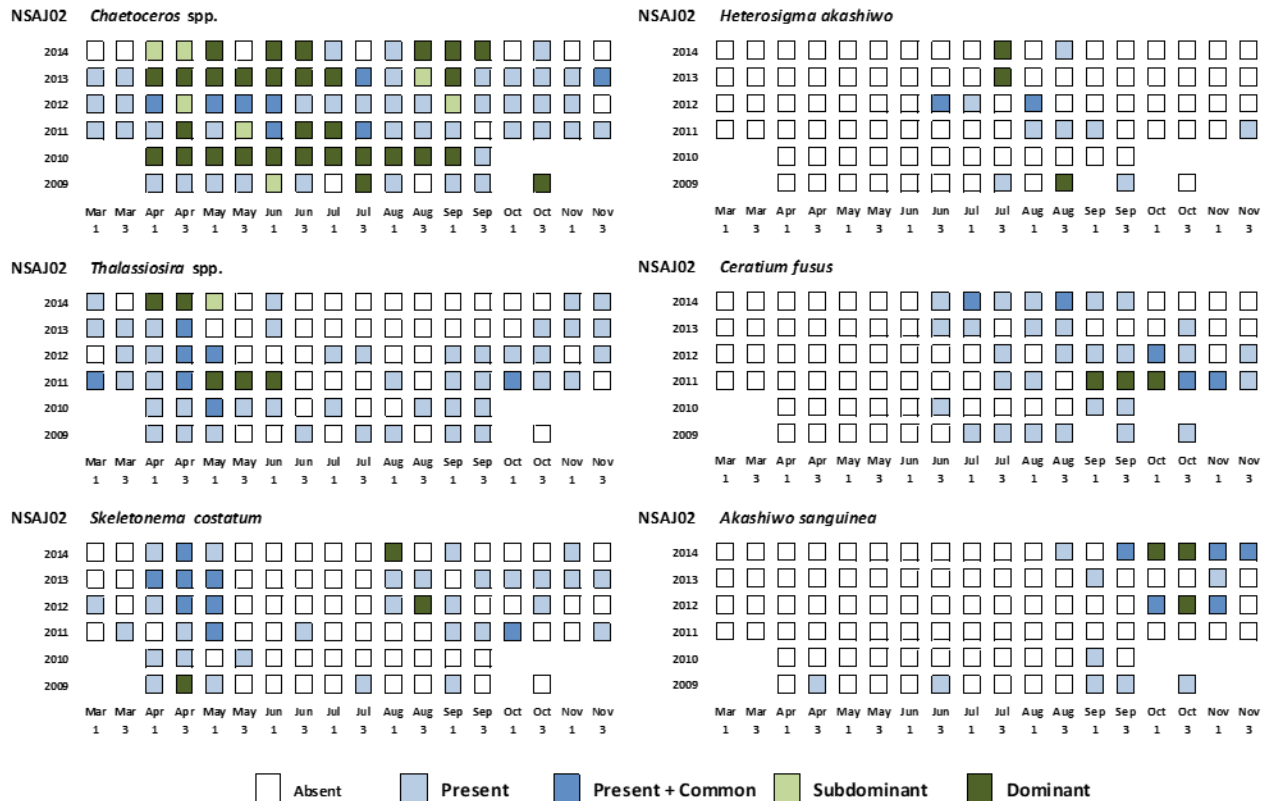


Figure 6. Seasonal and year to year differences in relative abundance at Dockton (NSAJ02) (2009 - 2014), based on semi-quantitative and qualitative assessments. Shown are six taxa that were dominant at least three times during this period. Numerals below months indicate first or third week of the month.

3.2 Dominant Diatom Species

The genus *Chaetoceros* is represented by at least 19 species in Puget Sound (Horner, 2002), forming blooms from spring to late summer and contributing almost half the annual phytoplankton biomass. Most species form straight or twisted chains that can at times be difficult to identify. The two most common species in the Central Basin (Figure 7), however - *C. debilis* and *C. socialis* - exhibit conspicuously different and unique morphologies: the former has large cells arranged in a spiraling chain, and the latter very small cells loosely connected to form a spherical colony. *C. debilis* is often dominant in the spring bloom. The relative proportions of *Chaetoceros* species have remained stable since 2010 (note that fewer species were identified in 2008 and 2009).

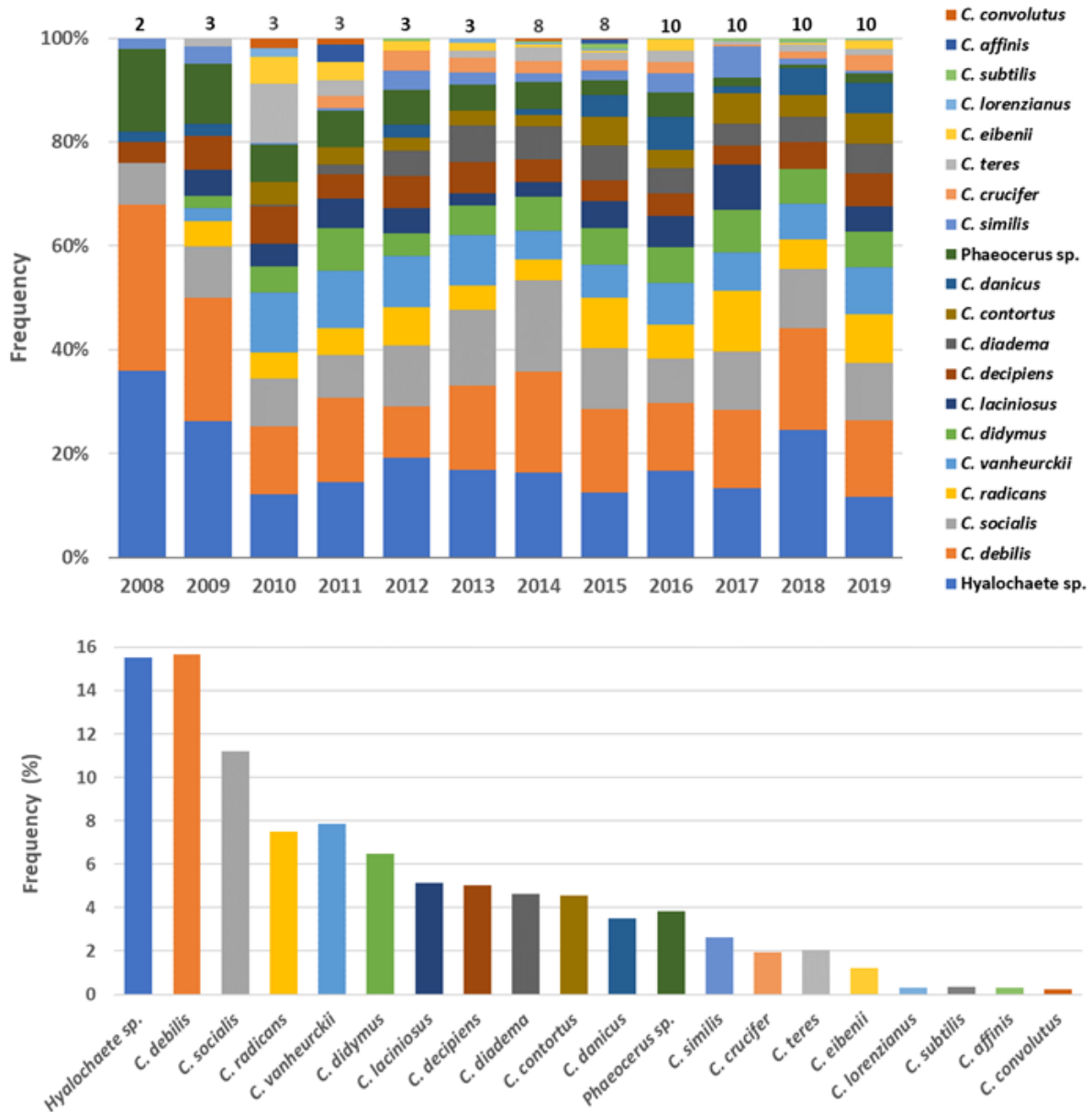


Figure 7. *Chaetoceros* species and their relative proportions (frequency), 2008 - 2019. Top panel shows interannual variations in relative proportions, bottom panel shows differences among species across all years. Proportions based on total of 3750 *Chaetoceros* qualitative observations, all stations combined (surface samples only). A qualitative observation refers to the presence of a particular species in a sample and does not reflect abundance. Numbers above bars indicate number of stations sampled each year. *Hyalochaete* sp. and *Phaeocerus* sp. indicate unidentified cells from these subgenera.

The genus *Thalassiosira* is represented by approximately 7 species in Puget Sound (Horner, 2002) and is the second largest biomass producer. Several *Thalassiosira* species typically initiate the spring bloom in large numbers but also contribute to the mixed diatom bloom later in the season. Except for *T. punctigera*, the cells form chains that can be very long,

especially *T. nordenskioldii*'s. The category *Thalassiosira* sp. includes cells, usually occurring singly or in “dirty” chains, that could not be identified to species (Figure 8). The category *T. pacifica/aestivalis* was added in 2010 and includes two species (and potentially also others of similar morphology) that are difficult to differentiate. The relative proportions of these five *Thalassiosira* species have some variations since 2010, notably an increase in the proportion of *T. pacifica/aestivalis* since 2015 and a gradual decrease in the proportion of *T. rotula*.

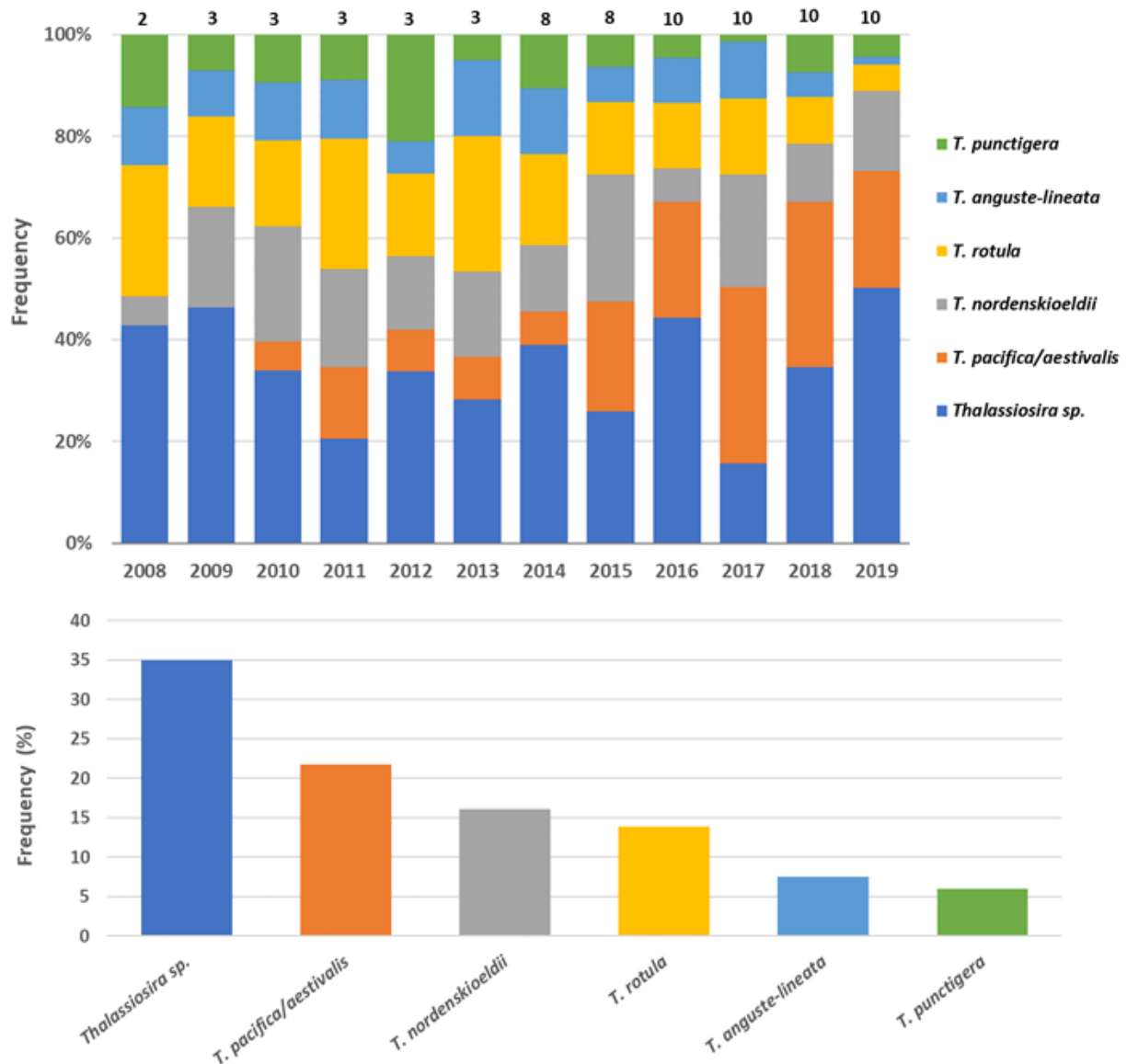


Figure 8. *Thalassiosira* species and their relative proportions (frequency), 2008 - 2019. Top panel shows interannual variations in relative proportions, bottom panel shows differences among species across all years. Proportions based on total of 1796 *Thalassiosira* qualitative observations, all stations combined (surface samples only). A qualitative observation refers to the presence of a particular species in a sample and does not reflect abundance. Numbers above bars indicate number of stations sampled each year. *Thalassiosira* sp. indicates cells that could not be identified to species level.

3.3 Inter-Annual Patterns in Species Composition

As shown in Table A-1 (Appendix A) many taxa were observed year after year at most stations. Aside from the two dominant genera, *Chaetoceros* and *Thalassiosira*, several common diatoms such as *Skeletonema*, *Asterionellopsis* and *Eucampia* formed blooms only during some years. Similarly, some dinoflagellate taxa, e.g., *Ceratium fusus*, were more abundant and ubiquitous in some years than others.

A few taxa were rare or observed only sporadically from 2008 - 2019. Notably the diatom *Guinardia striata* was only seen in 2016 and 2017 and *Bacteriastrum delicatulum* was present (and common) only in 2017. *Tropidoneis antarctica* disappeared from samples in 2016 and 2017. The dinoflagellate *Ceratium lineatum* was observed in 2017 and then again only in 2019. *Prorocentrum micans* was first observed in 2015, becoming common thereafter. It is apparent that some shifts in community composition may have occurred in 2016-2017, possibly related to environmental conditions such as the marine heat wave.

3.4 Harmful Algal Bloom (HAB) Species

Four common genera are considered recurrent HABs in Puget Sound ([SoundToxins](#), [NANOOS](#)) (*Dinophysis*, *Alexandrium*, *Heterosigma*, and *Pseudo-nitzschia*); four additional taxa are considered “of interest” due to their ability to form blooms that can cause adverse effects (*Akashiwo sanguinea*, *Mesodinium rubrum*, *Phaeocystis* sp. and *Protoceratium reticulatum*).

The dinoflagellate *Dinophysis* is responsible for diarrhetic shellfish poisoning (DSP); there have been concerns of its increase in Puget Sound in recent years (Trainer *et al.*, 2013). These cells do not occur in large numbers in the Central Basin, but large concentrations are not necessary for the toxin to be expressed in shellfish. Except for *D. parva*, all species identified are most likely toxin producers (Reguera *et al.*, 2014). Qualitative data indicate that occurrence of *Dinophysis* was highest from 2008 to 2012 (Figure 9, top). In subsequent years their presence dropped to 0–36% of samples across stations, with a sharp drop in 2019. *D. acuminata* was the most frequently observed species (Figure 9, bottom). Overall, these data suggest a decreasing trend in the occurrence of *Dinophysis* in the Central Basin.

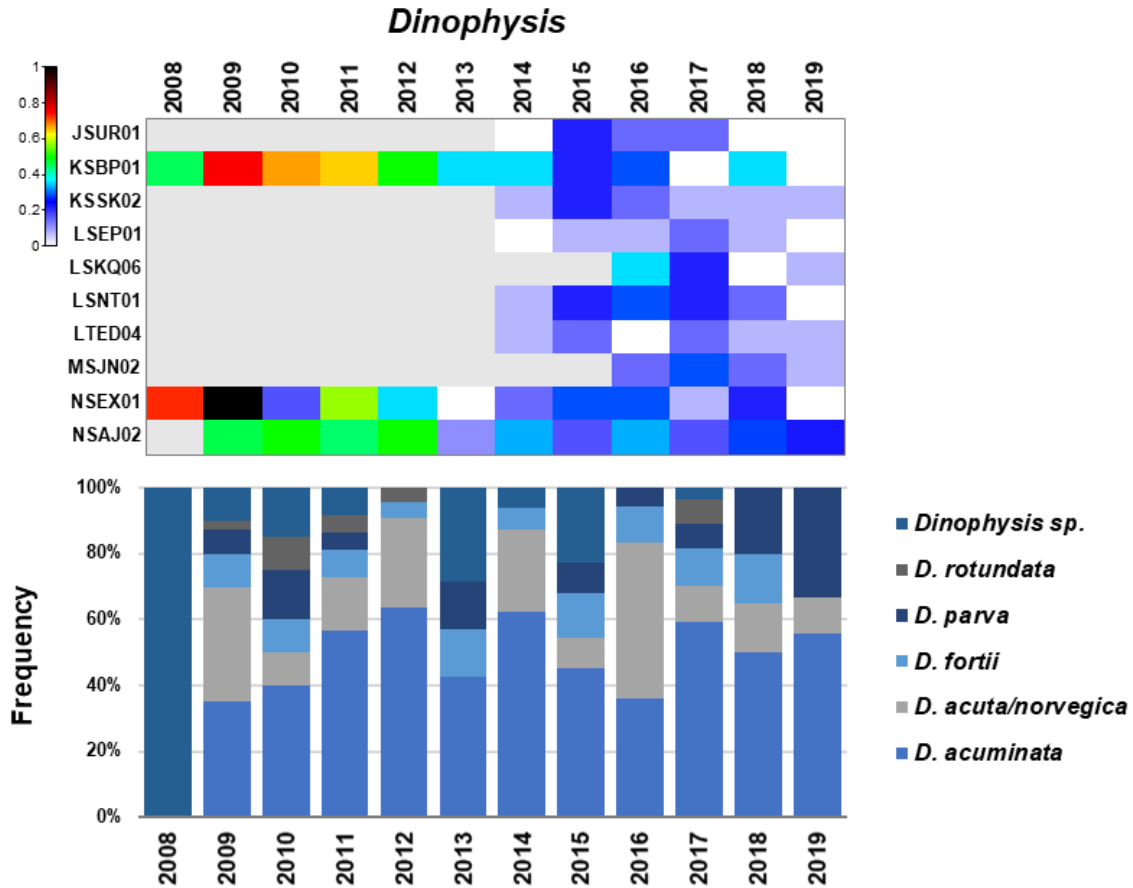


Figure 9. Relative proportions (frequency) of *Dinophysis* at ten stations, 2008 - 2019, between April and October (2009 - 2019, March–November at NSAJ02). Top panel: Relative proportions of all species combined (number of qualitative observations / number of samples). Grey areas indicate no sample. Bottom panel: Relative proportions of each species. Total 269 *Dinophysis* qualitative observations made (surface samples only). A qualitative observation refers to the presence of a particular species in a sample and does not reflect abundance. *D. acuta/norvegica* includes two species with similar morphologies. *Dinophysis* sp. indicates cells not identified to species level. *Dinophysis rotundata* is a former name for *Phalacroma rotundatum*.

The dinoflagellate *Alexandrium catenella* produces the toxin responsible for paralytic shellfish poisoning (PSP), the most concerning biotoxin in Puget Sound. *A. catenella* cells thrive in warmer embayments such as Dockton and are seldom encountered in mainstem Central Basin samples (Figure 10). Live *A. catenella* cells can only be easily identified when they occur in chains; single cells were therefore recorded as *Alexandrium* sp., given that several other, non-toxic *Alexandrium* species have been described for this region (Horner, 2002). At Dockton, *Alexandrium* occurrence was highest in September (Figure 10, bottom panel). *Alexandrium* was observed in 61 samples at this site (2009 – 2019, March - November), representing 11% of all samples.

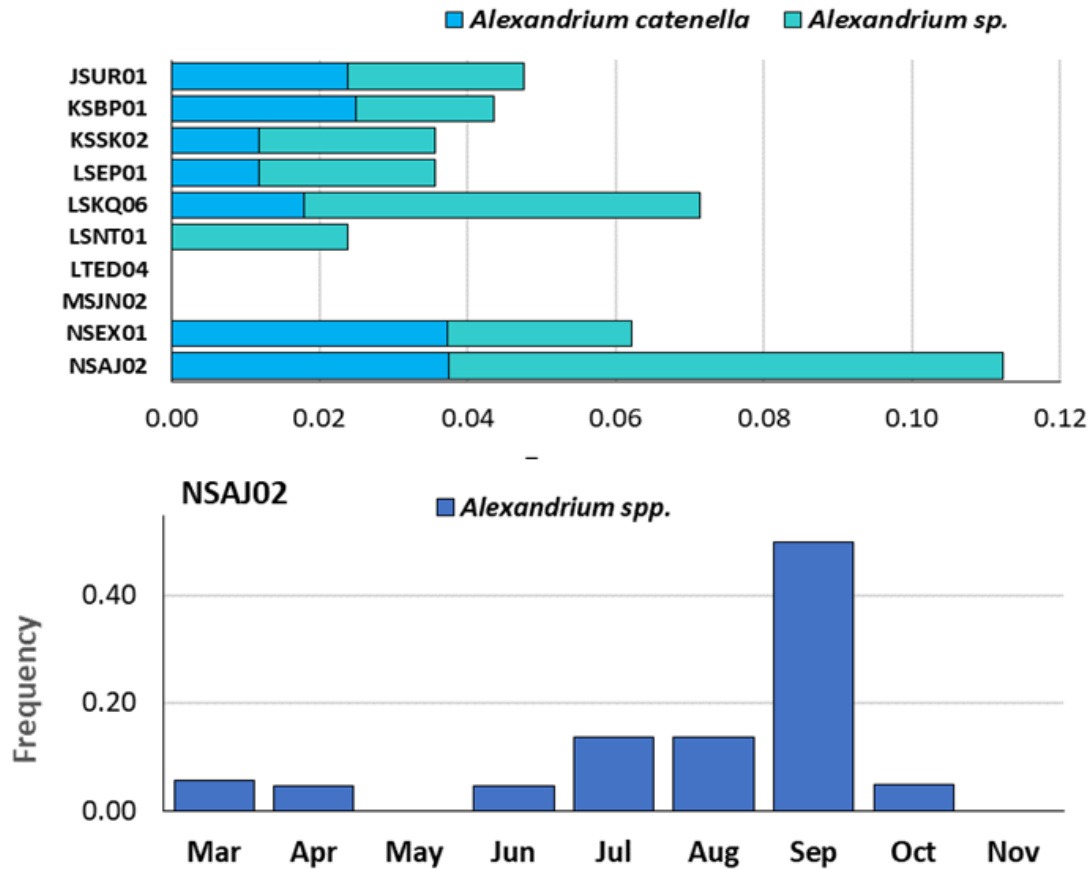


Figure 10. Relative proportions (frequency) of *Alexandrium* at ten stations, 2008 – 2019, between April and October (2009 - 2019, March - November at NSAJ02). Top panel: Relative proportions by station, all years combined. Bottom panel: Seasonal pattern at Dockton (NSAJ02), all years combined. Relative proportions calculated as number of qualitative observations / number of samples collected. A qualitative observation refers to the presence of a particular species in a sample and does not reflect abundance. *Alexandrium sp.* indicates cells not identified to species level, and *Alexandrium spp.* indicates all cells in genus.

The raphidophyte *Heterosigma akashiwo* is a small flagellate that has been linked to fish kills in Puget Sound (Rensel, 2007). Between March and November (2008 - 2019), *H. akashiwo* was observed in 168 surface samples, representing 13.9% of all samples. Occurrence of *Heterosigma* cells did not show a clear geographical or interannual pattern. The highest frequencies were observed from June to September (Figure 11), but note that this only refers only to presence/absence and is unrelated to cell density. Semi-quantitative and quantitative data shown in this section indicate short *Heterosigma* blooms in 2009, 2013, 2015, 2018 and 2019, with a particularly large bloom at Dockton in 2014 (see Section 4.5).

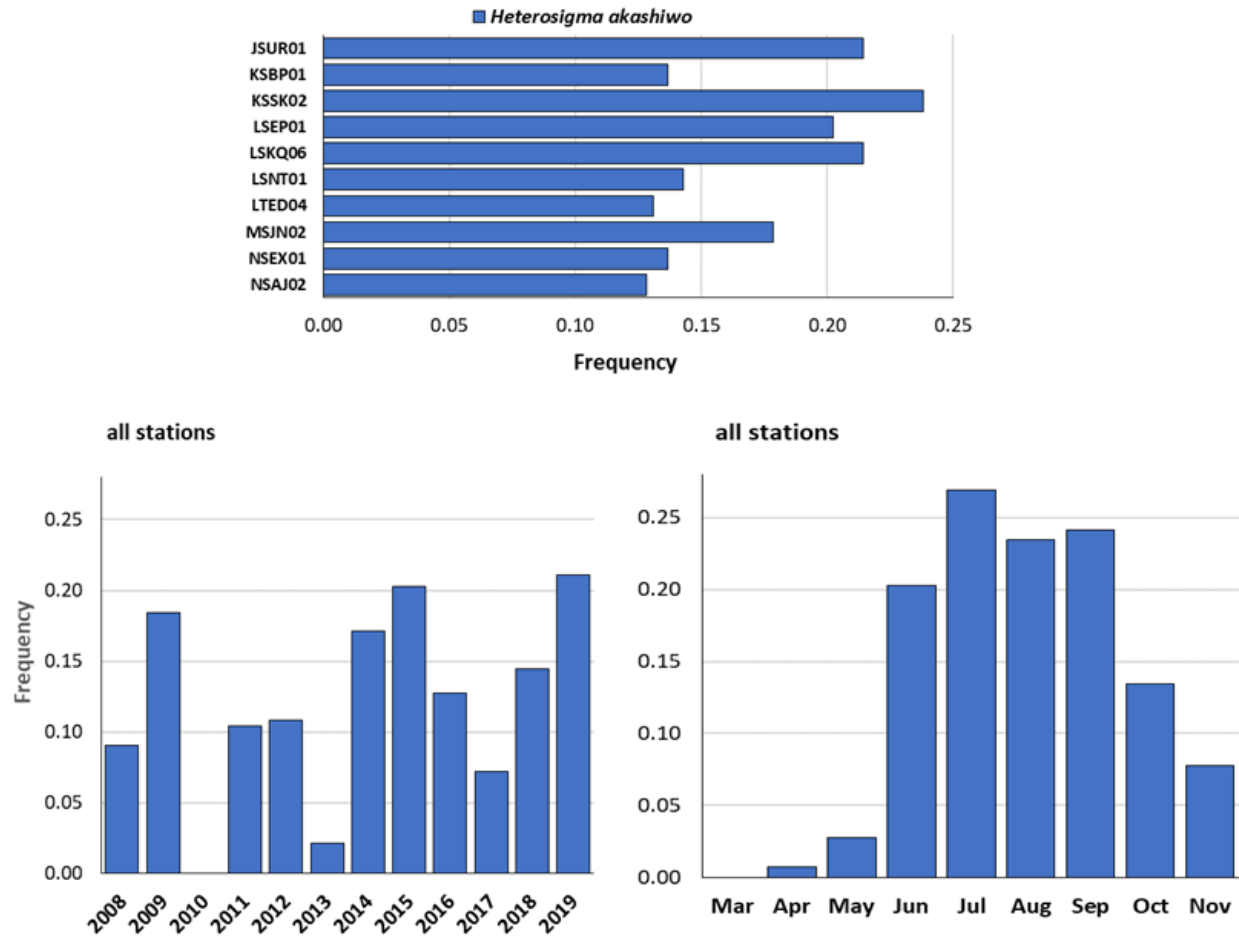


Figure 11. Relative proportions (frequency) of *Heterosigma akashiwo* at ten stations, 2008 - 2019, between April and October (2009 - 2019, March–November at NSAJ02). Top panel: Relative proportions by station, all years combined. Bottom panels: Interannual and seasonal patterns, all stations combined. Relative proportions calculated as number of qualitative observations / number of samples collected for a particular station (top panel), year, or month (lower panels). A qualitative observation refers to the presence of a particular species in a sample and does not reflect abundance.

Some species of the pennate diatom *Pseudo-nitzschia* can produce domoic acid, the toxin responsible for amnesic shellfish poisoning (ASP) which has only been detected in Puget Sound waters since 2003 (Bill *et al.*, 2006). The toxigenic species cannot be identified by light microscopy except as belonging to a group of chain forming small-celled species. These species were far less common in our samples than the large-celled species.

Between March and November, from 2008 to 2019, there was a total of 214 small-cell *Pseudo-nitzschia* observations in surface samples, representing 17.7% of all samples. High frequencies of occurrence were observed in 2016 and 2017, which likely explains the higher number of occurrences at Alki (LSKQ06) and Vashon (MSJN02) shown in Figure 12, since monitoring at these stations didn't start until 2016 (refer to Figure 9 for sampling

schedule). Small-celled *Pseudo-nitzschia* were most often present between April and August.

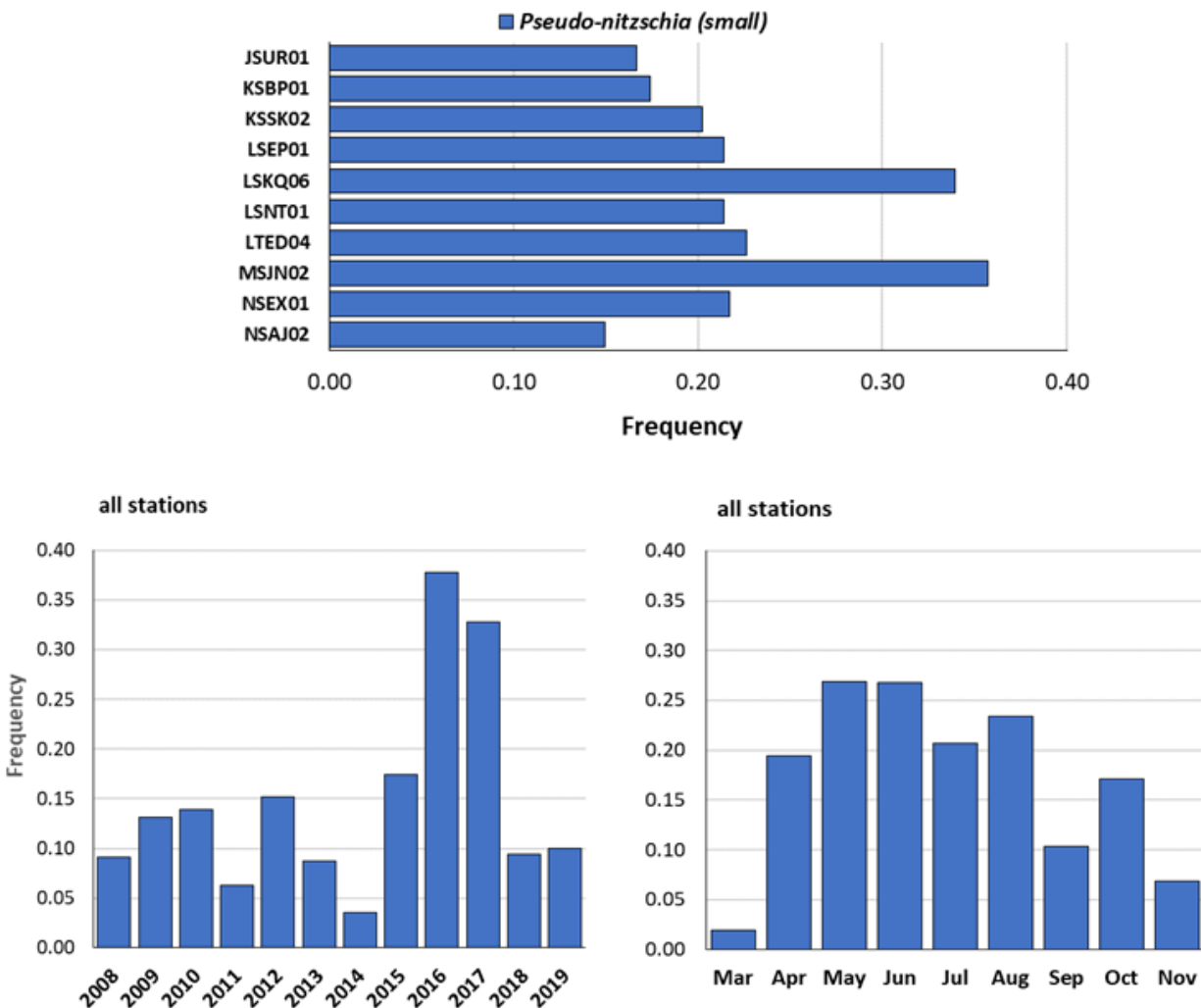


Figure 12. Relative proportions (frequency) of small-celled *Pseudo-nitzschia* observations at ten stations, 2008 - 2019, between April and October (2009 - 2019, March–November at NSAJ02). Top panel: Relative proportions by station, all years combined. Bottom panels: Interannual and seasonal patterns, all stations combined. Relative proportions calculated as number of qualitative observations / number of samples collected for a particular station (top panel), year, or month (lower panels). A qualitative observation refers to the presence of a particular species in a sample and does not reflect abundance.

Akashiwo sanguineum is a large, mixotrophic dinoflagellate that is common in the Central Basin. It produces surfactants that can harm marine wildlife when present at high concentrations. These cells are most common in late summer and fall (Figure 2 and Figure 3). During the report period there was a total of 151 *Akashiwo* observations in surface samples, representing 14.5% of all samples (Figure 13). A high percentage (24%) of all

Akashiwo observations were at Dockton, where it often forms autumn blooms following the nutrient decline caused by diatom blooms (see Section 4.0, Figure 24).

The toxigenic dinoflagellate *Protoceratium reticulatum* was present in only 4.7% of all samples and was not observed every year (Figure 13). Late summer basin-wide blooms occurred in 2009, 2017, 2018 and 2019.

The red photosynthetic ciliate *Mesodinium rubrum* is ubiquitous, and does not pose any direct threat to humans or wildlife but is sometimes considered harmful due to its ability to form dense blooms that could impact aquaculture. Monitoring of this organism started in 2014 (Figure 13) and it was subsequently observed in 36% of all microscope samples. It is present year-round.

Overall, these data do not indicate a trend in the frequency of occurrence of HABs in the Central Basin.

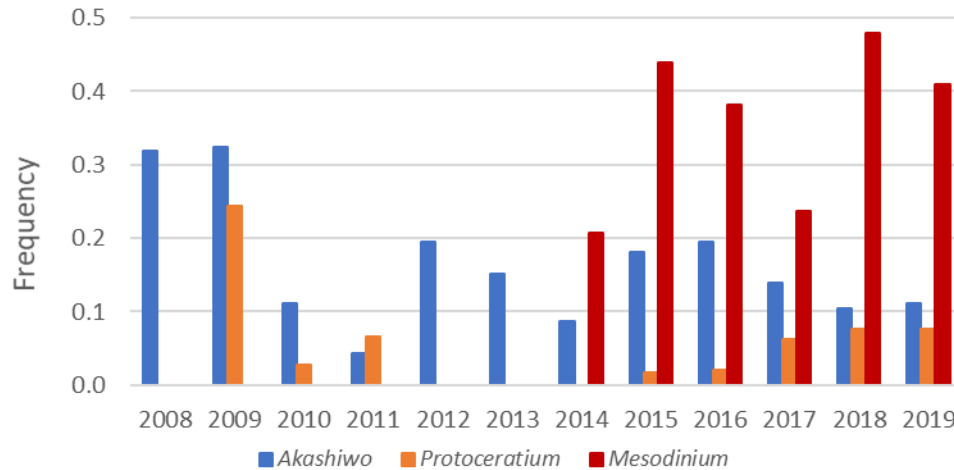


Figure 13. Relative proportions (frequency) of *Akashiwo*, *Protoceratium*, and *Mesodinium* at ten stations, 2008 - 2019, between April and October (2009 - 2019, March–November at NSAJ02). No *Mesodinium* data prior to 2014. Relative proportions calculated as number of qualitative observations / number of samples. A qualitative observation refers to the presence of a particular species in a sample and does not reflect abundance.

4.0 QUANTITATIVE DATA RESULTS

Samples for quantitative analysis by FlowCAM were collected between May 2014 and 2019, initially at 8 stations, and increasing to 10 stations in 2016 (Table 2). The primary endpoint of these analyses was biovolume which was estimated from particle images and is used here as a proxy for biomass (see Section 5.0).

4.1 Biovolumes and Seasonality

The seasonal pattern of the two major taxonomic groups, diatoms and dinoflagellates (Figure 14 and Figure 15), indicated:

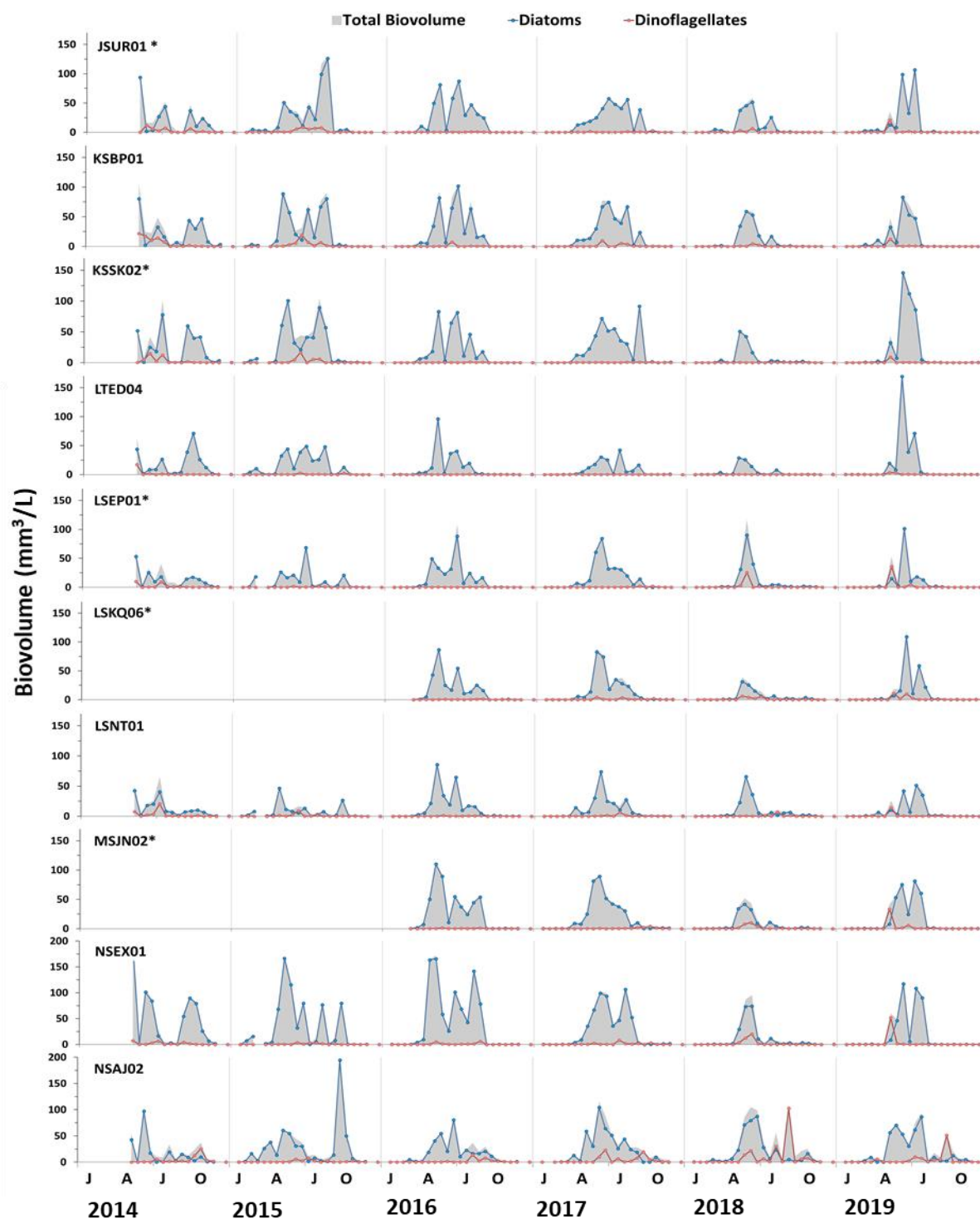
- Consistent diatom dominance throughout the seasons
- Small differences between mainstem stations
- Interannual shifts in the onset of the spring bloom
- Interannual differences in length of the bloom season
- Interannual differences in the shape and magnitude of the seasonal biovolume curves

Early spring phytoplankton blooms typically started in late March or early April but did not peak until mid-April or May, some years even as late as June. There was no consistent north-south pattern in the timing of the spring bloom (Table 4). However, clear inter-annual differences were seen with blooms starting later in 2018 and 2019 than in previous years. A side-by-side comparison of seasonal bloom patterns at Pt. Jefferson (northernmost) and East Passage (southernmost) stations shows similar timing of increases and decreases in phytoplankton but a larger late season bloom in some years at East Passage (Figure 16). Late summer / early fall blooms were observed some years, but cells usually disappeared from the surface layer by early September, if not earlier. The growing season was particularly short in 2018 and 2019. Seasonal phytoplankton patterns at Dockton were less consistent and often did not align with observations for the mainstem stations.

Phytoplankton bloom dynamics in Puget Sound were studied in detail by Winter *et al.* (1975), who showed that algal seed stock is supplied from depth and high productivity is due to persistent upwelling of nutrients, which rarely become exhausted in the photic zone. Spring and early summer freshwater runoff creates a less dense surface layer that promotes algal growth; growth is primarily limited by hydrodynamic factors (e.g., turbulent mixing and upwelling) and modulation of underwater light intensity. Several days of bright sunshine can be sufficient to promote massive growth, whereas nitrate limitation and a succession of cloudy days can cause a decline in bloom intensity, or blooms can be removed by sustained winds.

It is not uncommon for phytoplankton biomass to undergo a succession of peaks and troughs, as shown here for most years, (Figure 14), which can be caused by disruption from

wind events, tidal cycles, or zooplankton grazing (Erga and Heimdal, 1984; Sournia *et al.*, 1987). Some of the observed interannual differences may be due to timing of individual bloom events relative to timing of sampling events, as natural conditions and blooms may change quickly and peaks can thus easily be missed by twice-monthly sampling (Winter *et al.*, 1975). In general, interannual differences observed from biovolume data closely tracked our observations from chlorophyll-*a* data (Section 4.12, King County, 2022c).



* Indicates outfall stations

Figure 14. Seasonal changes in biovolume of diatoms, dinoflagellates and total microplankton (100-300 µm) for all stations, 2014 - 2019. Note different scales for NSEX01 and NSAJ02.

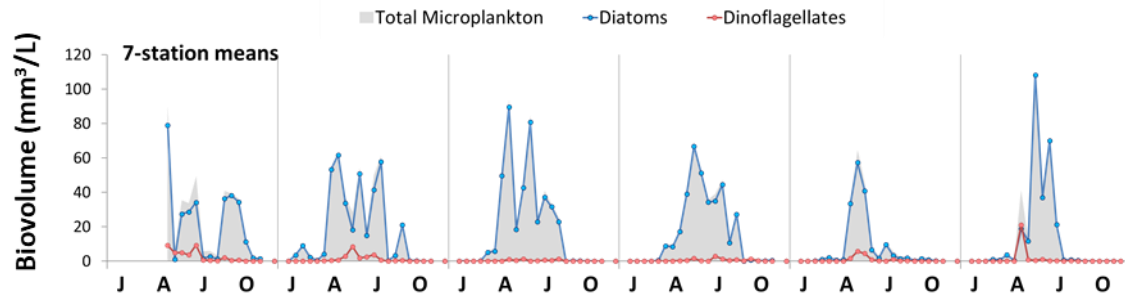


Figure 15. Seasonal changes in mean biovolume of diatoms, dinoflagellates and total microplankton (100-300 μm) for 7 stations sampled 2014 - 2019 (Dockton excluded). See Table 2 for station names.

Sharp interannual differences in seasonality, as observed in the Central Basin, are characteristic of plankton communities at the land-sea interface as opposed to terrestrial or open ocean environments where the annual climate cycle is the primary driver of biomass variability (Cloern and Jassby, 2008). Phytoplankton seasonality at the land-sea interface is driven by more than a few climatic factors (e.g., riverine inputs, tidal cycles, weather events, wind waves), making it more difficult to generalize the processes which determine seasonality of plankton production.

Table 4. Timing of spring diatom bloom at all stations, based on biovolume, 2015 - 2019. Dates indicate timing of first biovolume measurement $>5 \text{ mm}^3/\text{L}$, roughly $5 \mu\text{g/L}$ chlorophyll-*a* (Feb. data excluded). The color progression (yellow, orange, red) illustrates earlier to later timing.

Station	2015	2016	2017	2018	2019
JSUR01	4/6	3/21	4/3	3/7	5/6
KSBP01	4/6	3/21	4/3	5/7	4/1
KSSK02	4/20	3/21	4/3	5/7	5/6
LTED04	4/20	4/18	5/1	5/7	5/6
LSKQ06		4/19	4/4	5/8	5/7
LSEP01	4/21	4/5	4/3	5/8	5/7
LSNT01	4/21	4/5	4/3	5/8	4/2
MSJN02		4/5	4/4	5/8	5/7
NSEX01	4/21	4/5	4/17	5/8	5/7
NSAJ02	3/18	4/20	4/5	4/18	3/20

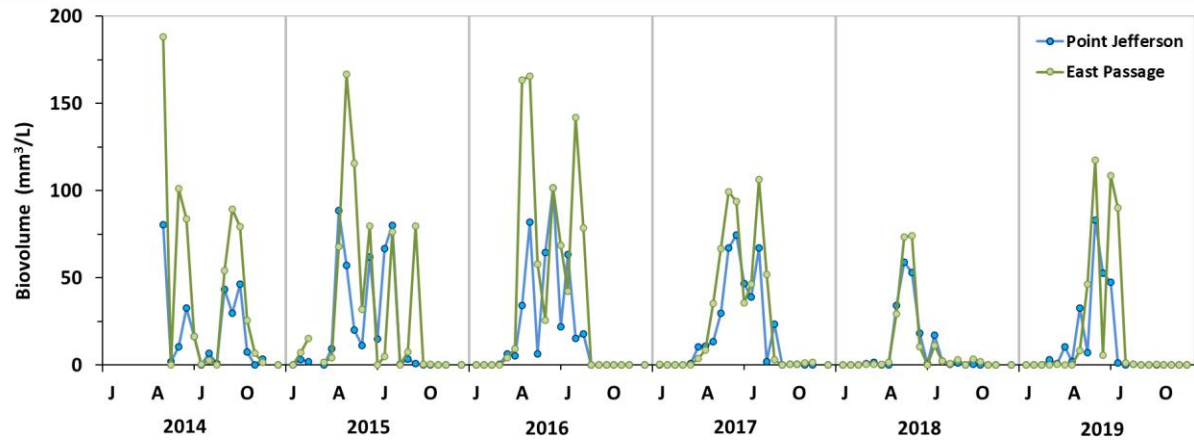


Figure 16. Comparison of seasonal changes in diatom biovolume at Pt. Jefferson and East Passage (2014 - 2019).

4.2 Growth and Water Column Stratification

It has been well established that growth of photosynthetic phytoplankton in temperate regions is greatly influenced by water column stability (Mahadevan *et al.*, 2012, van de Poll *et al.*, 2013). A stable, stratified water column allows cells to remain close to the surface where light can be harvested for photosynthesis. However, stratification also inhibits exchange with nutrient-rich deep water, potentially leading to nutrient limitation. Water column stability can be dependent on factors such as temperature, currents, wind, and freshwater input, but in Puget Sound, stratification is mostly influenced by freshwater inflows and mixing over sills (Moore *et al.*, 2008a). Stratified conditions are typically seen in spring due to river discharge and warmer temperatures, conditions which are all favorable for algal growth. Climatic and oceanographic events can disrupt this layering at any time, although stratified conditions often persist throughout the growth season.

The relationship between primary productivity and stratification is of great importance when considering the effects of climate change, as continued ocean warming will likely produce increasingly (thermally) stratified surface waters (Elsworth *et al.*, 2020), and Puget Sound will likely experience changes in the timing and volume of streamflow, which will lead to changes in timing and magnitude of stratification, nutrient loading, and turbidity related to freshwater inputs (Moore *et al.*, 2008b).

This monitoring program's subset of data, comprised of phytoplankton biovolumes together with water column characteristics, offers an opportunity to examine the relationship between density stratification and phytoplankton growth in the Central Basin. Density stratification calculations evaluate the rate at which water density varies with depth and look for a steep change in density signaling the convergence between two layers (the pycnocline). This steep change in density is the maximum density gradient and is expressed in kg/m^4 (King County, 2022b).

Figure 17 and Figure 18 show the relationship between microplankton biovolume and the maximum density gradient, a measure of pycnocline strength. The data suggest that:

- Higher cell concentrations generally occur above a maximum density gradient threshold of about 0.035-0.05 kg/m⁴ if other growth requirements are met (temperature, light, nutrients)
- No significant correlation between biovolume and stratification was seen above this threshold (based on regression analyses, not shown)
- Some sites, such as Pt. Williams (LSNT01), are less stratified, which may help explain the lower chlorophyll and biovolume values observed here

Moore *et al.* (2008a) have defined stratified conditions as when the maximum density gradient is > 0.1 kg/m⁴, which is higher than the stratification strength that may be necessary for persistence of surface phytoplankton as suggested by this dataset.

Seasonal changes in biovolume and stratification strength are shown in Figure 19 for Pt. Wells (JSUR01) and East Passage (NSEX01), stations at the north and south ends of the sampling area (Figure 1) that exhibit strong seasonal stratification (King County, 2022b). It is apparent that stratification strength varies throughout the growing season and year to year, yet mostly remains > 0.05 kg/m⁴ from mid-March to early or mid-September, when vertical mixing sets in and cells dissipate from the surface layer.

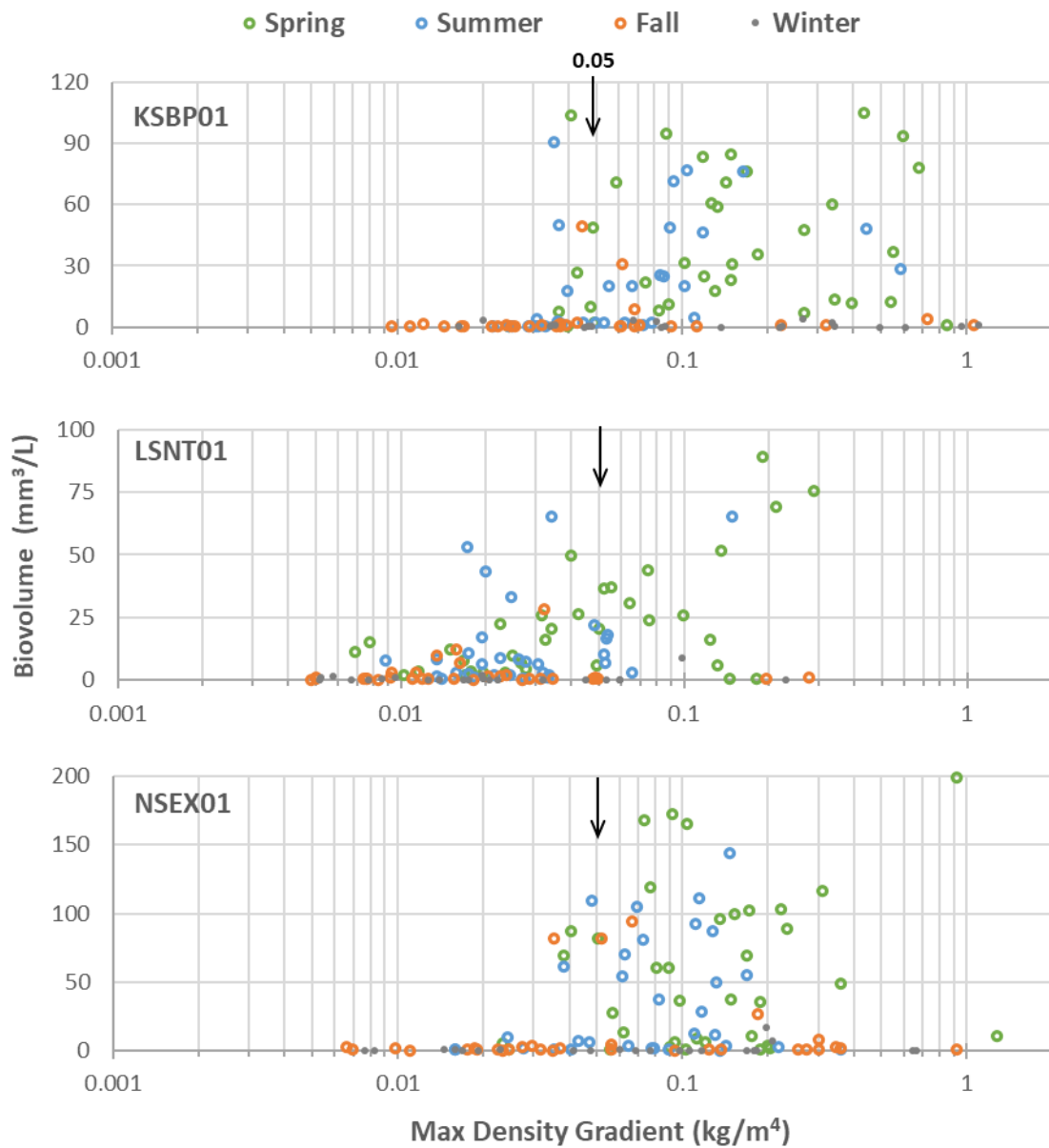


Figure 17. Total biovolume as a function of maximum density gradient at time of sampling for three ambient stations, showing seasonal and geographic differences (2014 - 2019, n=120-121). North to south: Pt. Jefferson (KSBP01), Pt. Williams (LSNT01), East Passage (NSEX01). Arrows indicate 0.05 cutoff shown in Figure 19. Note different biovolume scales.

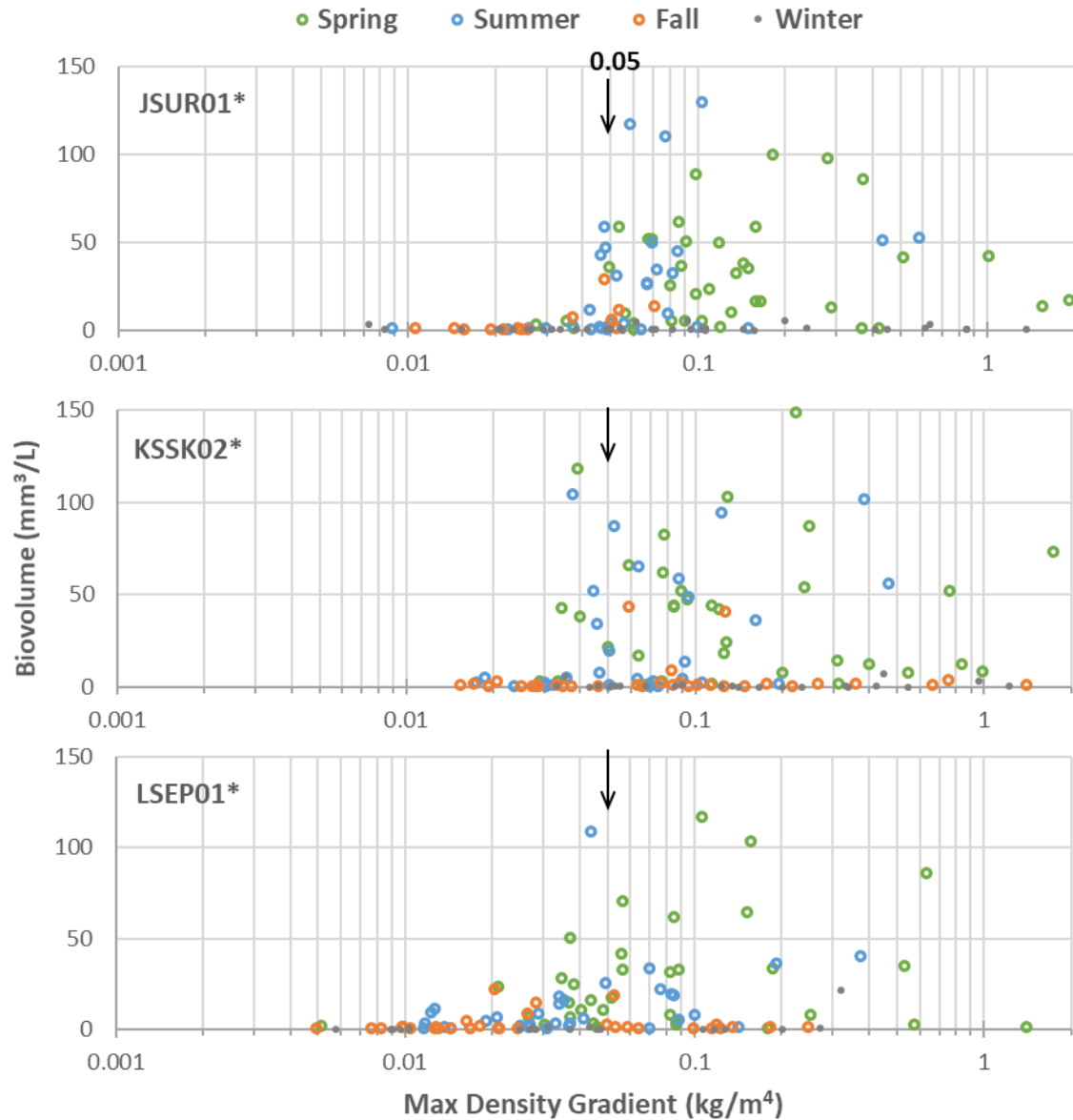


Figure 18. Total biovolume as a function of maximum density gradient at time of sampling at three outfall stations (2014 - 2019, n=120-122), showing seasonal and geographic differences. North to south: Pt. Wells (JSUR01), West Pt. (KSSK02), South Plant (LSEP01). Arrows indicate 0.05 cutoff shown in Figure 19.

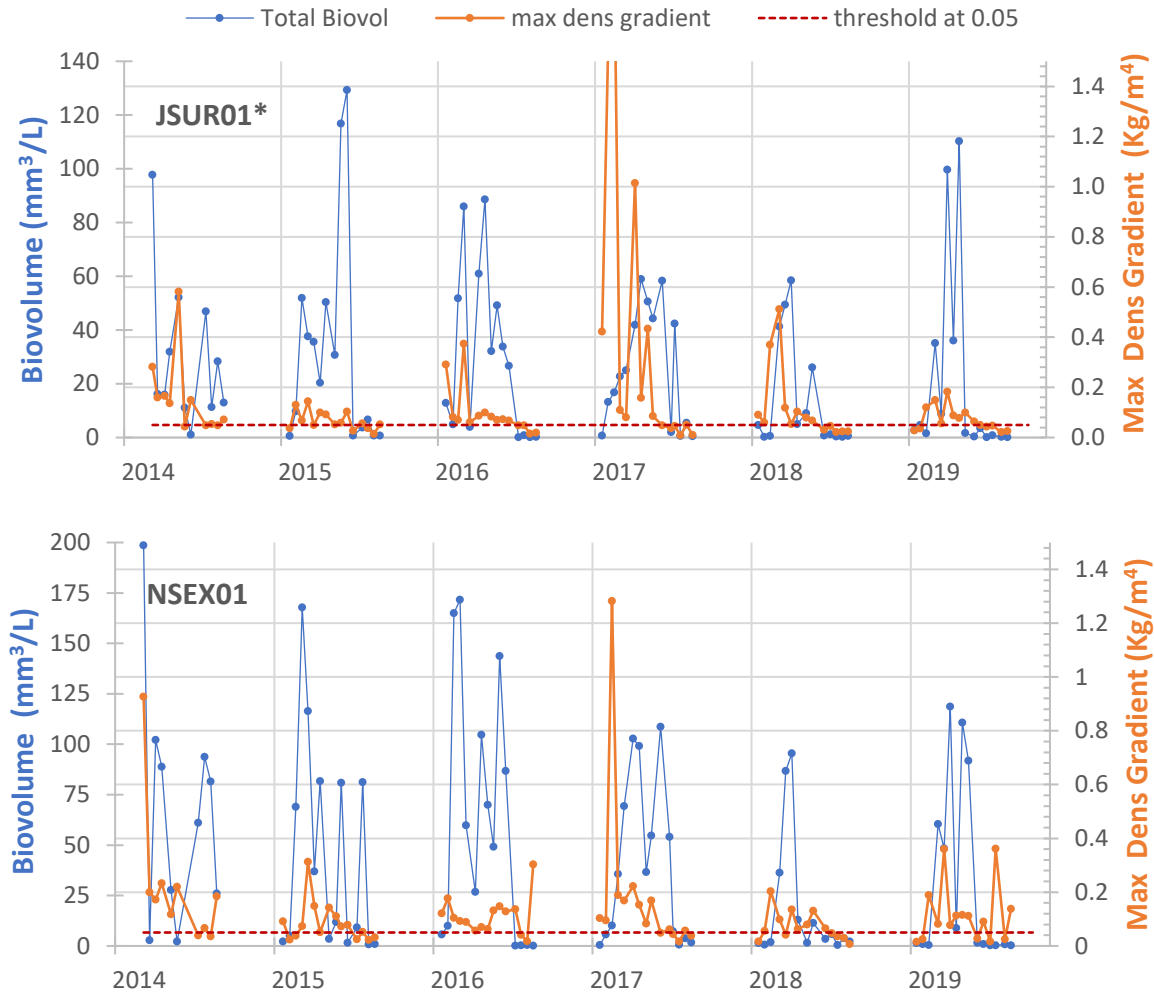


Figure 19. Seasonal pattern of total biovolume and maximum density gradient at time of sampling at Pt. Wells (JSUR01) and East Passage (NSEX01) (2014 - 2019; only mid-March-October samples). The red stippled line indicates a suggested stratification cutoff at 0.05 kg/m^4 .

4.3 Seasonal Succession

The seasonal pattern of the most prevalent phytoplankton species in the Central Basin indicates that some taxa are consistently abundant every year, whereas others are only abundant in some years and do not exhibit a predictable pattern (Figure 20). The growing season (2014 – 2019) typically started with an early (March) bloom of various species of *Thalassiosira* which was soon followed by a persistent bloom of multiple species of *Chaetoceros*. A few other diatom taxa became abundant in different years during spring/summer, e.g., *Lauderia/Deinonula* (2015-2016), *Skeletonema* (2017) and *Rhizosolenia* (2018), all of which represent long skinny chain forms. Mid to late season blooms typically consisted of larger celled taxa, e.g., *Ditylum* (2014, 2016), *Eucampia* (2016) and *Coscinodiscus* (2018). An unusually early bloom of *Coscinodiscus* occurred in

February of 2015, when marine conditions led to stratification along with 1-2 °C warmer than average surface temperatures due to the marine heat wave. *Noctiluca* cells were frequently among the top 6 taxa by biovolume; but since these large cells are mostly filled with large vacuoles they have a much lower carbon to biovolume ratio, precluding comparisons with other taxa on a biomass basis.

Thalassiosira species are vital primary producers in temperate and polar regions (Chappell *et al.*, 2013) and frequently form the initial major component of the spring diatom bloom due to their ability to proliferate in low light regimes, reduced temperatures, and well-mixed water in comparison with competitor species (Langdon, 1988, Haigh *et al.*, 1992, Harris *et al.*, 1995). Early *Thalassiosira* blooms followed by persistent *Chaetoceros* blooms are common in other systems as well (Shinada *et al.*, 1999, Booth *et al.*, 2002). Within the North Water of the Arctic Ocean, *Chaetoceros socialis* were able to persist for up to six months because of their ability to survive at low nutrient levels, serving as an important planktonic food source as well as a major carbon contributor to the benthic environment. Booth *et al.* (2002) suggest that if cells can maintain their population at low productivity until nutrients are replenished, a series of blooms can occur with the appearance of a single prolonged bloom. The observations likewise suggest that *Thalassiosira* blooms in the Central Basin are linked to early spring high nutrient levels, along with relatively low temperatures and irradiance, and are then taken over by *Chaetoceros* when temperatures and irradiance increase, and ambient nutrients decline.

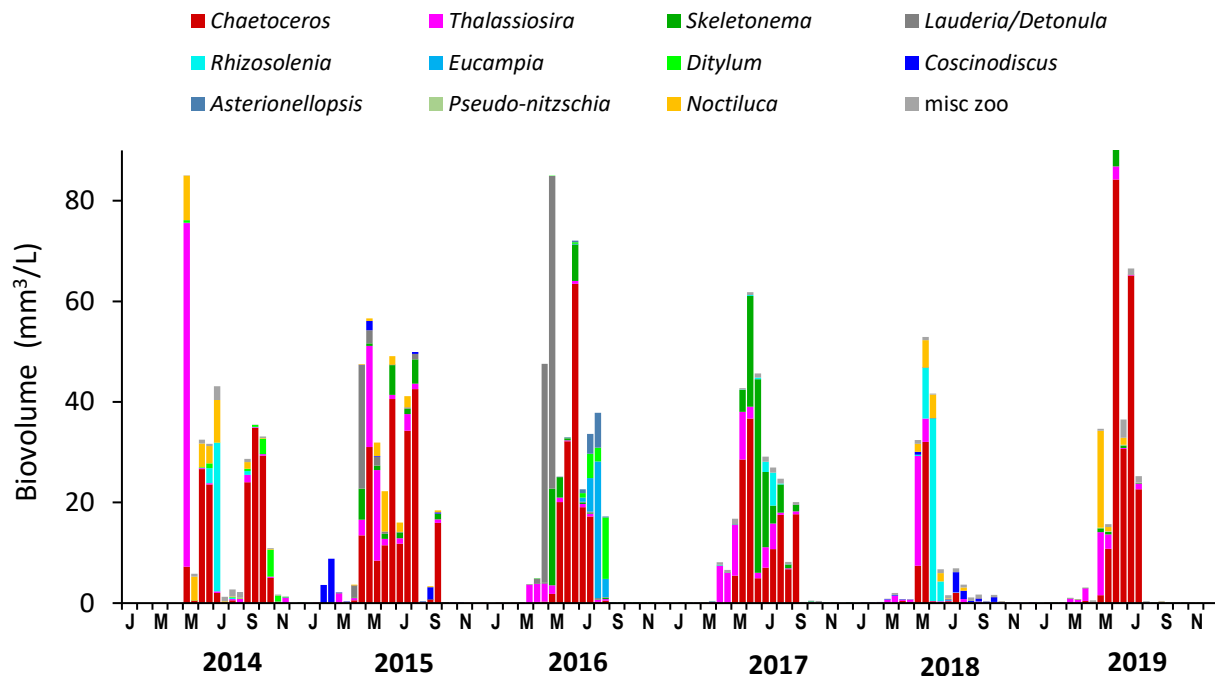


Figure 20. Seasonal succession in mean biovolumes for 6 top taxa (based on biovolume) for each year. Values represent mean biovolume for 7 (2014 - 2015) or 9 (2016 - 2019) Central Basin stations for each sampling event.

4.4 Diatom Biovolume

Diatoms were always the dominant group, and most of the biomass was dominated by just a few genera (Figure 21). The extensive and diverse cosmopolitan genus *Chaetoceros*, locally represented by at least 18 species, contributed on average 49% of the total annual biomass, followed by *Thalassiosira* (14%), *Rhizosolenia* and *Skeletonema* (8%).

Chaetoceros and *Thalassiosira* were the most predictable diatom genera, with recurring blooms every spring and summer (Figure 20 and Figure 22). Other common diatom taxa, while always present, did not form blooms every year and rarely overlapped with each other. Most notably, *Lauderia/Detonula* in 2016, *Skeletonema* in 2017 and *Rhizosolenia* in 2018 (Figure 22). Most of these blooms were recorded throughout the Central Basin albeit differing in intensity between stations. For example, the 2017 *Skeletonema* bloom was largest in mid-June at Pt. Jefferson (KSBP01) and East Passage (NSEX01), and the 2018 *Rhizosolenia* bloom was largest in early June at Pt. Wells (JSUR01), Pt. Jefferson (KSBP01) and East Passage (NSEX01), consistent with the observed geographic pattern in total biovolume discussed below.

Many common diatoms form chains, a morphological adaptation that (along with a large vacuole) allows them to stay afloat as their cells lack flagella. Species of *Chaetoceros* also share the presence of setae – hair-like extensions that further increase their surface area - which might help explain this genus’s success in staying near the water surface. The 2018 shortened bloom season and reduced stratification greatly impacted the *Chaetoceros* population, resulting in overall low annual biovolumes for that year (Figure 21). The *Chaetoceros* population rebounded in 2019, dominating for most of the season in the absence of competing blooms (Figure 21 and Figure 22).

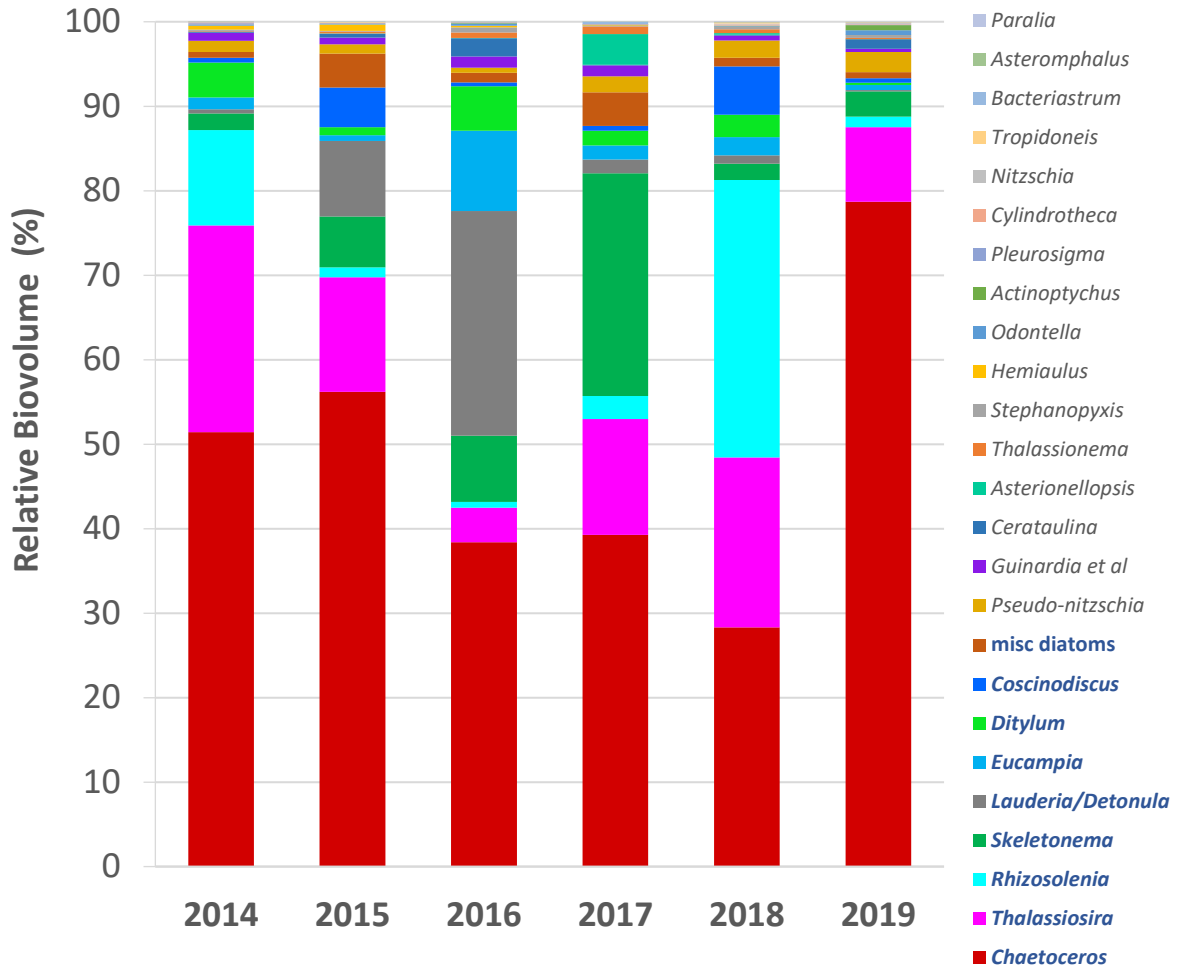


Figure 21. Relative biovolumes of the 25 diatom taxonomic categories. Relative % biovolume based on 7 (2014-2015) or 9 (2016-2019) stations (Dockton excluded). The nine taxa with names shown in blue contribute roughly 90-95% of annual biovolume. Only May-December data available for 2014.

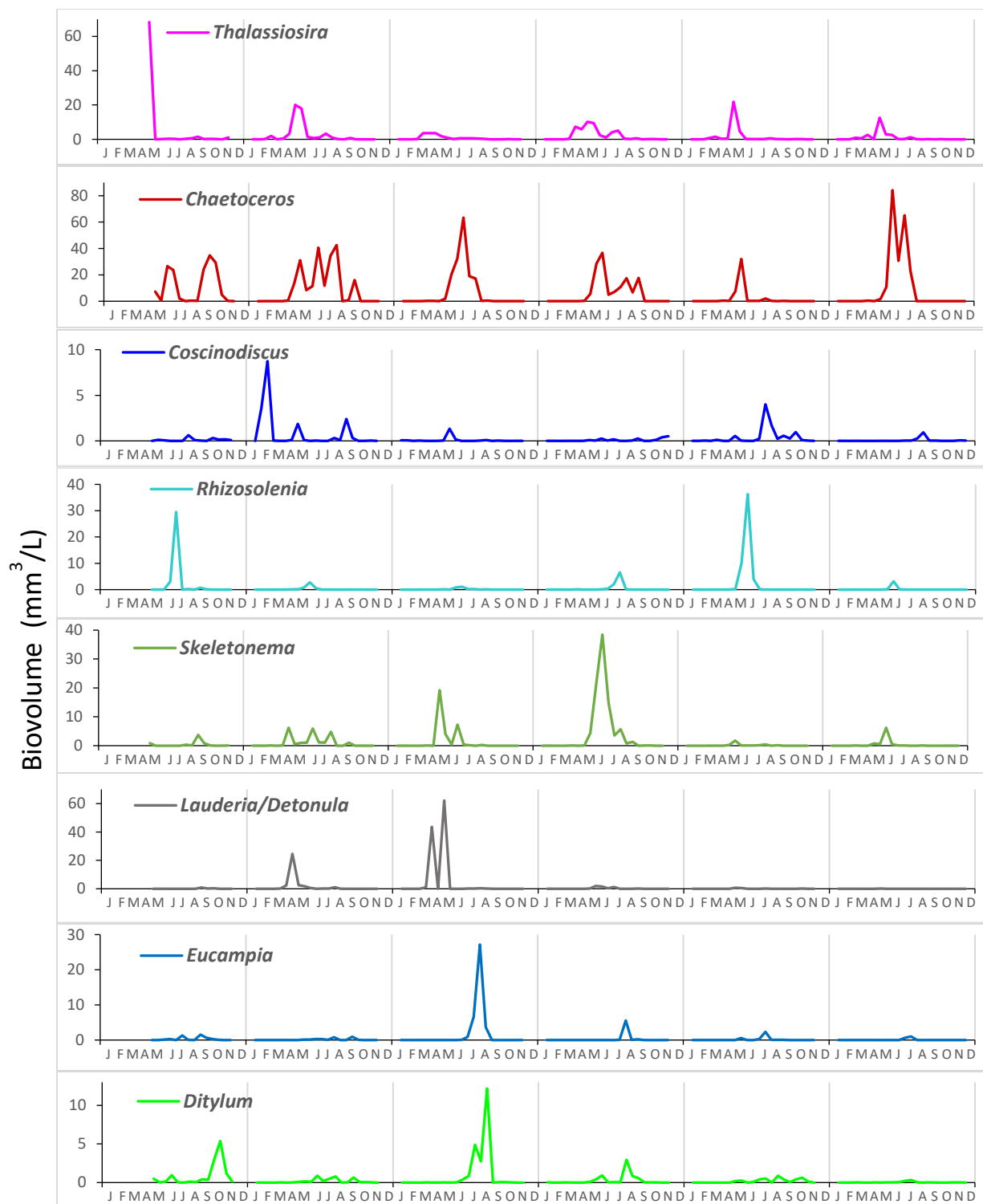


Figure 22. Seasonal and interannual changes in biovolume for 8 top diatom taxa (2014-2019). Values represent mean biovolume for 7 (2014-2015) or 9 (2016-2019) stations (Dockton excluded). Top 8 taxa determined from 6-year biovolume means for each taxon. Note different biovolume scales.

4.5 Flagellate Abundance and Biovolume

Since flagellate cells typically occur singly it is possible to use FlowCAM particle densities to estimate cell abundance (whereas this is largely not appropriate for diatom taxa). Given that flagellates comprise a large range of cell sizes, relative abundance and biovolume patterns are drastically different (Figure 23).

Ceratium (primarily *C. fusus*), gymnodinioid dinoflagellates and *Akashiwo sanguinea* were the largest contributors to flagellate biomass, together making up on average 55% of the total flagellate biovolume (Figure 23, top panel). This is explained by their relatively large size and regular occurrence. On the other hand, small unidentified dinoflagellates and *Heterosigma* were the most abundant flagellate categories (Figure 23, bottom panel), followed by *Prorocentrum* and unidentified gymnodinioid dinoflagellates.

Flagellate proportions did not exhibit large variations from year to year. While some top taxa were more abundant during certain years, the general hierarchical pattern was consistent. There were some differences among stations which can mostly be explained by spatial differences in total biovolume shown in Section 4.1. For example, *Heterosigma* blooms were usually densest at Pt. Wells (JSUR01), Pt. Jefferson (KSBP01) and East Passage (NSE X01) and lightest in Elliott Bay (LTED04).

Several flagellate taxa exhibited similar patterns each year, e.g., *Ceratium* and the two categories that include unidentified dinoflagellates (Figure 24). Small dinoflagellates (<25 µm) were present well into the fall months. Three conspicuous flagellate bloom events occurred during this period:

- A very unusual bloom of large unidentified gymnodinioid cells (e.g., Gyrodinium and Gymnodinium) in spring 2019
- *Prorocentrum* (2 species) in fall 2017
- Unprecedented densities of the harmful raphidophyte *Heterosigma akashiwo* in summer 2019

Brief *Akashiwo sanguinea* blooms were recorded most years. Gymnodinioids are all heterotrophs, whereas *Akashiwo*, *Prorocentrum* and *Heterosigma* are likely mixotrophs.

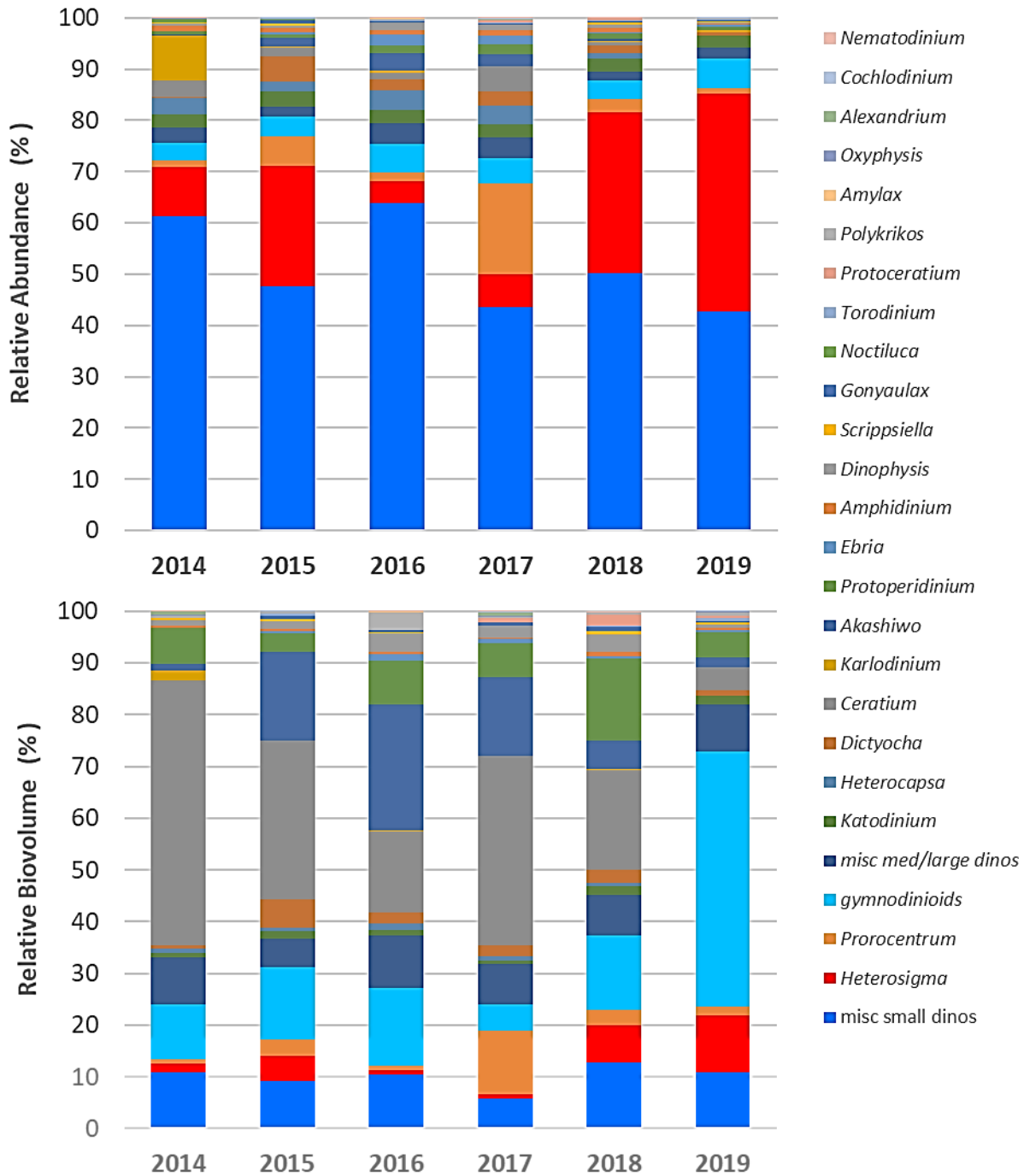


Figure 23. Relative mean abundances (top) and biovolumes (bottom) of 26 flagellate taxonomic categories in mainstem stations by year. Flagellate groups include *Heterosigma*, *Dictyocha*, *Ebria* and all dinoflagellates. *Noctiluca* omitted from relative biovolume calculations. Relative % mean abundance based on mean annual biovolumes for 7 (2014 - 2015) or 9 (2016 - 2019) stations (Dockton excluded).

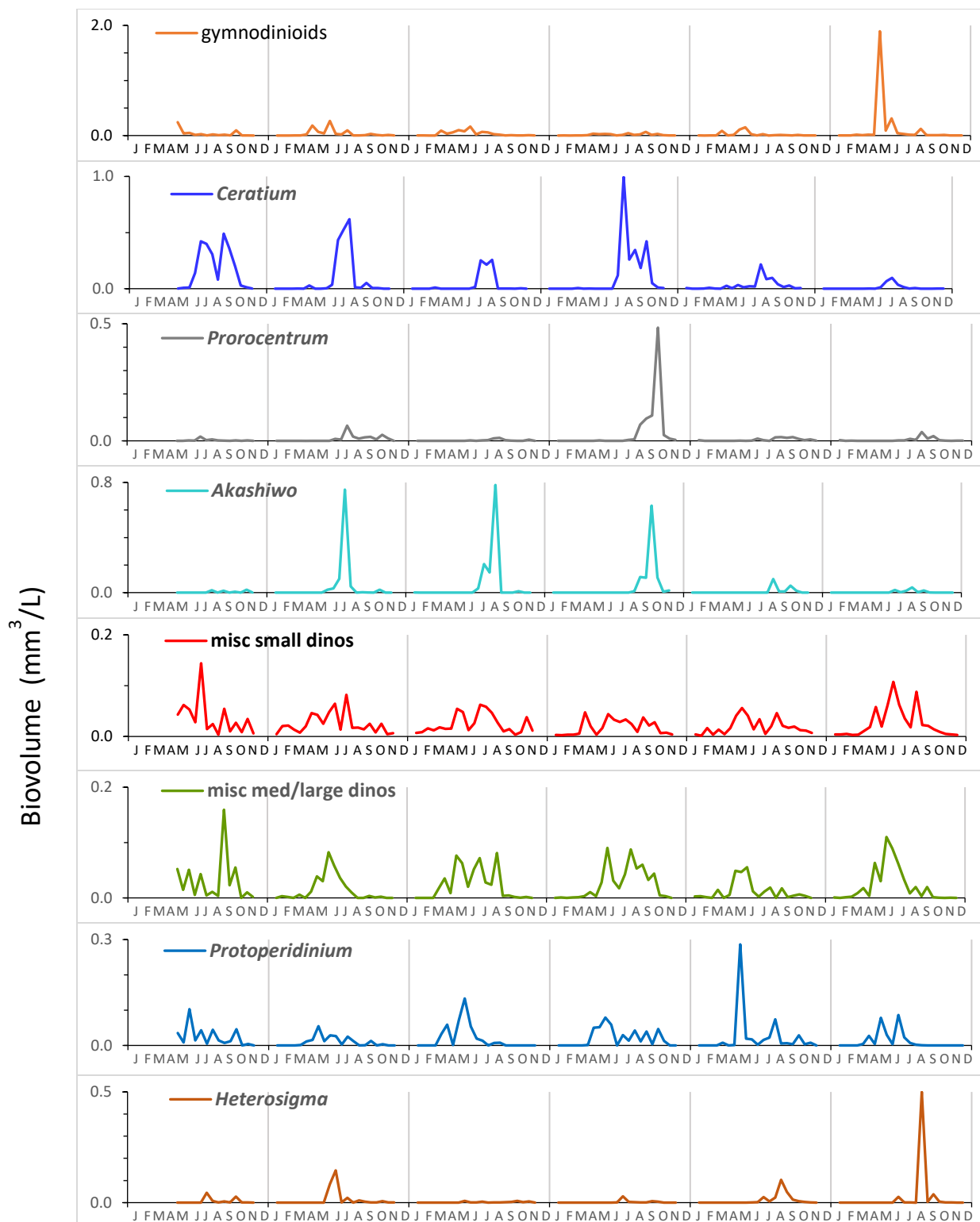


Figure 24. Seasonal and interannual changes in biovolume for 8 top flagellate taxa (2014 – 2019). Values represent mean biovolume for 7 (2014 - 2015) or 9 (2016 - 2019) stations for each sampling event (Dockton excluded). The top 8 taxa were determined from 6-year means for each taxon. Note different biovolume scales.

4.6 *Noctiluca*

The large (200-2000 μm), balloon-shaped phagotrophic dinoflagellate *Noctiluca scintillans* produces visible blooms that can color the water bright red. While not a toxic species, *Noctiluca* blooms are of concern due to their ability to release high concentrations of ammonium, which may be toxic to fish (Horner, 2002). Given that the cells are phagotrophic, the frequency and size of blooms can impact phytoplankton populations and the food web (Pool *et al.*, 2015). To monitor *Noctiluca* densities we record cell abundances using a dissecting microscope in addition to sample analysis using the FlowCAM method which excludes larger cells.

Blooms were observed in spring and/or summer of every year, with a notable drop in bloom size following the 2015 marine heat wave (Figure 25). Cell densities tended to be highest at Pt. Jefferson (KSBP01) and East Passage (NSEX01), but very low in Elliott Bay (LTED04), presumably due to boat traffic (data not shown). Since these cell aggregations can move very quickly with wind and currents, it is important to note that our 2-week sampling interval yields a somewhat incomplete picture of *Noctiluca* blooms in the sampling area.

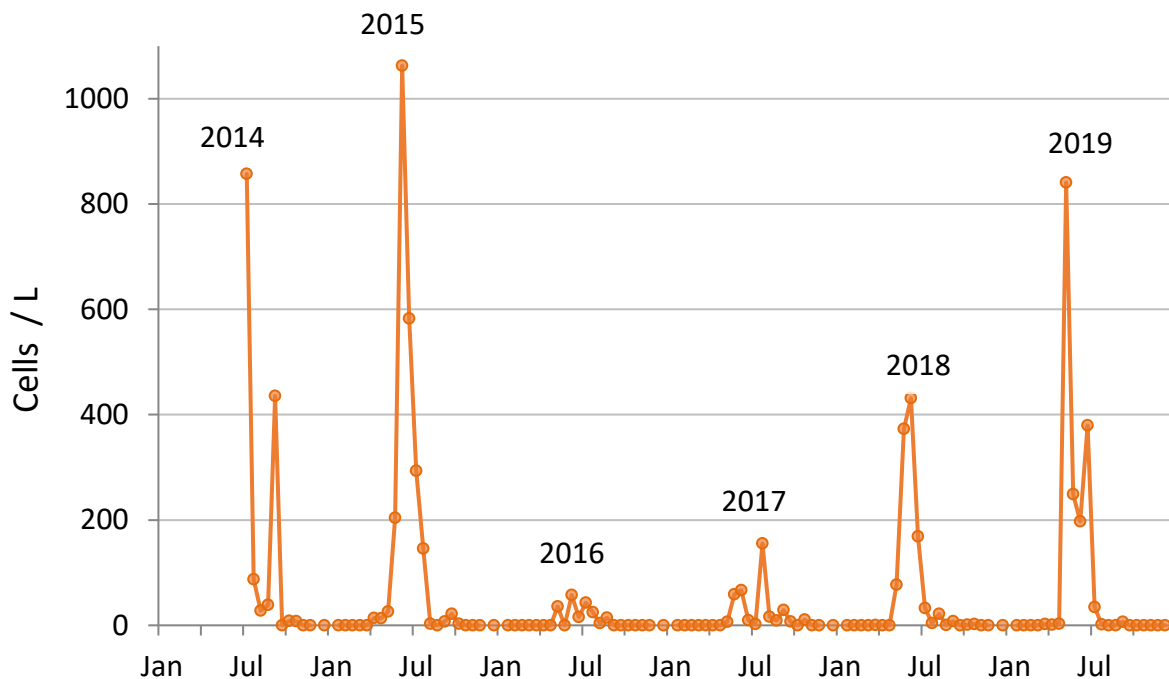


Figure 25. Cell concentrations of the large heterotrophic dinoflagellate *Noctiluca scintillans*. Values plotted represent mean cell concentrations for 7 (2014 - 2015) or 9 (2016 - 2019) stations (Dockton excluded). Both FlowCAM and dissecting microscope data included.

4.7 Community Analysis

Results of community analysis by nMDS indicated a high degree of similarity in community composition between samples (Figure 26, top panel). Season was the factor that had the greatest effect on community composition, as compared with year or locator. There was clear evidence of seasonal separation in community composition, with data points arranged in a temporal sequence within the two-dimensional space (Figure 26, Figure 27). Cluster analysis on seasonal means showed highest similarity between spring and summer (75%) and lowest similarity between summer and winter (47%, Figure 26, bottom panel).

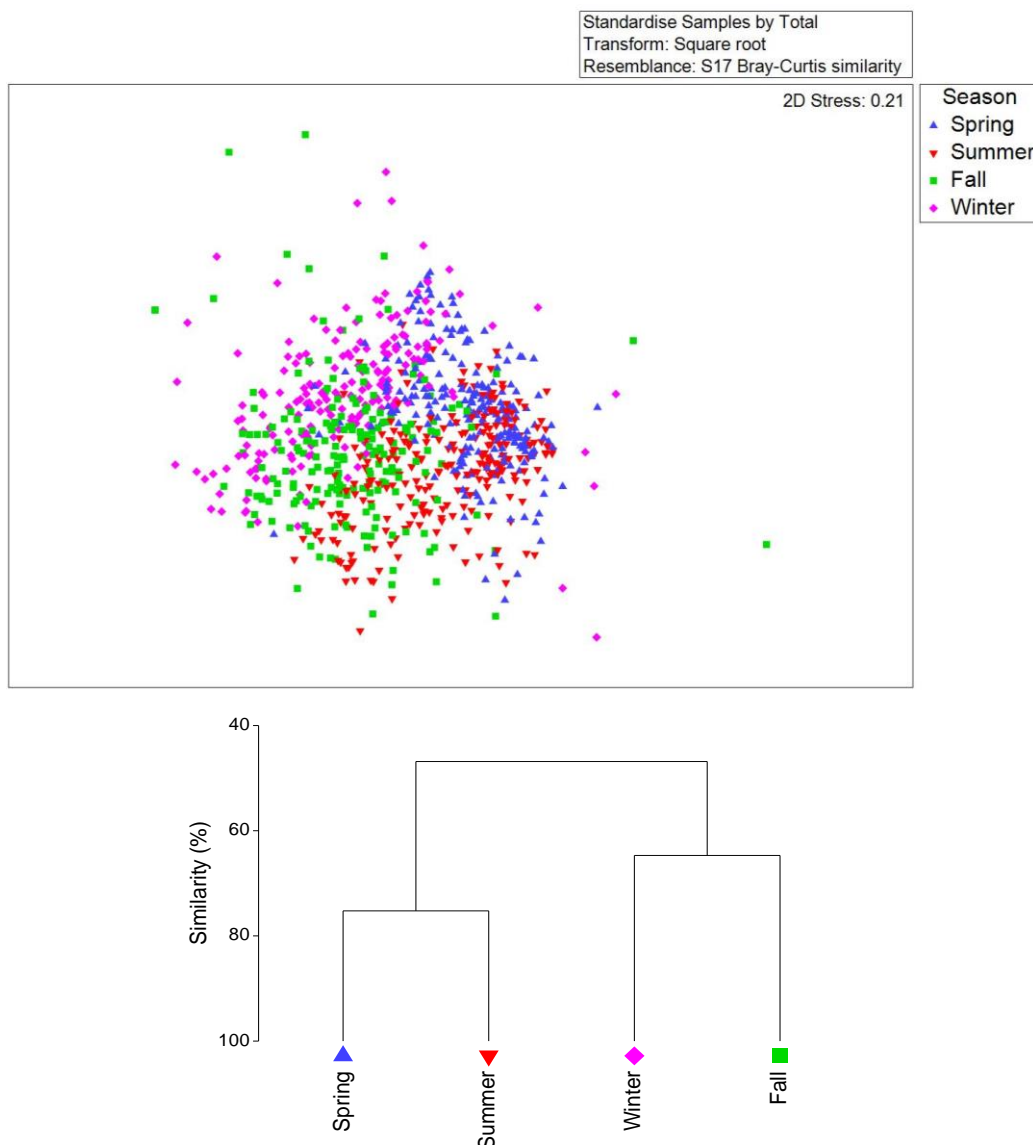


Figure 26. Non-metric multidimensional scaling (nMDS) of microplankton community composition, highlighted by season (top panel), and cluster analysis by season (bottom panel). Analyses based on relative abundances of 54 taxonomic categories at 8 stations sampled 2015 - 2019, n=872 samples. Each symbol in nMDS plot represents one sample. Cluster analysis based on overall mean abundance for each season.

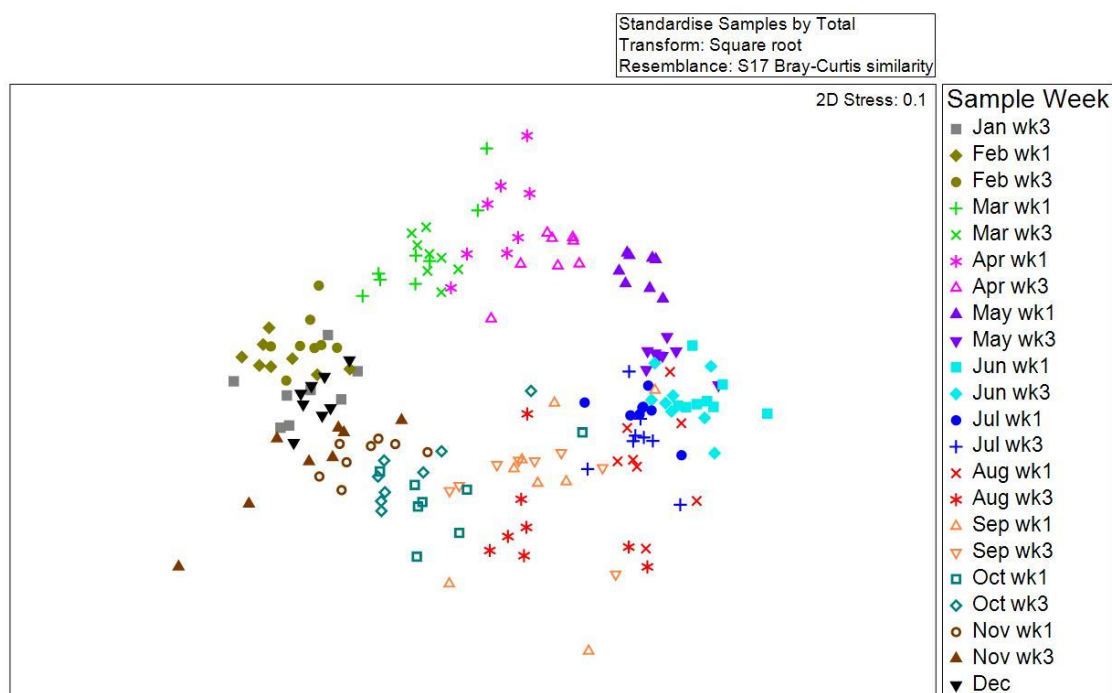


Figure 27. Non-metric multidimensional scaling (nMDS) of microplankton community composition, showing separation by sample week consistent with seasonal succession (clockwise). Analysis based on relative abundance of 54 taxonomic categories at 8 stations sampled 2015 - 2019. Each datapoint represents one station (5-year mean) and sample week.

Further nMDS analyses based on annual total abundance at each station showed a clustering of community composition by year (Figure 28). However, interannual differences were small, with similarities ranging from 74% (2016 and 2019) to 83% (2015 and 2019, the years with highest relative abundance of *Chaetoceros*). These data confirm our observations that year to year changes in taxonomic composition were relatively minor.

Differences in community composition between stations were generally small as well (Figure 28). Six of eight stations monitored since 2015 (JSUR01, KSBP01, KSSK02, LSEP01, LSNT01 and NSEX01) formed a cluster with >90% similarity. Only Elliott Bay (LTED04) and Dockton (NSAJ02) stood apart; this is to be expected given the different physical characteristics of these locations removed from the mainstem Central Basin. Elliott Bay's water quality and circulation are influenced by the Duwamish River, and Dockton has very limited circulation. Elliott Bay also stood out as having the lowest number of taxonomic categories (an indication of species richness) and lower diversity as determined by the Shannon diversity index (Figure 29), which accounts for both species number and evenness. Observed values are within the typical range of 1.5 to 3.5 for this index.

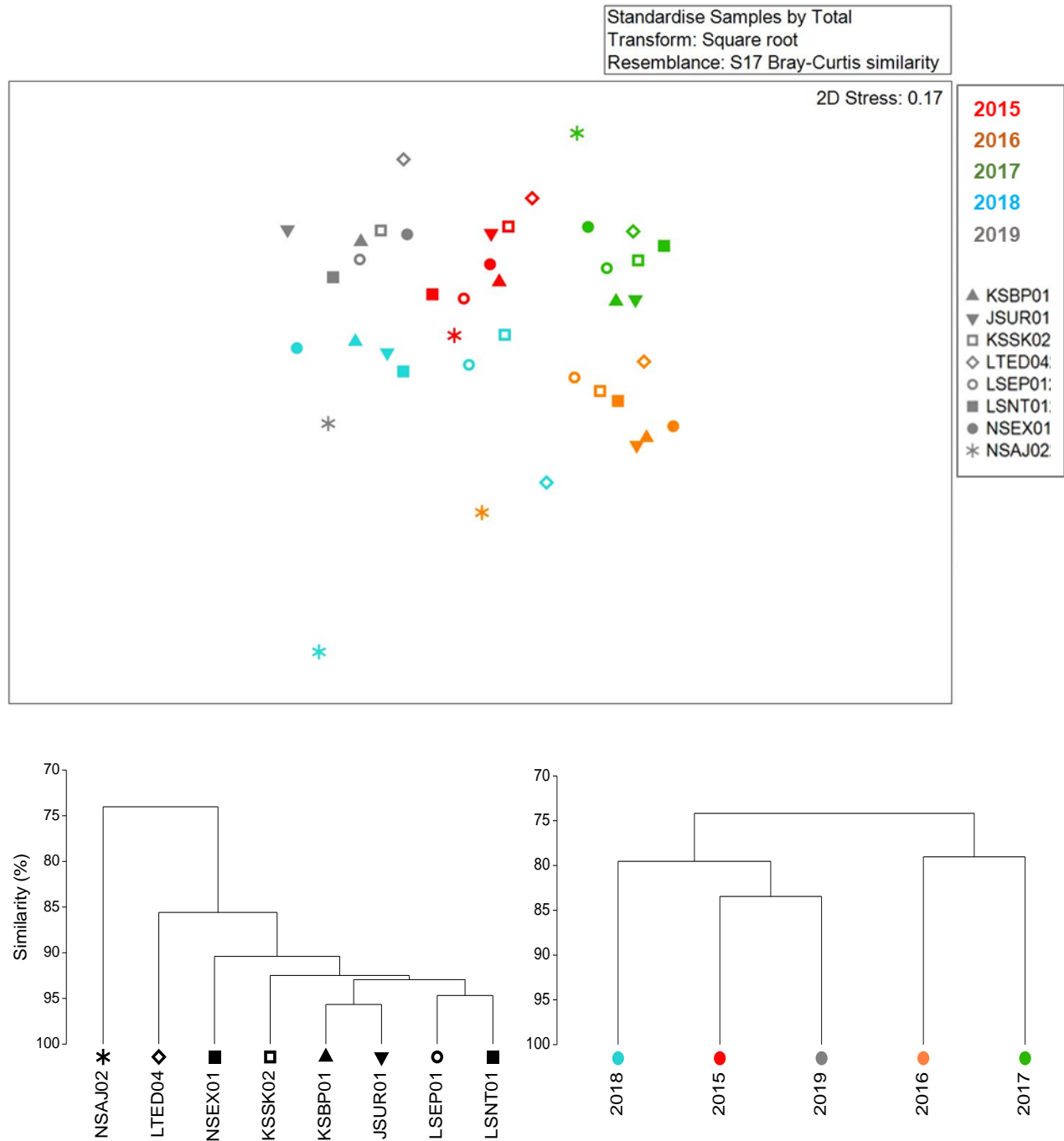


Figure 28. Non-metric multidimensional scaling (nMDS) of microplankton community composition, highlighted by locator and year (top panel), and cluster analyses by locator and year (bottom panels). Analyses based on relative abundances of 54 taxonomic categories at 8 stations sampled 2015 - 2019. Each nMDS datapoint represents annual sum at each station. Cluster analyses based on overall means for each locator and year.

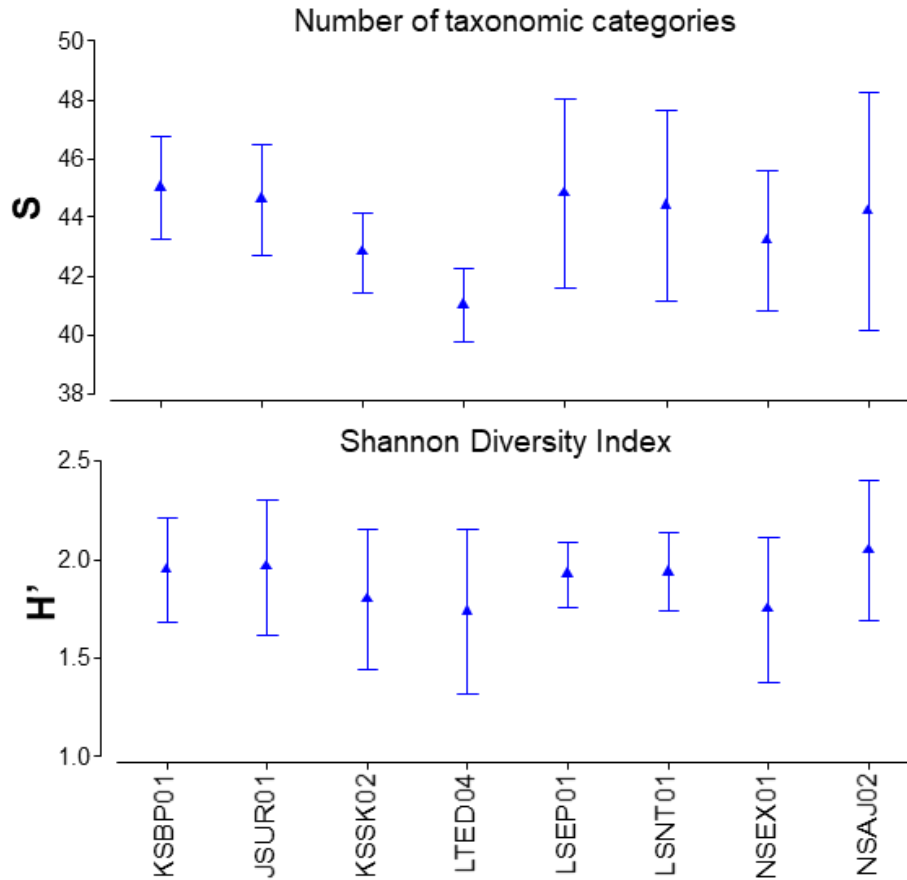


Figure 29. Species richness (as number of taxonomic categories) and Shannon's diversity index at 8 stations sampled 2015 - 2019. Indices calculated from annual sums in abundance of 54 taxonomic categories. 5-year means and standard deviations shown.

4.8 Size Class Distribution

As community composition changes seasonally so does its particle size structure. A preponderance of small particles was present during the fall and winter months, giving way to larger particles in spring and summer (Figure 30). A suite of phytoplankton biochemical functions is controlled by size, such as metabolic rate, growth, nutrient uptake, light absorption and sinking rates, as well as grazing (Cloern, 2018). As such, these seasonal changes in size structure may be of importance for trophic interactions and for explaining community composition in response to nutrient availability, stratification, and mixing.

The smallest size class, 10-25 μm ABD (area-based diameter) contains primarily unidentified, or incompletely identified biological particles, including many flagellate cells. This class was by far the most numerous yet represented a very small proportion of the total biovolume. Single diatom cells and most dinoflagellates fall into the 25-100 μm size class, whereas large diatom chains characteristic of spring and summer blooms typically

fall into the 100-300 μm size class (or larger). The latter class, while very low in abundance, contributed a significant portion of the total biovolume nearly year-round.

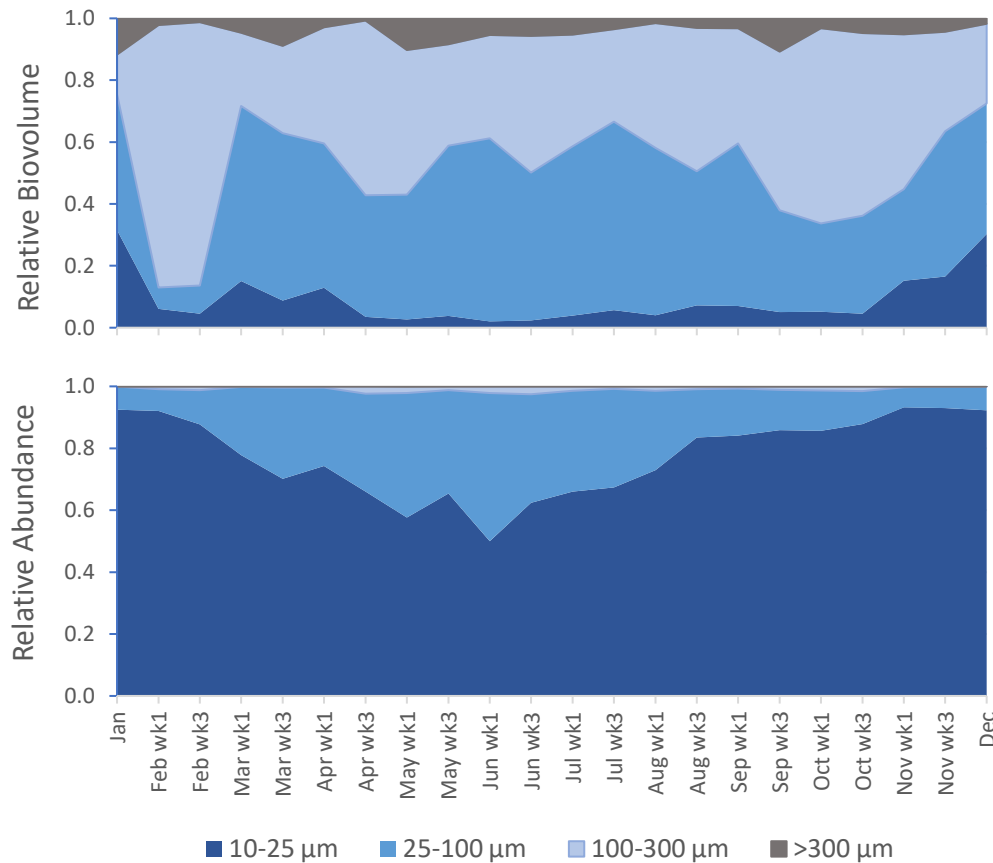


Figure 30. Seasonal changes in particle size structure quantified for 7 (2014 - 2015) or 9 (2016 - 2019) stations, expressed as relative biovolume (top panel) and relative abundance (bottom panel). Class sizes refer to area-based diameters (ABD). While most particles $>300 \mu\text{m}$ are filtered out during sample preparation, a small portion fall into a $>300 \mu\text{m}$ category as measured by the software.

4.9 Trends by Mode of Nutrition

As mentioned above, diatoms - which are entirely autotrophic - were the dominant component of the microplankton throughout all seasons in the Central Basin (Figure 31). Colorless flagellates, while often considered part of the phytoplankton community, are heterotrophic and therefore belong to a higher trophic level along with the microzooplankton. On the other hand, many flagellates that contain photosynthetic pigments (dinoflagellates in particular) have been shown to have a mixed mode of nutrition; it is for that reason that mixotrophy has been assumed for all colored flagellates in the present dataset. The seasonality of these groups indicates that while there was an increase in absolute numbers of mixotrophs and heterotrophs during spring and summer,

their relative proportion within the microplankton community was highest during winter and fall when diatoms declined significantly (Figure 31).

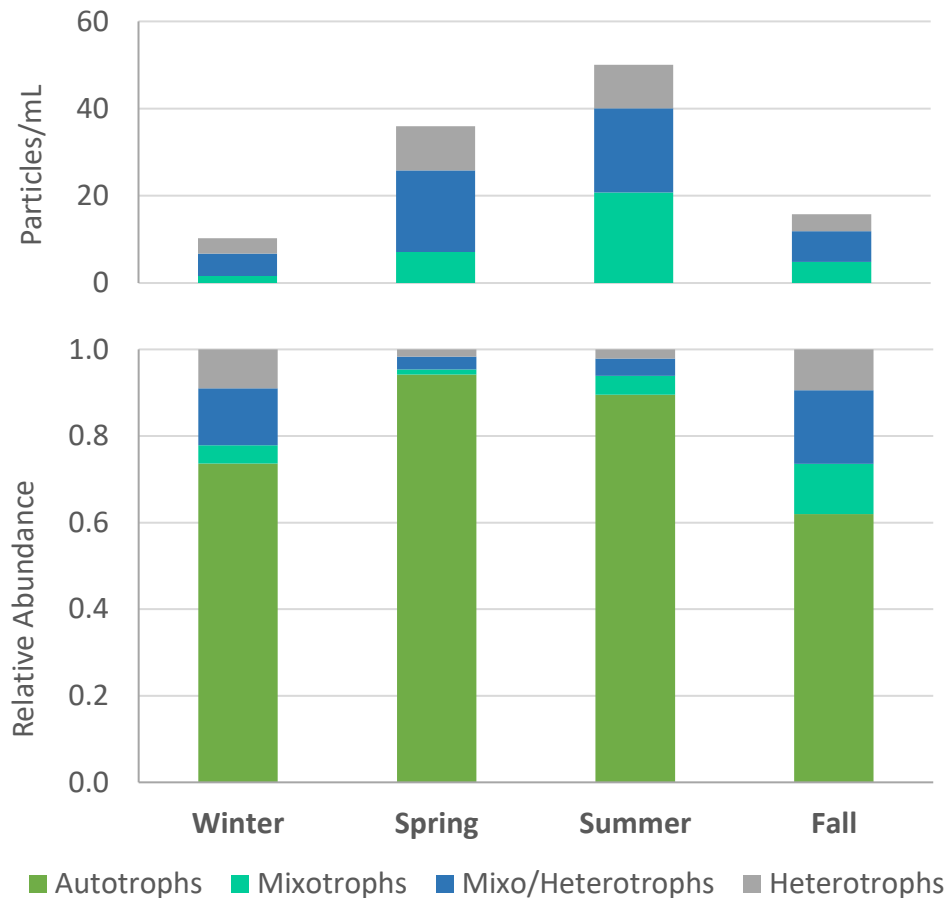


Figure 31. Abundance of autotrophic, mixotrophic and heterotrophic microplankton. Abundance means of 7 (2015) or 9 (2016 - 2019) stations (Dockton excluded), expressed as particle concentration (autotrophs excluded) and as relative particle abundance. Mixo/heterotrophs consist of unidentified dinoflagellates; other unidentified particles excluded. Note that abundance is determined from particle numbers, which are not representative of cell numbers for colonial diatoms (autotrophs).

4.10 Microzooplankton

FlowCAM images of microzooplankton are separated into three categories: The common red colored ciliate *Mesodinium rubrum*, all other ciliates (mostly in 10-100 μm range), and all other non-ciliate organisms, consisting primarily of larval plankton. Copepod nauplii are a dominant component of the latter group.

Mesodinium abundance changed very little throughout the seasons (Figure 32). These ciliates favor cryptomonads, which contain red pigments, in their diet; cryptomonads are observed year-round in microscope samples. Abundances of all other microzooplankton

were much higher in spring and summer than in winter and fall. Inter-annual differences in microzooplankton abundance were generally small, except for a large increase in 2018, notably a year characterized by low chlorophyll and low phytoplankton biomass.

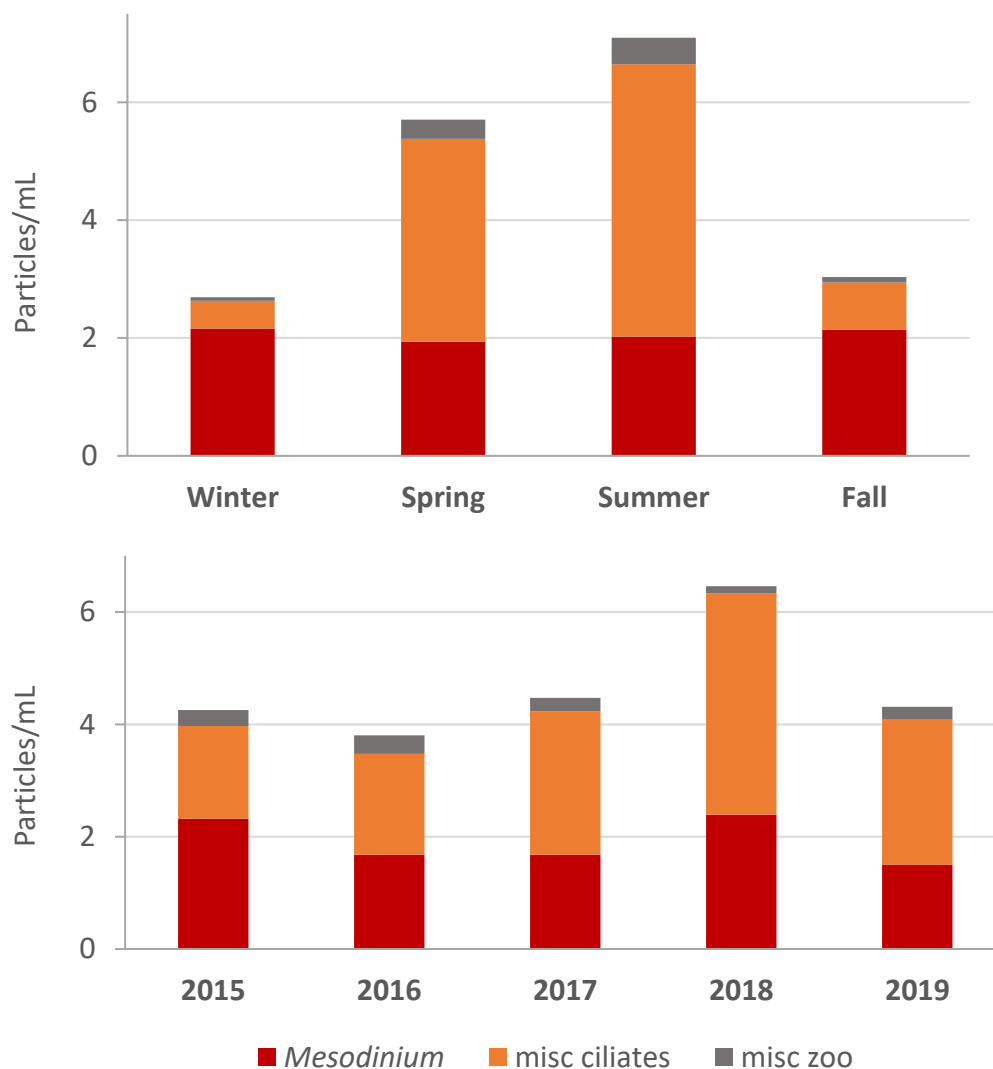


Figure 32. Abundance of ciliates and other microzooplankton. Mean particles/ml for 7 (2015) or 9 (2016-2019) stations, pooled by season (top panel) and year (bottom panel). *Mesodinium rubrum* is a common, pigmented ciliate.

4.11 Cumulative Biovolume

Total annual biovolumes, or cumulative biovolumes ($\text{mm}^3/\text{L} \times \text{d}$), were calculated for each station by linear interpolation between sample dates, and correspond to the grey area in Figure 14. They include all biological particles in the 10-300 μm range. Cumulative

biovolume is an informative metric for assessing spatial and inter-annual patterns in standing stock (Figure 33).

Cumulative biovolumes remained consistent from 2015 - 2017 but in 2018 fell to <50% of levels seen in previous years due to an unusually short growth season (see Figure 15). Values increased again in 2019 (also a short growth season year) yet remained low relative to the first three years of the monitoring period. The highest biovolumes were consistently observed at the southern stations (East Passage and Dockton) while the lowest were seen at the central stations (Elliott Bay, South Plant, Alki and Pt. Williams). These differences are most likely related to the different degrees of mixing among these sites, which arise from differences in wind stress and circulation patterns.

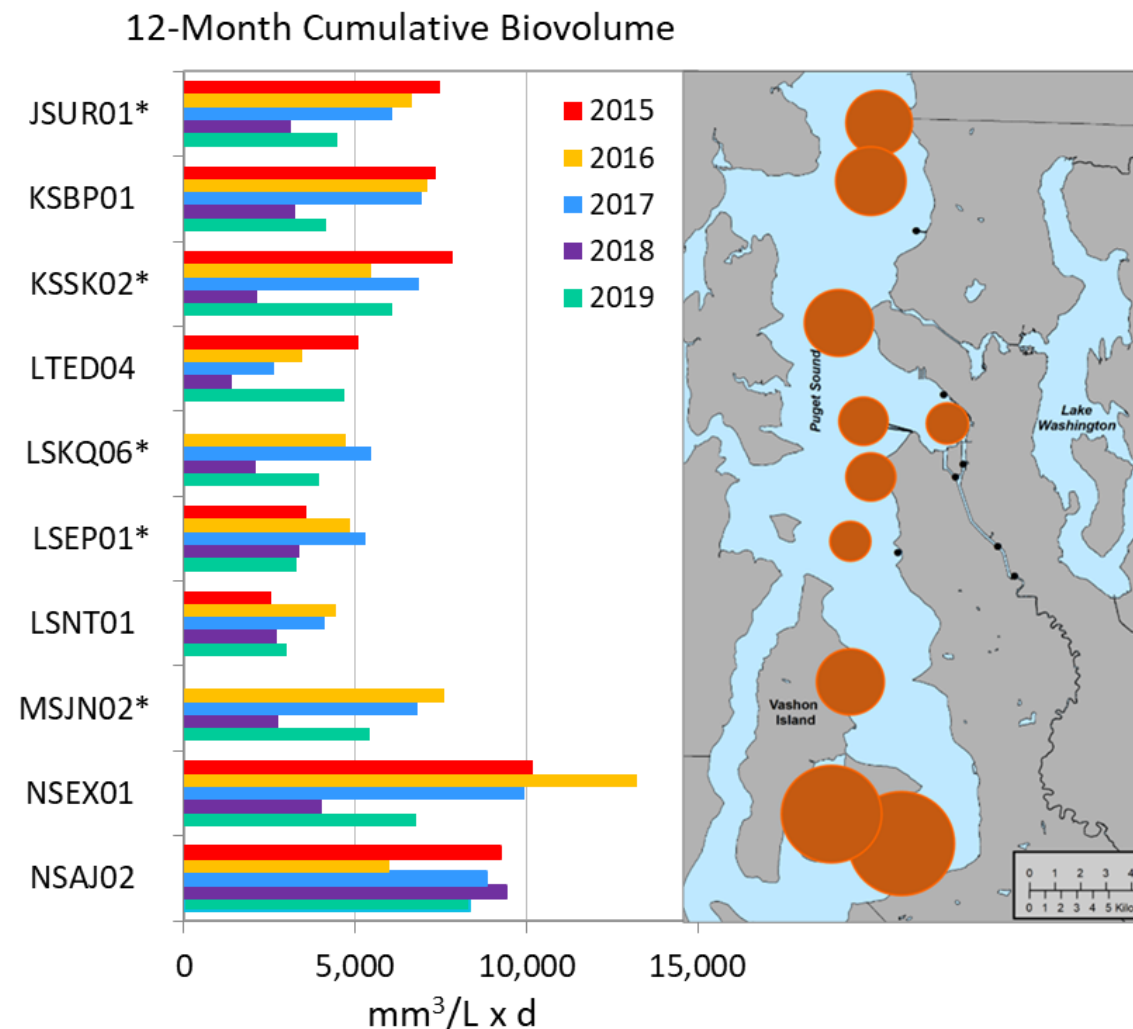


Figure 33. Twelve-month cumulative phytoplankton biovolumes by station and year (left panel) and geographic distribution (right panel). Bubble diameters represent mean cumulative biovolume for all years (2015 - 2019), ranging from 3361 at LSNT01 to 8347 ($\text{mm}^3/\text{L}) \times \text{d}$ at NSAJ02. Biovolumes include all biological particles in 10-300 μm range. *Outfall station.

4.12 Chlorophyll-*a* and Biovolume

The relationship between chlorophyll-*a* and biovolume is best described as a power function (Figure 34). The biovolumes included in this analysis consist primarily of pigmented cells, i.e., autotrophic, mixotrophic and a small category of miscellaneous unidentified dinoflagellates (a mix of mixotrophic and heterotrophic); of which diatoms are by far the largest contributors of pigmented cells in terms of biovolume (97% of total).

This chlorophyll-*a* vs. biovolume relationship tells us that the chlorophyll-*a*/biovolume ratio decreases as phytoplankton biovolume increases, indicating a seasonal shift that may be related to the seasonal changes in taxonomic composition (as larger cells tend to have lower chlorophyll densities), and possibly also to light-induced seasonal changes in the chlorophyll-*a* content of cells (Figure 35). For biovolumes in the 0.5-100 mm³/L range (~ 1.5-21 mg Chl-*a*/L), predicted chlorophyll-*a* content per unit cell volume ranges from 0.21 to 3.07 µg/mm³. These values are somewhat lower than ranges reported by Philips *et al.* (1999) for Florida Bay (1.4-7.7 µg/mm³) and Tolstoy (1979, in Hoyer *et al.* 2002) for four marine systems (1.9-6.3 µg/mm³).

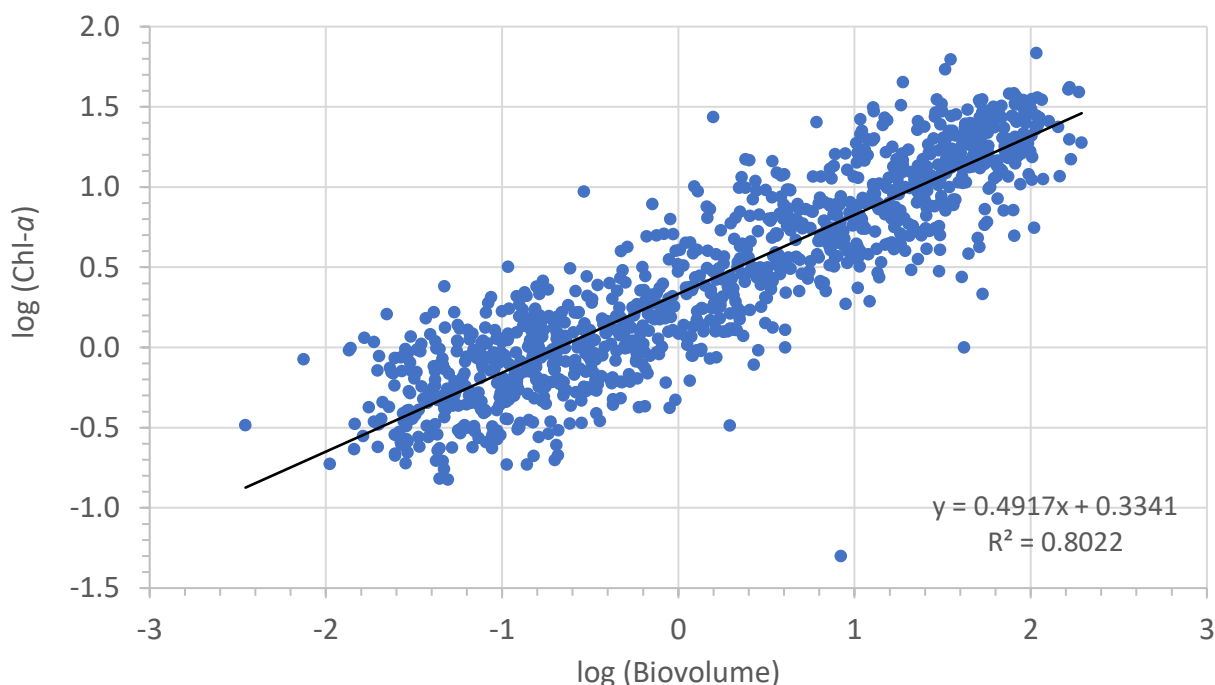


Figure 34. Relationship between chlorophyll-*a* (µg/L) and biovolume (mm³/L) for surface data collected at all stations (2014 - 2019) (*n* = 1116). Biovolumes include only autotrophic and mixotrophic taxa. The strong log-log linearity indicates a power relationship, where $\text{Chl-}a = 2.1582 (\text{Biovolume})^{0.4917}$.

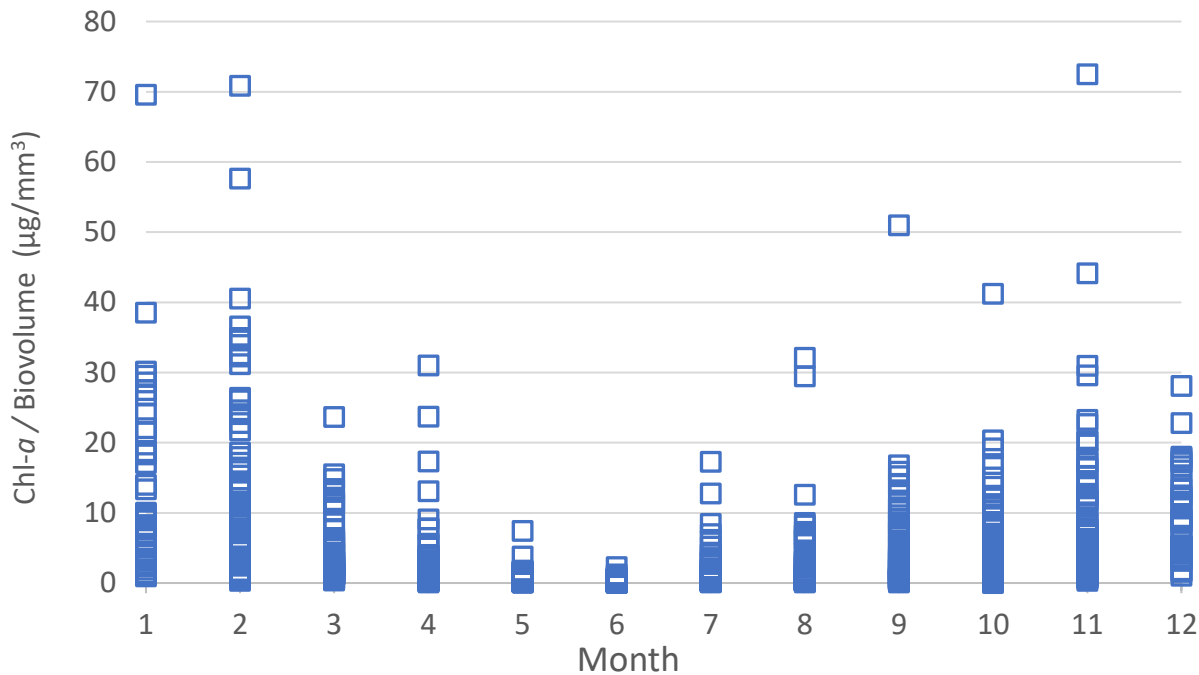


Figure 35. Seasonal changes in chlorophyll-*a* to biovolume ratio for surface data (2014 - 2019) at all stations ($n = 1112$). Biovolumes include autotrophic and mixotrophic taxa. Note that 89% of values are $\leq 10 \mu\text{g}/\text{mm}^3$ and large ratios correspond to very small biovolumes which have low analytical accuracy.

4.13 Dockton: Growth and Species Composition

Conditions at Dockton (NSAJ02), located at the entrance to Quartermaster Harbor, are markedly different than at other stations. As an enclosed, shallow bay with poor flushing it experiences strong seasonal stratification and elevated spring surface temperatures, conditions that favor early phytoplankton growth when nutrients from spring freshwater runoff are plentiful. From May to August (2014-2019) surface temperatures were 3-4 °C higher than at other monitoring stations (Figure 36). During the spring bloom nutrients become depleted but are then replenished in late summer. As shallow surface waters stay warmer longer, these favorable conditions prolong phytoplankton growth into late September.

FlowCAM data indicate that seasonal biovolume patterns were more variable at Dockton than at other stations, with growth usually extending later into the fall months (Figure 14). Cumulative biovolumes indicated high total annual biomass at Dockton, comparable to values observed at East Passage (NSEX01, Figure 33). The great majority of this biomass was produced in spring and summer and primarily comprised of a few genera (Figure 37). Species of *Chaetoceros* contributed 39% of the total annual biomass, followed by *Rhizosolenia* (11%) and *Thalassiosira* (5%). As elsewhere, *Thalassiosira* usually initiated the spring bloom and was followed by extensive growth of *Chaetoceros* species throughout

the summer (Figure 38). The harmful algal bloom (HAB) species *Heterosigma akashiwo* and *Akashiwo sanguinea*, as well as *Ceratium fusus*, are common flagellates at this site (Figure 38). Especially large flagellate blooms occurred in some years (e.g., *Heterosigma* in 2014 or *Akashiwo* on 2019) but conditions that lead to these events are difficult to discern.

Recurrent blooms of the toxic dinoflagellate *Alexandrium catenella* have been reported by others in this bay and bottom surveys have revealed unusually high concentrations of cysts in surface sediments (Greengrove *et al.*, 2018) but these cells were rarely observed in our samples.

Unlike open water stations, Dockton did not experience a sharp drop in biomass during 2018 even though *Chaetoceros* biomass was also unusually low that year (Figure 37). Instead, a very large spring bloom of *Rhizosolenia* occurred that continued until early July, followed by a large bloom of *Ceratium* from August to October. Dockton's lowest biomass year was 2016, a year with very high temperatures that started earlier than usual at this site (Figure 36).

Analysis of community composition showed no differences in species richness (evaluated using the number of FlowCAM taxonomic categories) between Dockton and open water stations but slightly higher diversity (Figure 29). Analyses also showed ~74% similarity in taxonomic composition between Dockton and open water stations (Figure 28), substantially lower than the >90% similarity amongst those open water stations. These dissimilarities point to the higher proportions of mixotrophs and heterotrophs at Dockton (Figure 39 and Figure 40).

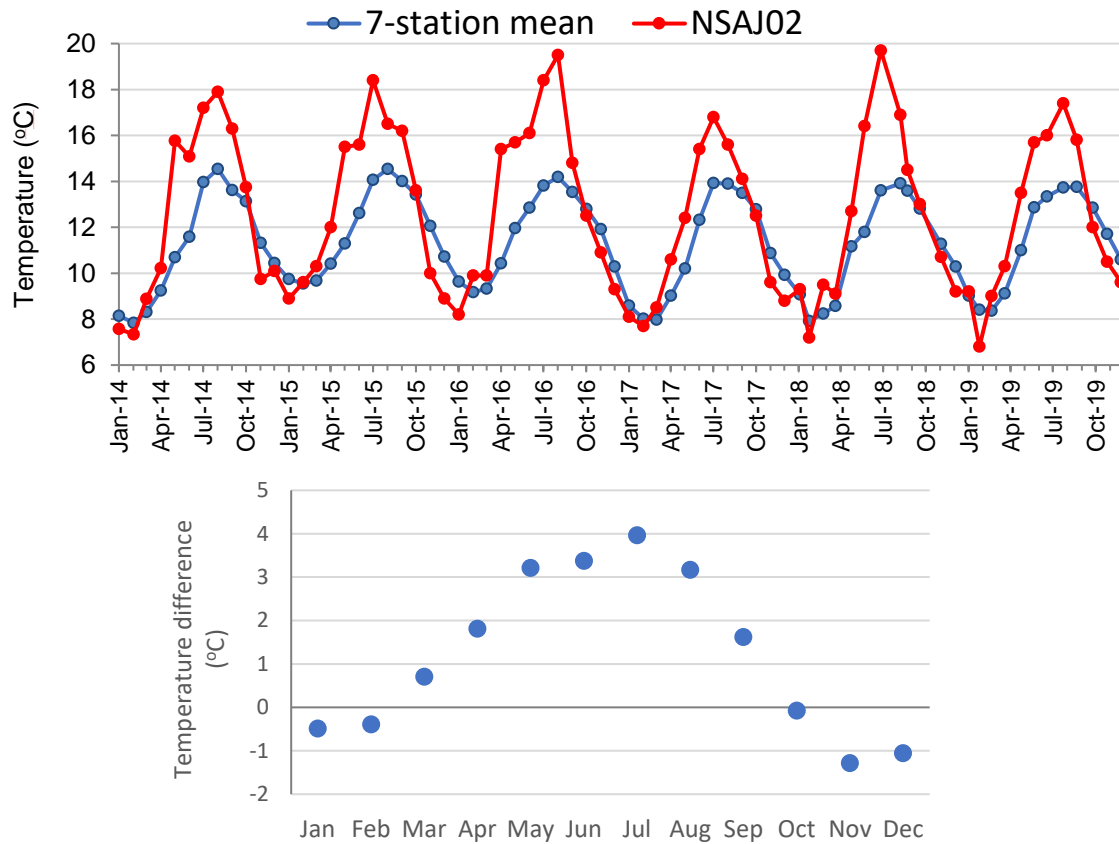


Figure 36. Monthly surface temperatures (<2 m) at Dockton (NSAJ02) (2014 - 2019). Top panel: Comparison of Dockton with mean temperature (2014 - 2019) for 7 mainstem stations. Bottom panel: Difference in temperature by month between Dockton and the 7 mainstem stations.

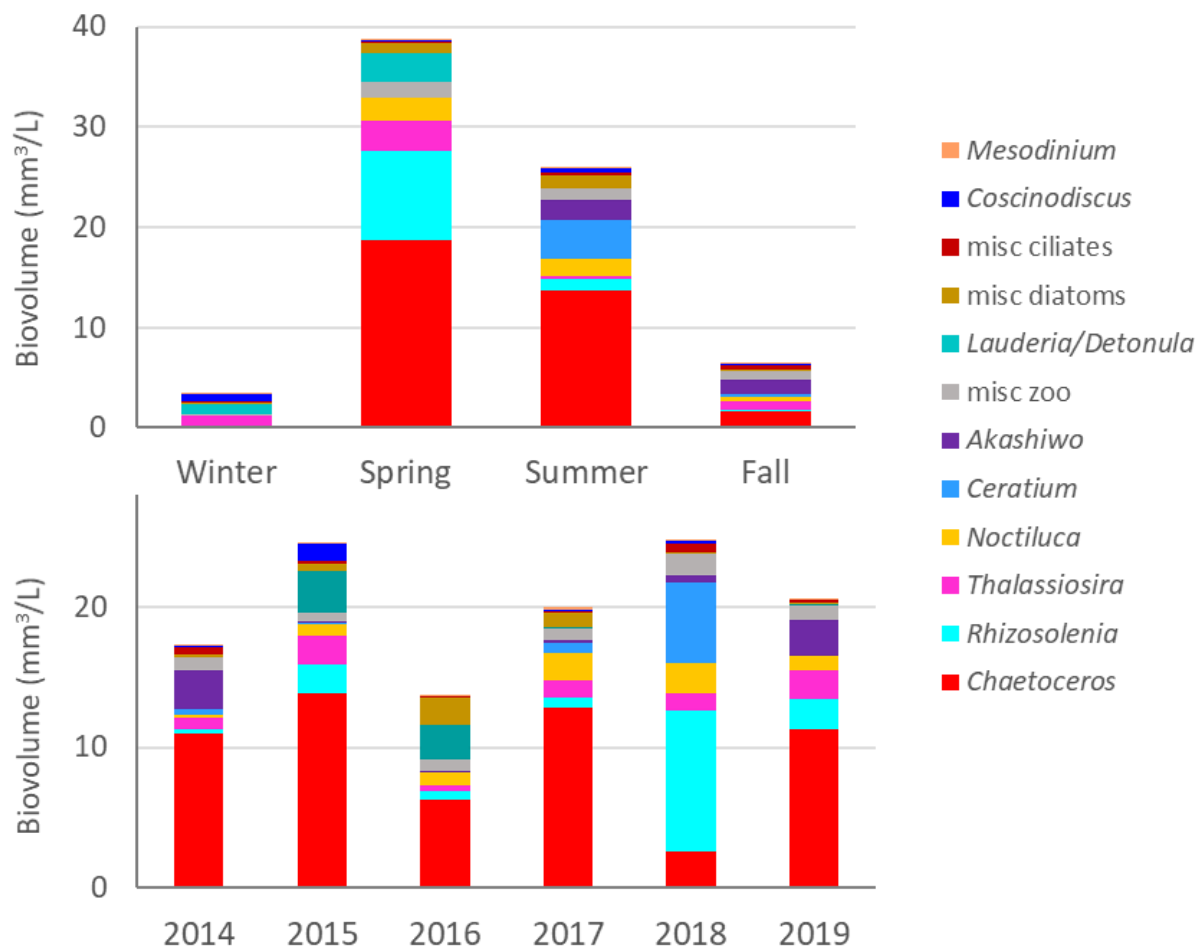


Figure 37. Biovolumes of top 12 taxonomic categories at Dockton (NSAJ02) (2014 - 2019). Mean biovolume by season (top panel) and year (bottom panel). Note different biovolume scales.

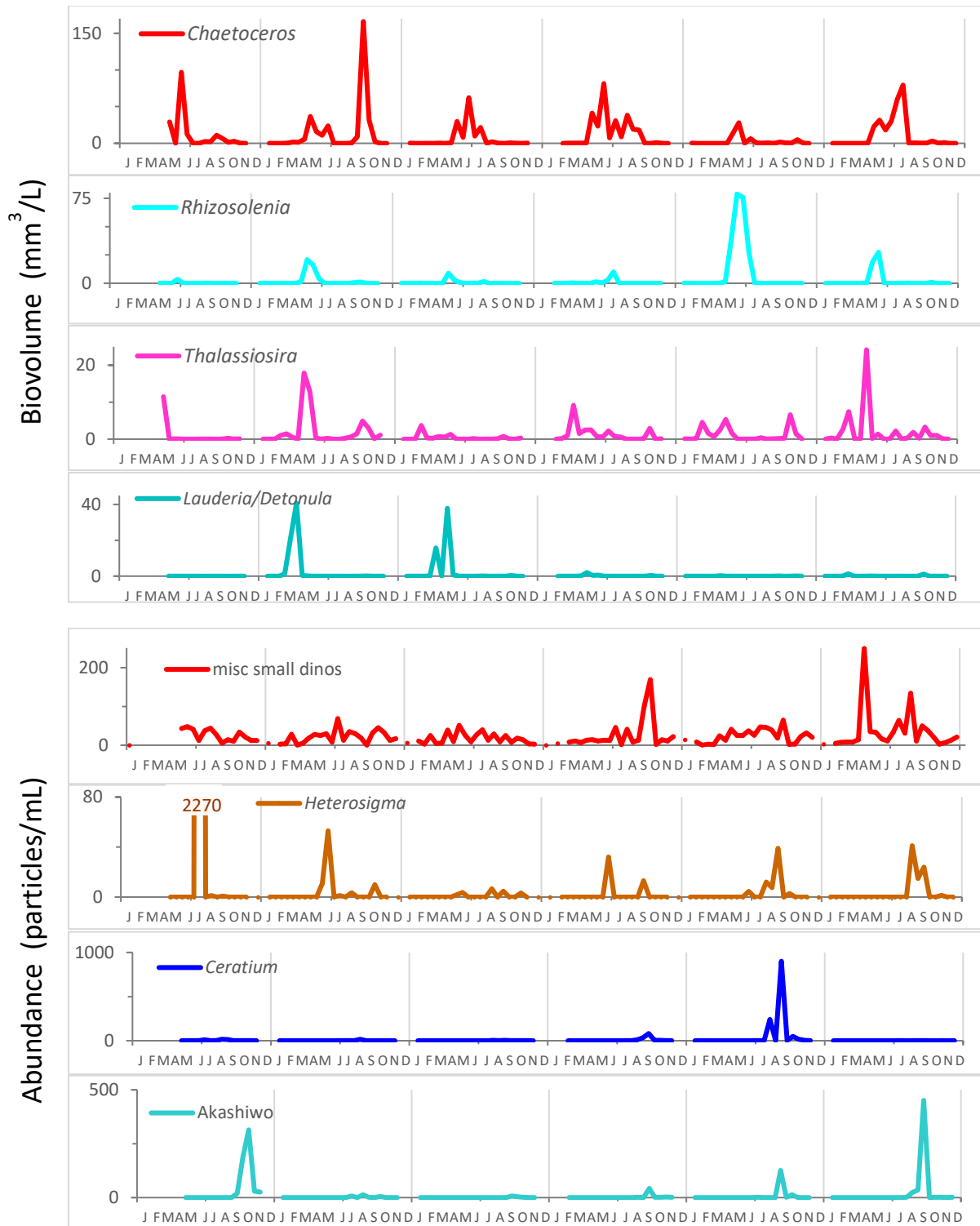


Figure 38. Seasonal and interannual changes in biovolume for 4 top diatoms (top panels) and abundance for 4 top flagellate taxa (bottom panels) at Dockton. Abundance concentrations represent single observations for each sampling event. Top taxa determined from 6-year abundance means for each taxonomic group. Note different abundance and biovolume scales.

4.14 Dockton: Trends by Mode of Nutrition

At Dockton, diatoms dominated the microplankton community throughout the seasons, not unlike other stations (Figure 39). Total abundances were higher than at other stations throughout the year, especially during summer and fall (Figure 39, bottom panel) and reflect the extended growth season at this site relative to deeper stations. Mixotrophs (i.e., pigmented flagellates) were particularly abundant during these months, with summer values reaching close to 8 times those observed at other stations. Heterotrophs were generally highest in fall, averaging four times the numbers observed at other stations.

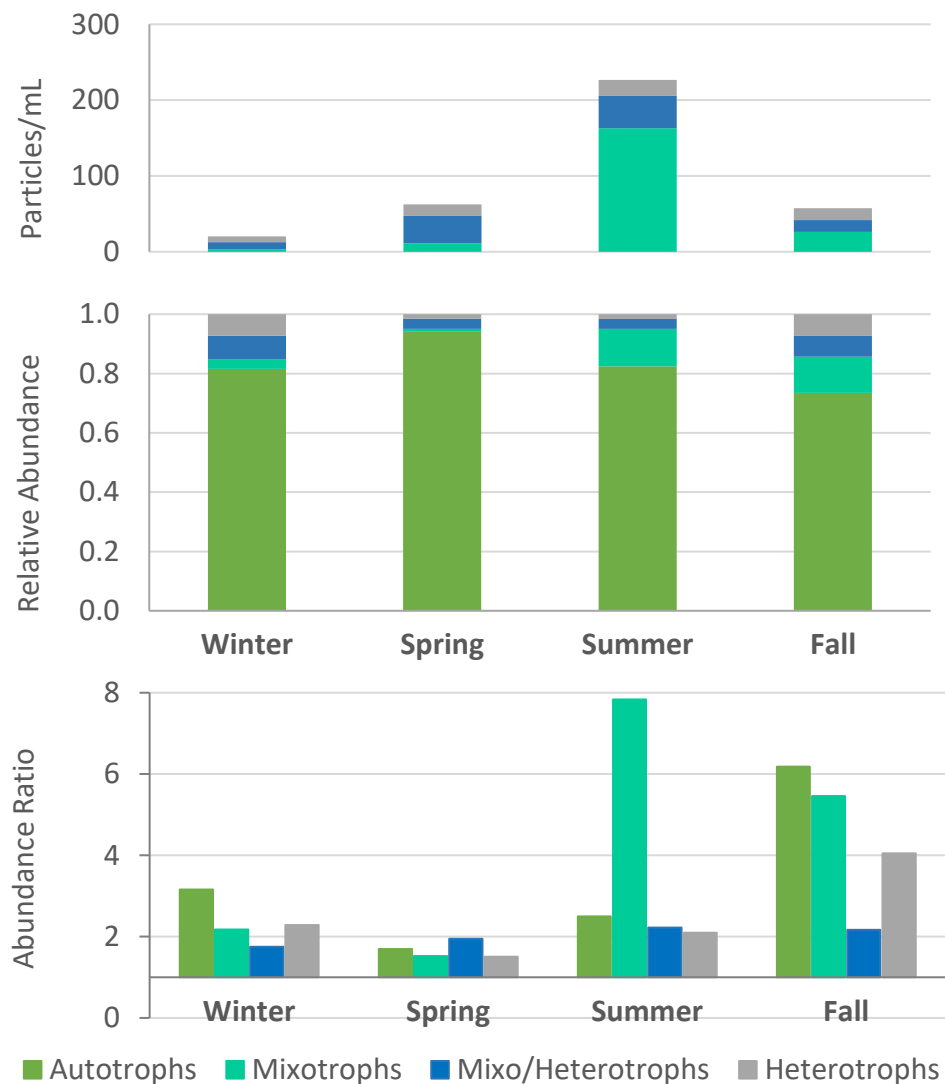


Figure 39. Abundances (top panel) and proportions (center panel) of autotrophic, mixotrophic and heterotrophic microplankton at Dockton. Bottom panel: Abundance ratios for Dockton compared to all other stations (Figure 31). Values in top and middle panels represent five-year mean abundance (2015 - 2019) by season (autotrophs omitted in upper panel). Values in bottom panel calculated as ratio of abundances at Dockton (shown here) to abundances at all other stations.

4.15 Dockton: Microzooplankton

Ciliates were most abundant during spring and summer at Dockton yet declined very little during fall and winter; abundances during these months were almost 7 times those observed at other stations (Figure 40). *Mesodinium* abundance, on the other hand, was highest in fall but then declined in winter. Overall, microzooplankton remained abundant through the fall, in sharp contrast with the seasonal pattern typically observed at other stations (Figure 31).

Inter-annual comparisons in microzooplankton abundance indicate moderate differences between years (Figure 40). *Mesodinium* populations increased in 2016 and 2017 relative to other years and stations; this was followed by an increase in miscellaneous ciliates in 2018.

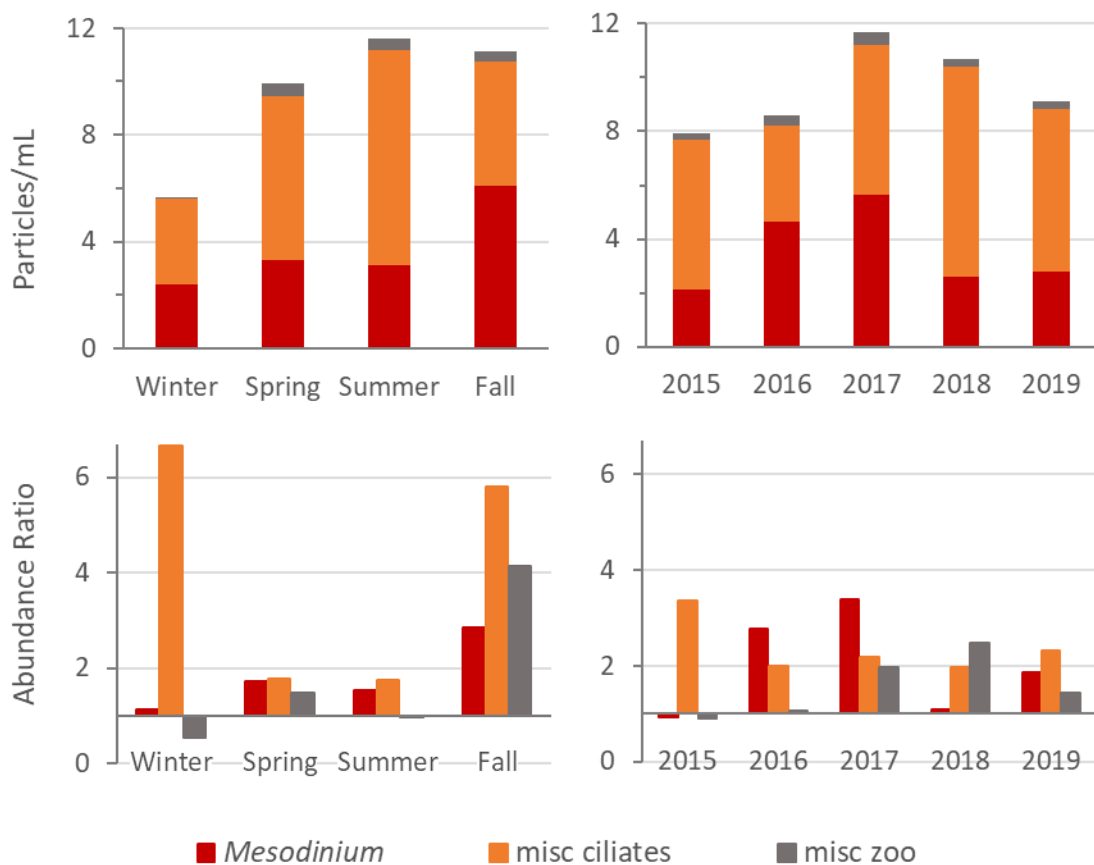


Figure 40. Abundance of ciliates and other microzooplankton at Dockton (NSAJ02). Top panels: Mean abundance by season and year. Bottom panels: Abundance ratios for Dockton compared to other stations (Figure 32). *Mesodinium rubrum* is a common, pigmented ciliate.

5.0 POC STUDY RESULTS

Results from this study were used to describe the relationships between FlowCAM-determined biovolume and POC and PON concentrations, and to evaluate if these relationships can be used as a predictive tool for Central Basin phytoplankton samples.

5.1 Data Overview

Raw POC and PON results for the 200 samples analyzed are presented in Appendix B (Tables B-1 and B-2) and include microplankton biovolume data generated concurrently as part of the phytoplankton component of the Marine Monitoring Program. Biovolumes were determined with the FlowCAM imaging particle analyzer using an area-based diameter (ABD) formula (KCEL, 2016a), regardless of cell shape. Quality control results are presented in Tables B-4 to B-6.

Results from this study were used to describe the relationships between FlowCAM-determined biovolume and POC and PON concentrations, and to evaluate if these relationships can be used as a predictive tool for Central Basin phytoplankton samples.

Seasonal changes in biovolume for the major taxonomic groups during the study period (2015 and 2016) are shown in Figure 41. These data illustrate how the 2015 POC/PON sampling window captured the late part of the bloom season, whereas the 2016 POC/PON sampling window captured the full bloom season. FlowCAM based particle size is shown to increase during peak bloom periods and decrease as population biovolumes get smaller.

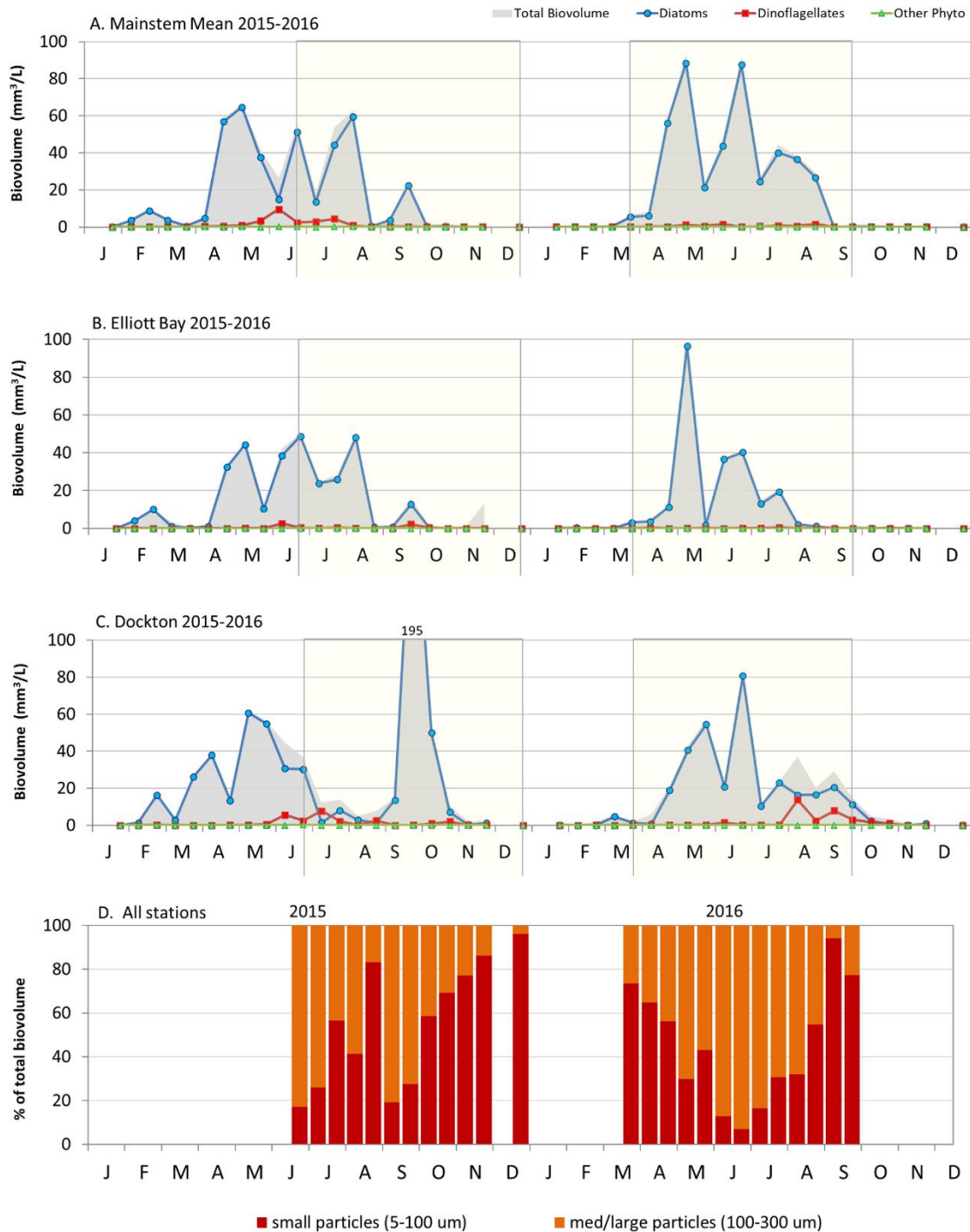


Figure 41. Seasonal variation in FlowCam based biovolumes for major taxonomic groups (2015 and 2016). (A) Mean monthly biovolume for 6 mainstem stations, JSUR01 (Pt. Wells), KSBP01 (Pt. Jefferson), KSSK02 (West Pt.), LSEP01 (South Plant), LSNT01 (Pt. Williams), NSEX01 (East Passage); all data combined. Individual observations for two non-mainstem sites: (B) LTED04 (Elliott Bay) and (C) NSAJ02 (Dockton). Yellow highlight represents POC and PON data collection period. D) % total mean biovolume for two size fractions analyzed for POC and PON for all 8 stations.

5.2 Relationship Between POC, PON and FlowCAM Biovolume

Multiple regressions of POC and PON vs FlowCAM biovolume suggest that a power function yields the best fit for small particles, whereas a linear or polynomial function yields the best fit for medium/large particles (Table 5 and Figure 42). Best fit was evaluated on R^2 values. Using Excel, linear, second order polynomial, and power functions were compared for both fractions separately or totaled: Fraction A (small particles), Fraction B (medium/large particles), and A+B. POC regressions always returned higher R^2 values compared to PON regressions, likely due to seasonal variations in the C/N ratio. For POC, the R^2 values for Fraction A ranged from 0.67 for the linear fit to 0.82 for the power fit. Visual inspection of the graphed data confirms that POC content is biovolume dependent in the small particle size range. R^2 values for POC in Fraction B, on the other hand, were in the 0.72 to 0.75 range for all three fits, indicating that a simple linear model is a reasonable approximation to data in the larger particle size range. Removing data points that fell outside of the calibration range (<25 $\mu\text{g C}$ per filter) did not alter these conclusions (data not shown).

A simple relationship between total sample biovolume (A+B, rather than per size fraction) and POC would be less accurate yet most practical for routine analysis of FlowCAM data. Regressions for the sum of the two fractions yielded the highest R^2 value for the power fit ($y = 127.67x^{0.4496}$, **Error! Reference source not found.**). The linear equation with intercept ($y = 9.0832x + 221.33$), explaining 78% of the variance, may also be a practical alternative for the conversion of biovolume data.

Table 5. Regression analysis results of POC and PON vs FlowCAM based sample biovolume. Best fits after comparing linear, second order polynomial and power equations for all samples. N=199, 36 values < lowest calibration standard for elemental carbon (<25 $\mu\text{g C}$) and 49 values < lowest calibration standard for elemental nitrogen (6 $\mu\text{g N}$). Units are mm^3/L for sample biovolume (x) and $\mu\text{g/L}$ for sample POC and PON (y).

Size Fraction	POC vs Biovolume	R^2	PON vs Biovolume	R^2
A (< 100 μm)	$y = 129.32x^{0.5303}$	0.821	$y = 23.758x^{0.5222}$	0.728
B (100 – 300 μm)	$y = -0.0106x^2 + 5.9426x + 38.202$	0.751	$y = 11.85x^{0.3146}$	0.571
	$y = 4.8895x + 45.581$	0.743		
A + B	$y = 127.67x^{0.4496}$	0.850	$y = 23.576x^{0.4556}$	0.771
	$y = 9.0832x + 221.33$	0.778		

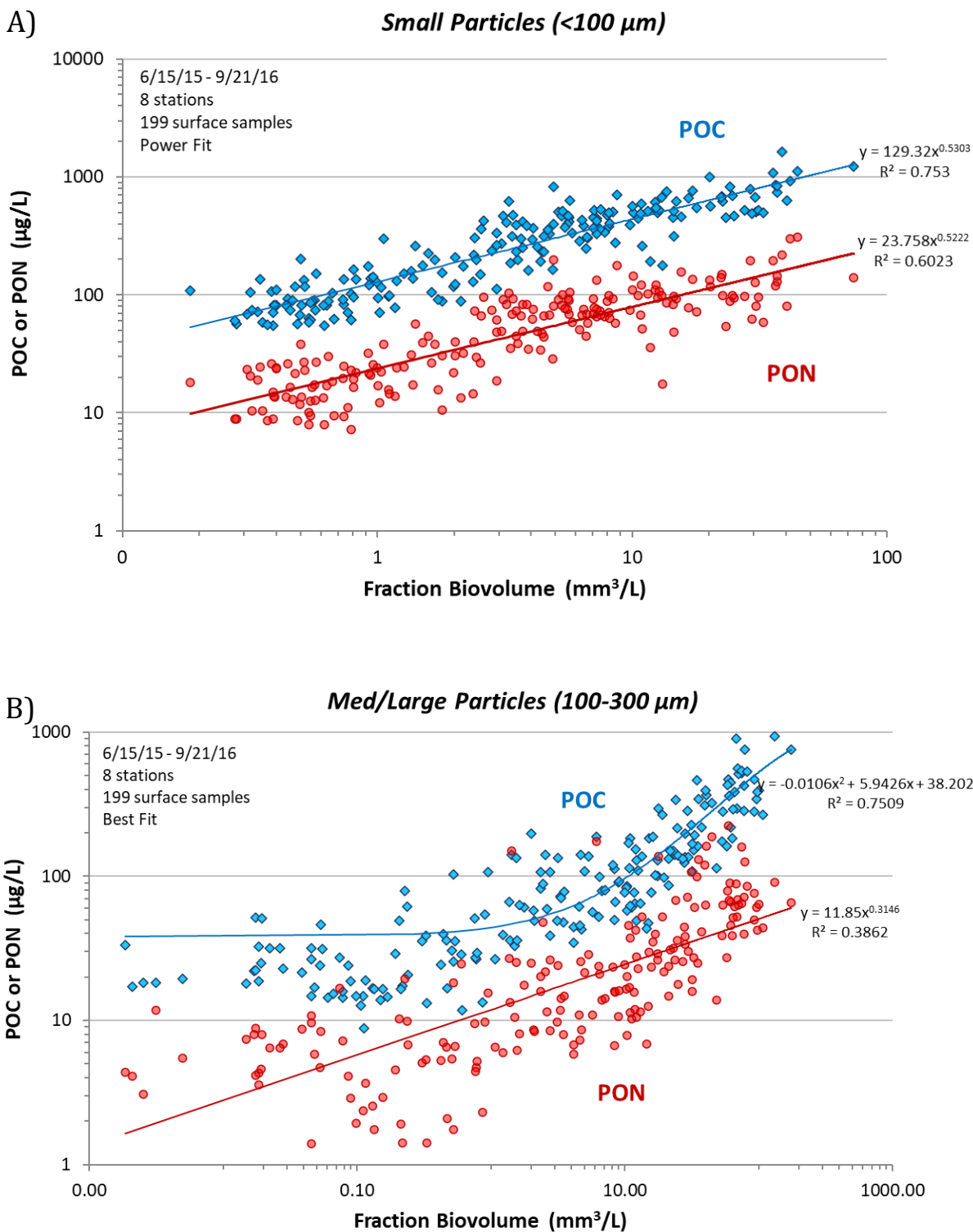


Figure 42. Regressions of POC and PON vs. FlowCAM based biovolume for A) Fraction A (<100 μm) and B) Fraction B (100-300 μm), showing best fit regression lines. Log-log scales used for easier visualization. Note the different scales between plots.

5.3 Carbon Density

There was a large difference in the slopes of the POC versus biovolume regression lines for the two particle size fractions; these slopes represent average carbon density of each fraction¹. The predicted carbon density, $\mu\text{g C}/\text{mm}^3$, for each fraction is represented in Figure 43 as a function of fraction biovolume (i.e. biovolume of fractions A and B) in the 10-90 mm^3/L range, the range of sample biovolumes typically observed during the bloom period (April – August or September, Figure 41). Fraction A, small particles that are most prevalent during off-season months (Figure 41 bottom panel), shows a 3-fold drop in carbon density across the selected range of biovolumes. Fraction B, with the larger particles typical of spring and summer blooms, shows only a slight drop in carbon density across the selected range of biovolumes. Across this range, the carbon density of the smaller size fraction is predicted to be, on average, 3.6 (range 2.9 – 4.3) times larger than carbon density of the larger size fraction. All natural samples contain a mix of both particle sizes, with seasonal differences in the proportion of each. Summing the two sample fractions (A+B) for all samples ($n=199$) yields a median carbon density of $32.5 \mu\text{g}/\text{mm}^3$ ($0.0325 \text{ pg}/\mu\text{m}^3$).

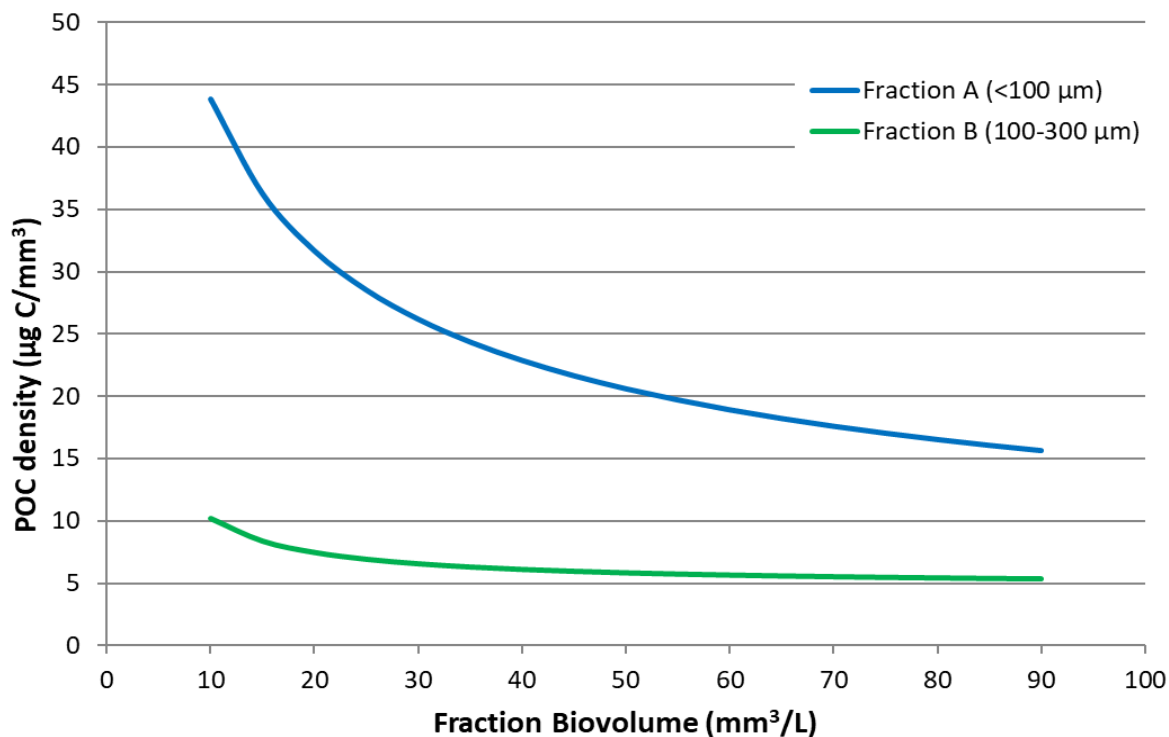


Figure 43. Predicted carbon density for two particle size fractions, A (<100 μm) and B (100-300 μm), over range of sample biovolumes typically observed during spring and summer. Carbon density calculated as $\text{POC}/\text{Biovolume}$, where POC determined as: $y = 129.32x^{0.5303}$ for Fraction A and $y = 4.7406x + 54.961$ for Fraction B.

¹ Note that the term ‘carbon content’ is generally used in the literature to refer to carbon quota per cell, whereas ‘carbon density’ refers to carbon per unit cell volume; carbon per cell cannot be calculated from this dataset

5.4 Measured Carbon Biomass Compared to Calculated Values

The carbon biomass determined by POC elemental analysis was compared with calculations based on the taxonomic composition of each sample and species-specific carbon content from the literature, as explained in Section 5.3. Published cell sizes of the different taxa, predictive equations and calculations can be found in Appendix B (Table B-3).

Regression analysis of measured carbon biomass vs. calculated carbon biomass for each sample showed that, for samples with >0.7 mg/L C, measured values were consistently lower than calculated values (Figure 44). Though the cause of this discrepancy is unknown, it could result from a) overestimation of biovolume by the FlowCAM image analysis software for certain morphological types, e.g., diatom chains, and/or b) overestimation of the carbon density of some common bloom forming diatom taxa.

Measured/calculated carbon biomass values ranged from 0.12 to 6.8 (mean = 1.02) (Figure 45); small values (≤ 25 $\mu\text{g C/L}$) were removed from the dataset to limit variations inherent in calculation of ratios of small numbers. Overall, lower measured/calculated values were observed in spring and early summer when colonial diatoms typically dominate.

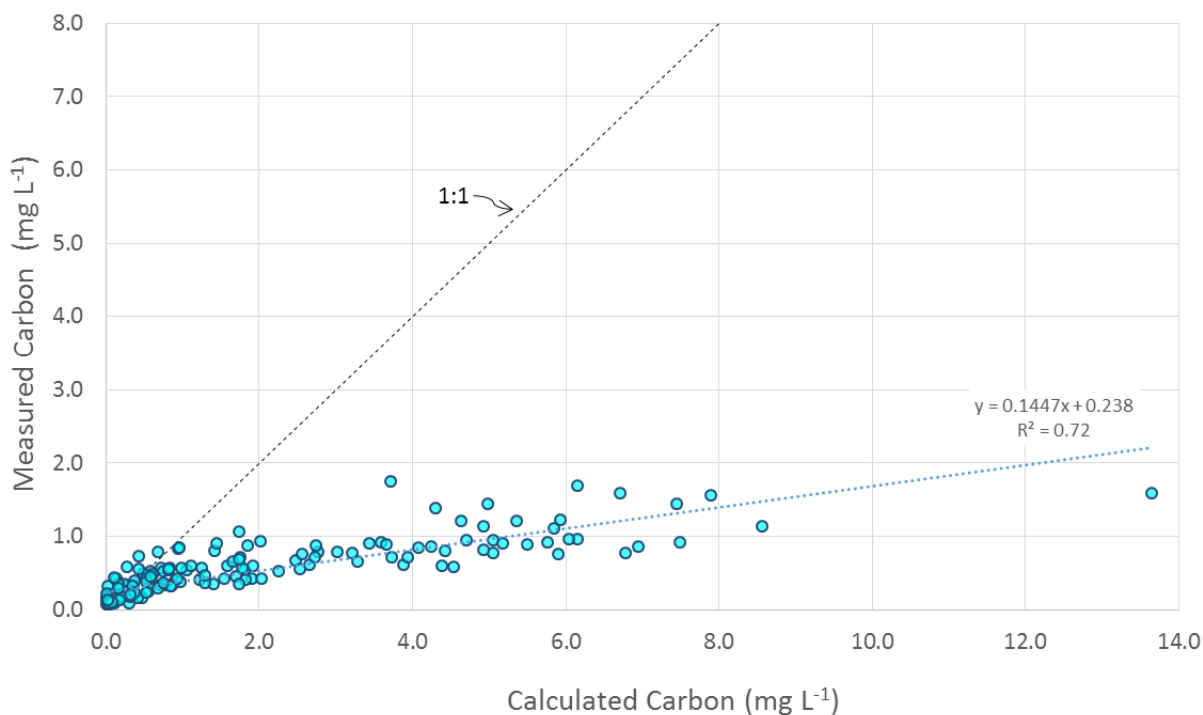


Figure 44. Measured vs. expected POC, as calculated from published cell sizes, carbon density and taxonomic composition of each sample. N = 199 samples.

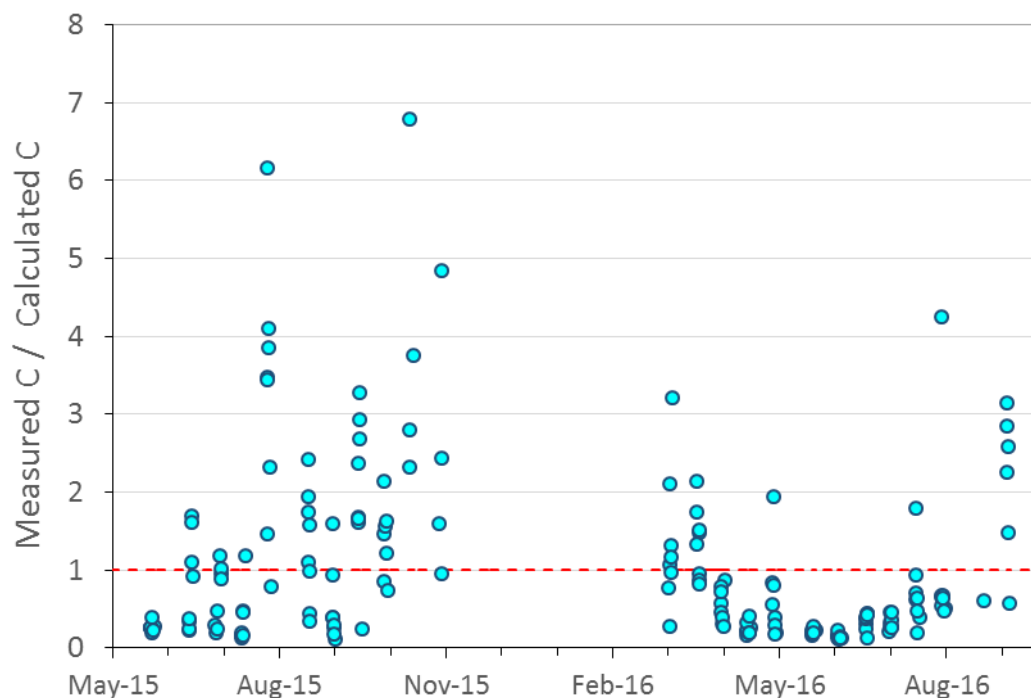


Figure 45. Variation in ratio of measured/calculated carbon biomass (2015-2016). Red stippled line indicates a ratio of 1. Ratios <1 indicate an overestimate of calculated carbon, while ratios >1 indicate an overestimate of measured carbon. Values $\leq 25 \mu\text{g C/L}$ excluded from ratio calculations; N=174.

5.5 Relationship Between POC, PON and Chlorophyll-*a*

Numerous studies have explored the relationship between marine phytoplankton POC and chlorophyll-*a*, with the goal of establishing empirical equations that can be used to infer POC from measurements of chlorophyll-*a*. This information can then be applied to models of carbon-based growth rates and primary production (e.g., Sathyendranath et al., 2009), or in food web models to estimate the carbon available to zooplankton (Legendre and Michaud, 1999). The variability in the relationship between particulate carbon and chlorophyll is due to a) variability in the proportion of non-phytoplanktonic particulate carbon, and b) variability in the carbon or chlorophyll content of the cells, which is known to vary both taxonomically and with environmental factors, especially irradiance and nutrients (Finenko et al., 2003, Jakobsen and Markager, 2016).

The sample aliquot for chlorophyll analysis was taken from the same Niskin sample used for the FlowCAM and particulate analysis for the routine monitoring program. It is important to note that chlorophyll-*a* data are for all particles $>0.7 \mu\text{m}$ and thus include particles $>300 \mu\text{m}$ not quantified by FlowCAM or in the POC study, which can be a significant portion of the total chlorophyll at the peak of a diatom bloom.

Regressions of log-transformed POC and PON data over chlorophyll-*a* indicate good linear fits, with R^2 values of 0.79 and 0.77, respectively (Figure 46). Our results for the parameters $\log a$ (intercept) and b (slope) are comparable to values reported by others for POC vs chlorophyll-*a* in coastal systems (Table 6).

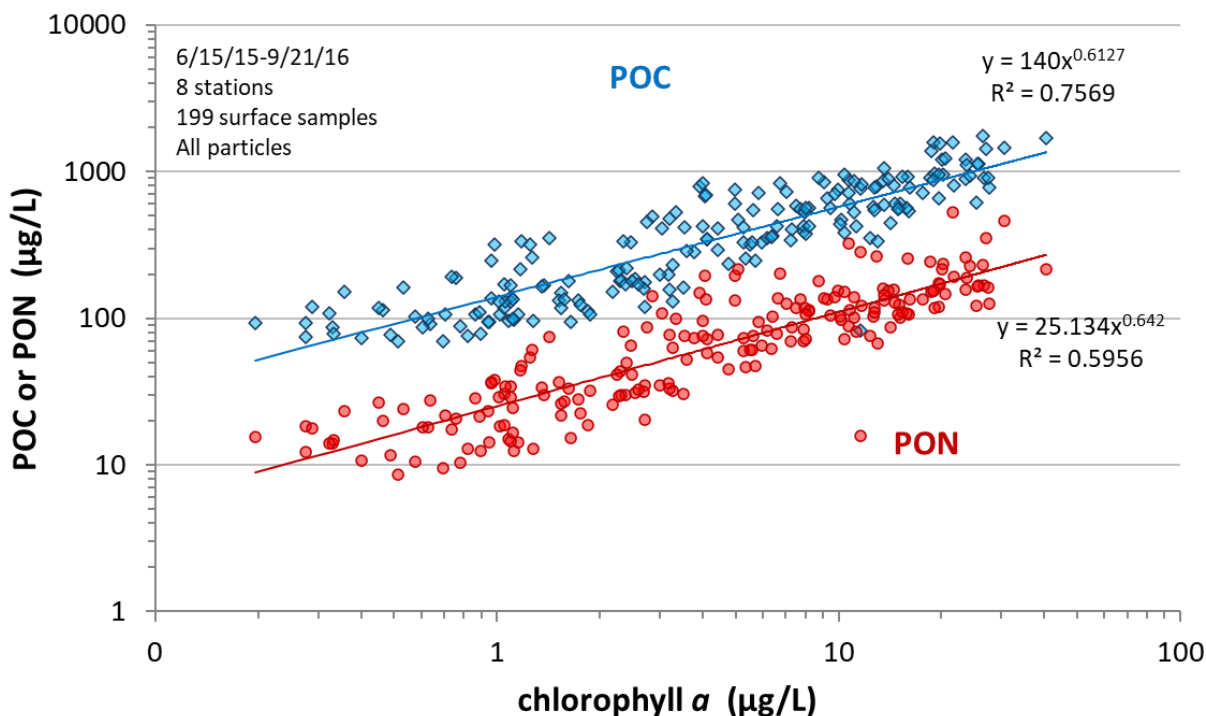


Figure 46. POC and PON as a function of chlorophyll-*a*. Shown are least-squares fits to log-transformed data.

Table 6. Fitted relationships between carbon and chlorophyll using linear least squares regression on log-transformed data for this and other studies. Relationships use $\log(y) = \log(a) + b[\log(x)]$, where y is particulate carbon and x is chlorophyll- a . Particulate carbon and chlorophyll- a have the same units. Studies listed for comparison may have used different methods to determine chlorophyll- a and particulate carbon

Study	$\log(a)$	b	N	R^2	Source
Puget Sound Central Basin, <i>Surface</i>	2.146	0.6127	199	0.79	This study
Baltic Sea, <i>Open water & Estuarine</i>	1.51	0.84	7578	NA	Jakobsen & Markager (2016)
NW Atlantic & Arabian Sea, <i>Offshore</i>	2.20-2.26	0.45-0.48	839-847	0.58-0.59	Sathyendranath <i>et al.</i> (2009)
Tokyo Bay	2.41-2.43	0.60-0.64	469-811	0.76-0.78	Sathyendranath <i>et al.</i> (2009)
North Atlantic	1.92	0.69	NA	0.60	Buck <i>et al.</i> (1996)
Global dataset <200 m depth	2.29	0.353	222	0.34	Legendre & Michaud (1999)

5.6 Seasonal Trends

The relative proportions of POC, PON and chlorophyll- a are expected to vary seasonally as ambient nutrient conditions and taxonomic composition change. On a timeline, POC:Chl- a ratios were variable and scattered (Figure 47, Table 7). Although these data do not show a clear seasonal pattern in the POC:Chl- a ratio, they do somewhat suggest a decrease in summer and an increase in fall and winter (but note that spring and summer ratios are negatively biased by inclusion of particles >300 μm in chlorophyll analysis). This pattern is to be expected if smaller, carbon dense particles that dominate in winter give way to larger particles that are chlorophyll-rich and less carbon dense in spring and summer. On the other hand, if nutrient limitation causes a significant drop in cellular chlorophyll content, then we would expect the opposite trend, an increase of this ratio in summer, as observed by Jakobsen and Markager (2016). The POC:Chl- a ratio can also be a valuable descriptor of a system's nutrient status, as eutrophication typically shifts the balance between primary and secondary producers. The POC:Chl- a median of 75 g/g is within the range of published values for phytoplankton (e.g., Jakobsen and Markager, 2016), but somewhat lower than the value given by Finenko *et al.* (2003) for a mesotrophic site in the Atlantic Ocean.

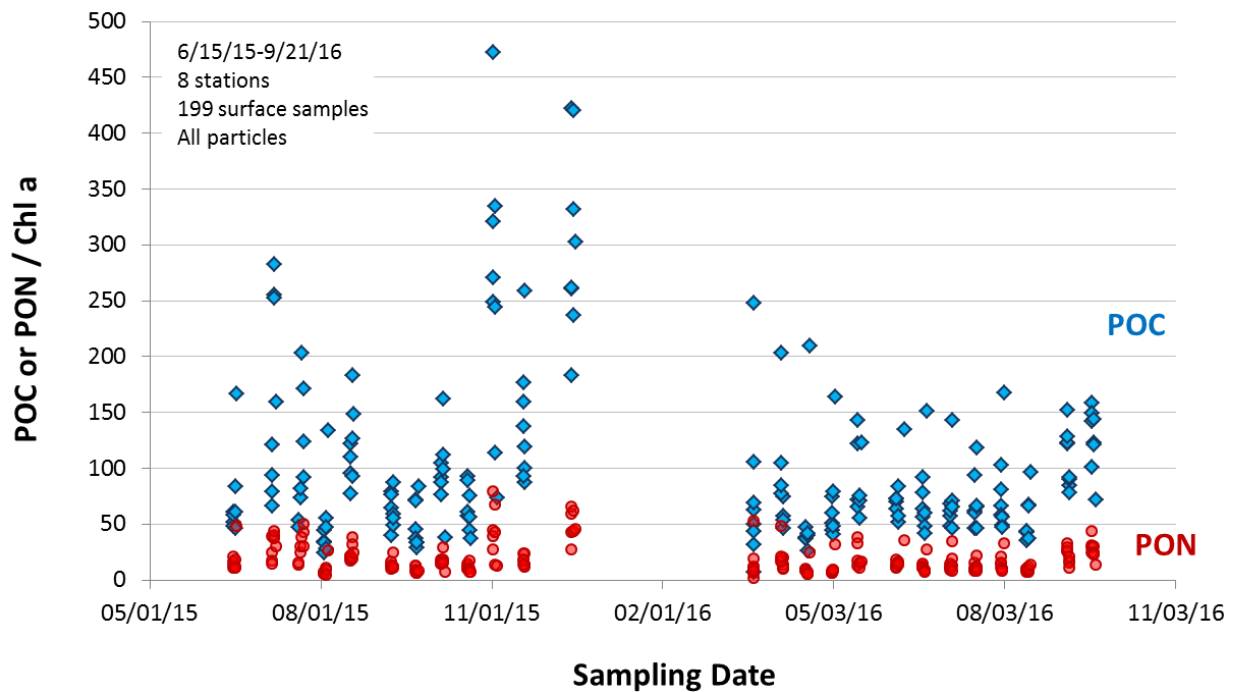


Figure 47. POC:Chl-*a* and PON:Chl-*a* seasonal variation (weight/weight ratios). POC and PON values are for 1.5-300 μm particles (i.e., sum of two size fractions), whereas Chl-*a* values are for all particles $>0.7 \mu\text{m}$. N=199 samples.

The Redfield ratio, based on historic observations of a consistent atomic ratio of C:N:P in both marine phytoplankton and throughout the deep oceans, continues to be a central principle in ocean biogeochemistry, though many exceptions have been noted. It was originally determined to be 106:16:1 (i.e., a C:N molar ratio of 6.6). Analysis of a large data set across all major ocean regions spanning from 1970 to 2010 yielded a global median C:N molar ratio of 6.6 (Martiny *et al.*, 2013, 2014). However, elemental ratios exhibited a clear latitudinal trend, with C:N below Redfield proportions (C:N=6) in colder, nutrient rich high latitude environments such as the Pacific Northwest.

POC:PON (i.e., C:N) ratios in this study were scattered and did not follow a clear seasonal pattern (Figure 48). The exception was an increase in the C:N ratio for small particles between September and December during 2015, which may reflect increasing nitrogen limitation as the season progressed. This trend was not observed for larger particles. Despite the considerable range in values, the median ratio was similar for the two fractions, and the median molar ratios (6.1 and 6.3) agree with the studies cited above (Table 7).

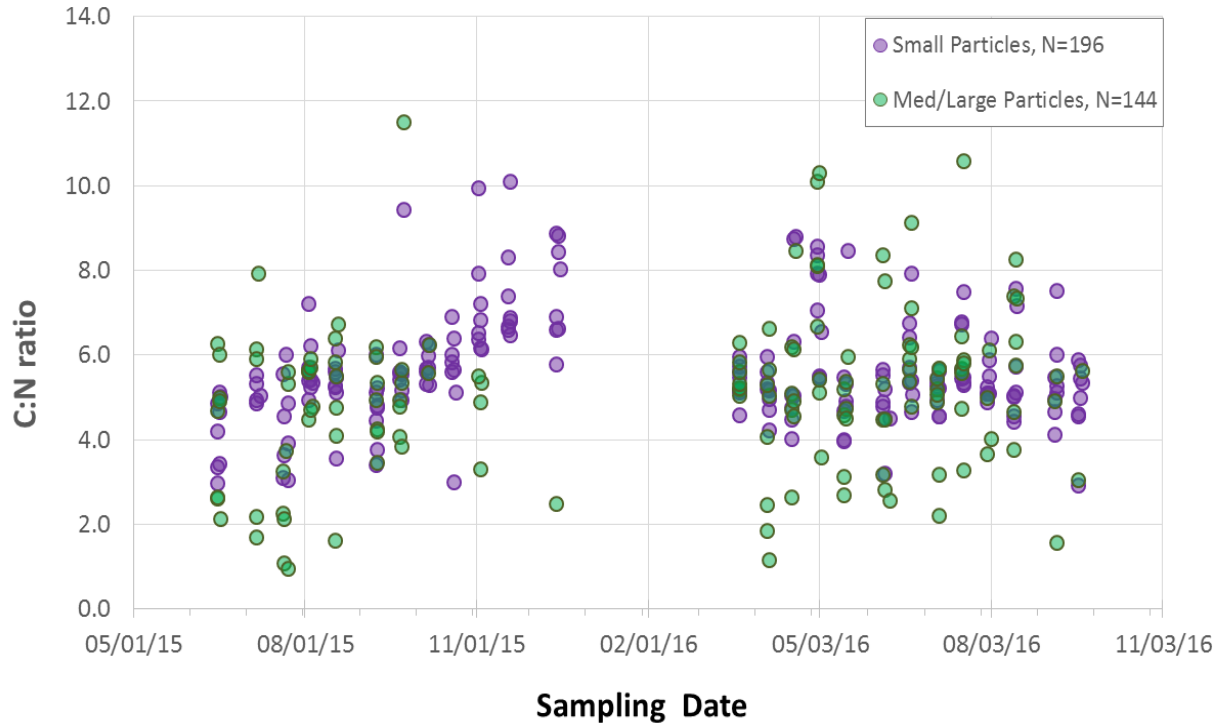


Figure 48. C:N seasonal variation for two particle size fractions (weight/weight ratios). Small Particles (<100 μm) and Med/Large Particles (100-300 μm). Only values within elemental C and N calibration ranges were used to calculate C:N ratios.

Table 7. Ratios of POC and PON to biovolume and chlorophyll-*a*. Values < lowest calibration standards for elemental carbon and nitrogen are included, except for POC:PON. Chlorophyll-*a* is for all particles >0.7 μm , including particles >300 μm not quantified by FlowCAM. w/w indicates weight/weight.

Ratio	Size Fraction*	N	Range	Median
POC:Biovolume ($\mu\text{g}/\text{mm}^3$)	A+B	199	7.2 - 482	32.5
PON:Biovolume ($\mu\text{g}/\text{mm}^3$)	A+B	199	0.8 - 99.2	6.8
POC:Chl- <i>a</i> (w/w)	A+B	199	7.1 - 472	74.7
PON:Chl- <i>a</i> (w/w)	A+B	199	1.4 - 78.7	13.9
POC:PON (w/w)	A	196	2.9 - 10.1	5.4
	B	144	0.9 - 11.5	5.2
POC:PON (molar)	A	196	3.4-11.8	6.3
	B	144	1.1-13.4	6.1

*Size fraction A: 1.5 -100 μm for particulate analysis, and 5-100 μm for FlowCAM determined biovolume; Size fraction B: 100-300 μm

6.0 PHYTOPLANKTON SUMMARY

6.1 Qualitative and Semi-Quantitative Results

- Seasonal changes in taxonomic composition show a basin-wide diatom-dominated community that peaks in April–August.
- The early spring bloom appeared in March–April and was dominated primarily by *Thalassiosira nordenskioldii* and *T. pacifica/aestivalis*; this was followed by a *Chaetoceros* bloom that usually started in April and continued at both stations through the summer with a number of different species.
- Other notable spring and summer taxa were *Cylindrotheca closterium*, *Ditylum brightwellii*, *Eucampia zodiacus*, *Paralia sulcata*, *Pseudo-nitzschia* spp. (large forms), *Rhizosolenia setigera*, *Skeletonema costatum*, *Thalassionema nitzschioides*, and small dinoflagellates.
- Many taxa were observed year after year at most stations, but several common diatoms (e.g., *Skeletonema*, *Asterionellopsis*, *Eucampia*) and some dinoflagellate taxa (e.g., *Ceratium fusus*) formed blooms only during some years.
- Species composition at Dockton differed somewhat from mainstem stations, yet there were many similarities, such as the dominance of *Thalassiosira* and *Chaetoceros* in spring and summer.
- Occurrence of the HAB dinoflagellate *Dinophysis* was highest from 2008 to 2012 and dropped in subsequent years.
- The toxic dinoflagellate *Alexandrium catenella* was rarely observed at mainstem stations. Occurrence of *Alexandrium* species was highest at Dockton, but was only 11% of all samples.
- Occurrence of *Heterosigma akashiwo*, a small HAB flagellate, did not show a clear geographical or interannual pattern. A large bloom was seen at Dockton in 2014.
- *Akashiwo sanguineum*, a harmful dinoflagellate, was most common in late summer and fall. A high percentage of observations were at Dockton.

6.2 Quantitative Results

- The seasonal pattern of the two major taxonomic groups, diatoms and dinoflagellates, indicated 1) consistent diatom dominance throughout the seasons, 2) small differences among the nine mainstem stations, 3) interannual shifts in the onset of the spring bloom, and 4) interannual differences in length of bloom season.
- Analysis of the relationship between phytoplankton biovolumes and water column stratification indicated that higher cell concentrations generally occur above a maximum density gradient threshold of about 0.035–0.05 kg/m⁴. Some sites, such as Pt. Williams, are less stratified, which may help explain the lower chlorophyll and biovolume values observed at this site.

- The first spring bloom typically started in late March or early April but didn't peak until mid-April or May, some years even as late as June. There was no consistent geographical pattern in timing of the spring bloom.
- Some taxa were consistently abundant every year, whereas others were only abundant in some years, thus exhibiting no predictable pattern
- Most of the biomass was comprised of just a few diatom genera. *Chaetoceros*, locally represented by at least 18 species, contributed on average 49% of the total annual biomass, followed by *Thalassiosira* (14%), *Rhizosolenia* and *Skeletonema* (8%).
- *Ceratium* spp., gymnodinioid dinoflagellates and *Akashiwo sanguinea* were the largest contributors to flagellate biomass, together making up on average 55% of the total flagellate biovolume. On a cell density basis, small unidentified dinoflagellates and *Heterosigma* were the most abundant flagellate categories, followed by *Prorocentrum* and unidentified gymnodinioid dinoflagellates.
- *Noctiluca* blooms were observed in spring and/or summer of every year, with a notable drop in bloom size following the 2015 marine heat wave. Cell densities tended to be highest at Pt. Jefferson and East Passage but very low in Elliott Bay.
- There was an increase in absolute numbers of mixotrophs and heterotrophs during spring and summer, but their relative proportion within the microplankton community was highest during winter and fall when diatoms declined significantly
- Abundance of the common red ciliate *Mesodinium* changed little seasonally, while abundances of all other microzooplankton were much higher in spring and summer than in winter and fall. Inter-annual differences in microzooplankton abundance were generally small.
- Community analysis by nMDS indicated a high degree of similarity in community composition among samples. Season was the factor that had the greatest effect on community composition, as compared with year or locator.
- Cumulative annual biovolumes remained consistent from 2015 to 2017 but fell to <50% of previous years in 2018 due to an unusually short growth season. The highest biovolumes were consistently observed at the southern stations (East Passage and Dockton) and lowest biovolumes at the central stations (Elliott Bay, South Plant, Alki and Pt. Williams). These differences are likely related to different degrees of mixing among sites.
- At Dockton, diatoms were also the dominant component of the microplankton community throughout the seasons. Seasonal biovolume patterns were more variable than at other stations, and growth usually extended later into the fall months. Cumulative biovolumes indicated high annual biomass, similar to East Passage. Species of *Chaetoceros* contributed 39% of total annual biomass, followed by *Rhizosolenia* (11%) and *Thalassiosira* (5%).
- Mixotrophs (i.e., pigmented flagellates) were particularly abundant at Dockton, with summer concentrations reaching close to eight times those observed at other stations. Heterotrophs were generally highest in fall, averaging four times the numbers observed at other stations.

- The relationship between chlorophyll-*a* and biovolume of pigmented cells is best described as a power function, where $\text{Chl-}a = 2.1582 (\text{Biovolume})^{0.4917}$.

6.3 POC Study

- A single power equation ($y = 127.67x^{0.4496}$) was adequate to describe the relationship between measured POC (y) and FlowCAM determined biovolume (x) for the 199 Central Basin samples analyzed for this study. However, when analyzed separately, the best fit for small particles (<100 μm) was described by a power function, whereas the best fit for medium/large particles (100–300 μm) was described by a linear or polynomial function.
- These empirical equations may prove useful to estimate POC from biovolume measurements during the bloom season in the Central Basin but should be used with caution. Additional validation is needed across years and conditions since species composition can vary from year to year.
- The non-linear relationship between measured POC and biovolume implies that samples with higher biomass, which typically occur during diatom blooms, are less carbon dense. This is consistent with the notion that larger cells - which have been shown to be less carbon dense - tend to dominate blooms in nutrient-rich estuarine areas (Cloern 2018).
- In bloom samples, the expected carbon content of our samples (based on calculations using equations and literature-based taxon-specific cell volumes) was generally higher than POC content measured by combustion. This discrepancy needs further study but suggests that for some shapes the FlowCAM image analysis settings may overestimate biovolume compared to traditional microscope methods, possibly overestimating biovolume of colonial taxa.
- The relationship between POC and chlorophyll-*a* was best described by a power equation, indicating increasing chlorophyll-specific carbon content with increasing chlorophyll concentration. Equation parameters were comparable to values reported for other systems. POC:Chl-*a* ratios did not follow a clear seasonal trend. The median POC:Chl-*a* ratio was 75.
- C:N ratios were highly variable and did not follow a clear seasonal trends, yet the medians (6.1–6.3) were in high agreement with molar ratios from global oceanographic studies.

7.0 REFERENCES

- Bill, B.D., F.H. Cox, R.A. Horner, J.A. Borchert, V.L. Trainer. 2006. The first closure of shellfish harvesting due to domoic acid in Puget Sound, Washington, USA. *S. Afr. J. Mar. Sci.*
- Booth, B.C; Larouche, P; Bélanger, S; Klein, B; Amiel, D; Mei, Z.-P (2002). Dynamics of *Chaetoceros socialis* blooms in the North Water. *Deep Sea Research Part II: Topical Studies in Oceanography*. 49 (22–23): 5003–5018. Bibcode:2002DSRII..49.5003B. [doi:10.1016/S0967-0645\(02\)00175-3](https://doi.org/10.1016/S0967-0645(02)00175-3).
- Chappell, D.P., Whitney, L. A. P., Haddock, T. L., Menden-Deuer, S., Roy, E. G., Wells, M. L., & Jenkins, B. D. 2013. *Thalassiosira* spp. community composition shifts in response to chemical and physical forcing in the northeast Pacific Ocean. *Frontiers in Microbiology*, 4(SEP), 273. <https://doi.org/10.3389/fmicb.2013.00273>
- Clark, KR, Gorley, RN, Somerfield, PJ, Warwick, RM. 2014. Change in marine communities: an approach to statistical analysis and interpretation, 3rd edition. PRIMER-E: Plymouth.
- Cloern, J.E. 2018. Why large cells dominate estuarine phytoplankton. *Limnol. Oceanogr.* 63:S392-S409.
- Cloern, J.E. and Jassby, A.D. 2008. Complex seasonal patterns of primary producers at the land–sea interface. *Ecology Letters* 11: 1294–1303.
- Dodson, A.M. and W.H. Thomas. 1978. Reverse filtration, pp. 104-107. In: A. Sournia (ed.), *Phytoplankton Manual*. Monographs on oceanographic methodology 6. UNESCO, Paris.
- Elsworth, G.W., Lovenduski, N.S., McKinnon, K.A. *et al.* 2020. Finding the Fingerprint of Anthropogenic Climate Change in Marine Phytoplankton Abundance. *Curr Clim Change Rep* 6, 37–46. <https://doi.org/10.1007/s40641-020-00156-w>
- Erga, S.R., and Heimdal, B.R. 1984. Ecological studies on the phytoplankton of Korsfjorden, western Norway. The dynamics of a spring bloom seen in relation to hydrographical conditions and light regime. *J. Plankton Res.* 6: 67–90
- Finenko, Z.Z., Hoepffner, N., Williams, R., Piontkovski, S.A., 2003. Phytoplankton carbon to chlorophyll *a* ratio: response to light, temperature and nutrient limitation. *Mar. Ecol. J.* 2:40-64. (<https://www.researchgate.net/publication/37615131>)

- Greengrove, C., J. Masura, T. Nguyen, and M. Schatz. 2018. Comparison of *Alexandrium* spp. surface sediment cyst maps from Quartermaster Harbor in 2007 and 2017. SIAS Faculty Publications, 1002. https://digitalcommons.tacoma.uw.edu/ias_pub/1002
- Haigh, R., Taylor, F., & Sutherland, T. 1992. Phytoplankton ecology of Sechart Inlet, a fjord system on the British Columbia coast. I. General features of the nano- and microplankton. *Marine Ecology Progress Series*, 89(2/3), 117-134.
- Harris, A., Medlin, L., Lewis, J., Jones, K., D Harris, A. S., Medlin, L. K., & Jones, K. J. (1995). *Thalassiosira* species (Bacillariophyceae) from a Scottish sea-loch. *European Journal of Phycology*, 30(2), 117–148. <https://doi.org/10.1080/09670269500650881>
- Harrison, P.J., Zingone, A., Mickelson, M.J., Lehtinen, S., Ramaiah, N., Kraberg, A., Jun, J., McQuatters-Gollop, A., Jakobsen, H.H., 2015. Cell volumes of marine phytoplankton from globally distributed coastal data sets. *Estuarine Coast. Shelf Sci.* 162:130-142.
- Hoppenrath, M., Elbrächter, M. and Drebes, G. 2009. *Marine Phytoplankton. Kleine Senckenberg-Reihe, E. Schweitzbart'sche Verlagsbuchhandlung (Nägele u. Obermiller), Stuttgart, 264 pp.*
- Horner, R.A. 2002. *A Taxonomic Guide to Some Common Marine Phytoplankton.* Biopress Ltd., Bristol, 195 pp.
- Hoyer, M.V., T.K. Frazer, S.K. Notestein, and D.E. Canfield, Jr. 2002. Nutrient, chlorophyll, and water clarity relationships in Florida's nearshore coastal waters with comparisons to freshwater lakes. *Can. J. Fish. Aquat. Sci.* 59: 1024–1031
- Jakobsen H.H. and Markager, S., 2016. Carbon-to-chlorophyll ratio for phytoplankton in temperate coastal waters: Seasonal patterns and relationship to nutrients. *Limnol. Oceanogr.* 61:1853-1868.
- King County. 2001. *Water Quality Status Report for Marine Waters, 1999 and 2000.* Prepared by the Marine Monitoring & Assessment Group, Water and Land Resources Division. Seattle, Washington.
- King County. 2006. *Chlorophyll-a and Pheophytin-a Analysis in Marine Water by Fluorometric Detection.* KCEL SOP #314 v.4. King County, Environmental Lab, Seattle, WA.
- King County. 2011. *Qualitative Analysis of Marine Phytoplankton.* KCEL SOP 459v0. King County Environmental Lab, Seattle, WA.

- King County. 2015. Qualitative analysis of marine phytoplankton. KCEL SOP #459v1. King County, Environmental Lab, Seattle, WA.
- King County. 2016a. Analysis of marine phytoplankton by FlowCAM. KCEL SOP #467v1. King County, Environmental Lab, Seattle, WA.
- King County. 2016b. Marine phytoplankton Monitoring Program Sampling and Analysis Plan. Prepared by Amelia Kolb, G. Hannach, L. Swanson. King County Water and Land Resources Division. Seattle, Washington.
- King County. 2020. Marine Offshore and Beach Water Monitoring: Sampling and Analysis Plan. Prepared by Kimberle Stark, Water and Land Resources Division. Seattle, Washington.
- King County. 2022a. Marine Conditions 2008–2019 Report Series: Marine Monitoring Program Overview. Prepared by Kimberle Stark and Taylor Martin, Water and Land Resources Division. Seattle, Washington.
- King County. 2022b. Marine Conditions 2008–2019 Report Series: Offshore Temperature and Salinity. Prepared by Taylor Martin, Water and Land Resources Division. Seattle, Washington.
- King County. 2022c. Marine Conditions 2008–2019 Report Series: Chlorophyll and Pheophytin. Prepared by Kimberle Stark, Water and Land Resources Division. Seattle, Washington.
- Langdon, C. 1988. On the causes of interspecific differences in the growth-irradiance relationship for phytoplankton. II. A general review. *J. Plankton Res.* 10 (6):1291–1312, <https://doi.org/10.1093/plankt/10.6.1291>
- Legendre, L., Michaud, J., 1999. Chlorophyll *a* to estimate the particulate organic carbon available as food to large zooplankton in the euphotic zone of oceans. *J. Plankton Res.* 21(11): 2067–2083.
- Mahadevan, A., D’Asaro, E., Lee, C. Perry, M.J. 2012. Eddy-driven stratification initiates North Atlantic spring phytoplankton blooms. *Science* 337 (6090): 54-58.
- Martiny, A., Pham, C., Primeau, F. *et al.*, 2013. Strong latitudinal patterns in the elemental ratios of marine plankton and organic matter. *Nature. Geosci.* 6, 279–283. (<https://doi.org/10.1038/ngeo1757>)

- Martiny, A.C.; Vrugt, J.A.; Lomas, M. W., 2014. "[Concentrations and ratios of particulate organic carbon, nitrogen, and phosphorus in the global ocean](#)". *Scientific Data*. **1** (1): 140048. [doi:10.1038/sdata.2014.48](#). [PMC 4421931](#). [PMID 25977799](#).
- Menden-Deuer, S., Lessard, E.J., 2000. Carbon to volume relationships for dinoflagellates, diatoms, and other protist plankton. *Limnol. Oceanogr.* 45:569-579.
- Montagnes, D.J.S., Berges, J.A., Harrison, P.J., Taylor, F.J.R., 1994. Estimating carbon, nitrogen, protein, and chlorophyll *a* from volume in marine phytoplankton. *Limnol. Oceanogr.* 39:1044-1060.
- Moore, S.K., N.J. Mantua, J.A. Newton, M. Kawase, M.J. Warner, J.P. Kellogg. 2008a. A descriptive analysis of temporal and spatial patterns of variability in Puget Sound oceanographic properties. *Estuarine, Coastal and Shelf Science* 80 (4):545-554. <https://doi.org/10.1016/j.ecss.2008.09.016>
- Moore, S.K., V.L. Trainer, N.J. Mantua *et al.* 2008b. Impacts of climate variability and future climate change on harmful algal blooms and human health. *Environ Health* **7**, S4. <https://doi.org/10.1186/1476-069X-7-S2-S4>
- Phlips, E.J., S. Badylak, T.C. Lynch. 1999. Blooms of the picoplanktonic cyanobacterium *Synechococcus* in Florida Bay, a subtropical inner-shelf lagoon. *Limnol. Oceanogr.*, 44(4), 1999, 1166–1175
- Pool, S., C. Krembs, J. Bos, and B. Sackmann 2015. Physical, chemical, and biological conditions during *Noctiluca* blooms in an urban fjord, Puget Sound. Washington State DOE Publication number 15-03-040.
- PSEMP (Puget Sound Ecosystem Monitoring Program) Marine Waters Workgroup. 2019. Puget Sound Marine Waters: 2018 Overview. S.K. Moore, R. Wold, K. Stark, J. Bos, P. Williams, N. Hamel, A. Edwards, C. Krembs, and J. Newton, editors.
- Reguera B, P. Riobó, F. Rodríguez, P.A. Díaz, G. Pizarro, B. Paz, J.M. Franco, J. Blanco. 2014. *Dinophysis* toxins: causative organisms, distribution and fate in shellfish. *Mar Drugs* 12(1):394-461.
- Rensel, J. E. 2007. *Fish kills from the harmful alga Heterosigma akashiwo in Puget Sound: Recent blooms and review*. Rensel Associates Aquatic Sciences. Arlington, Washington, USA. 58 pp.
- Sathyendranath, S., Venetia, S., Nair, A. and others, 2009. Carbon-to-chlorophyll ratio and growth rate of phytoplankton in the sea. *Mar. Ecol. Prog. Ser.* 383. 73-84.

- Shinada, Akiyoshi & Shiga, N. & Ban, Syuhei. (1999). Structure and magnitude of diatom spring bloom in Funka Bay, southwestern Hokkaido, Japan, as influenced by the intrusion of Coastal Oyashio Water. *Plankton Biology and Ecology*. 46. 24-29.
- Sournia, A., Birrien, J.-L., Douvillé, J.-L., Klein, B., and Viollier, M. 1987. A daily study of the diatom spring bloom at Roscoff (France) in 1985. I. The spring bloom with the annual cycle. *Estuarine Coastal Shelf Sci*. 25: 355–367.
- Tomas, C.R. 1997. Identifying marine phytoplankton. Academic Press, Inc., San Diego, New York, Boston, London, Sidney, Tokio, Toronto, 858 pp.
- Trainer VL, L. Moore, B.D. Bill, N.G. Adams, N. Harrington, J. Borchert, D.A. da Silva, B.T. Eberhart. 2013. Diarrhetic shellfish toxins and other lipophilic toxins of human health concern in Washington State. *Mar Drugs* 11(6):1815-35.
- van de Poll, W. H., Kulk, G., Timmermans, K. R., Brussaard, C. P. D., van der Woerd, H. J., Kehoe, M. J., Mojica, K. D. A., Visser, R. J. W., Rozema, P. D., and Buma, A. G. J. 2013. Phytoplankton chlorophyll a biomass, composition, and productivity along a temperature and stratification gradient in the northeast Atlantic Ocean. *Biogeosciences* 10, 4227–4240, <https://doi.org/10.5194/bg-10-4227-2013>
- Winter, D.F., Banse, K., Anderson, G.C. 1975. The dynamics of phytoplankton blooms in Puget Sound, a fjord in the Northwestern United States. *Mar. Biol.* 29, 139–176. <https://doi.org/10.1007/BF00388986>

Appendix A: Species List

December 2022

Table A-1 (contd.) p2

DIATOMS	Nutrition	2008		2009		2010		2011		2012		2013		2014						2015															
		KSBP01	NSEX01	MSWH01	KSBP01	NSEX01	NSAJ02	KSBP01	NSEX01	NSAJ02	KSBP01	NSEX01	NSAJ02	KSBP01	NSEX01	NSAJ02	JSUR01	KSBP01	KSSK02	LTED04	LSEP01	LSNT01	NSEX01	NSAJ02	JSUR01	KSBP01	KSSK02	LTED04	LSEP01	LSNT01	NSEX01	NSAJ02			
<i>Dactyliosolen fragilissimus</i>	A			●	●●	●●	●		●●	●	●●	●●	●	●●	●●	●		●	●	●	●		●	●	●	●●	●	●	●	●●	●	●	●		
<i>Detonula pumila</i>	A	●●	●●	●	●●		●	●●	●●	●	●●	●	●	●●	●●	●		●●	●		●			●	●	●●	●	●	●	●	●●	●	●		
<i>Ditylum brightwellii</i>	A	●●	●●	●	●●	●●	●	●●	●●	●	●	●●	●	●●	●●	●	●	●●	●	●	●	●	●	●●	●	●	●●	●	●	●	●●	●	●		
<i>Eucampia zodiacus</i>	A	●●	●●	●	●●	●●	●	●●	●●	●	●●	●	●	●●	●●	●	●	●●	●	●	●	●	●●	●	●	●●	●	●	●	●	●●	●	●		
<i>Guinardia delicatula</i>	A		●●		●●	●	●			●	●●	●	●●	●	●	●		●●	●	●	●	●	●●	●	●	●●	●	●	●	●	●	●	●		
<i>Guinardia striata</i>	A														●									●	●	●	●	●	●	●	●	●	●		
<i>Hemiaulus hauckii</i>	A	●●	●●				●●	●●	●	●			●●	●●	●	●	●●		●	●	●	●	●●	●	●	●●	●	●	●●	●	●	●●	●	●	
<i>Lauderia annulata</i>	A			●	●	●●	●	●●	●	●	●	●●	●	●	●●	●	●	●●	●	●	●	●	●●	●	●	●●	●	●	●●	●	●	●●	●	●	
<i>Leptocylindrus danicus</i>	A	●●	●●	●	●●	●●	●	●●	●●	●	●●	●	●●	●●	●	●	●●	●	●	●	●	●●	●	●	●●	●	●	●●	●		●	●	●	●	
<i>Leptocylindrus minimus</i>	A				●●	●●	●			●●	●●	●	●●	●●	●	●	●●			●		●●	●	●	●	●	●		●	●	●	●	●	●	
<i>Melosira moniliformis</i>	A					●		●	●●										●						●				●	●	●	●	●	●	
<i>Navicula</i> sp.	A							●	●●																			●							
<i>Nitzschia acicularis</i>	A	●●	●●	●	●●	●●	●	●●	●●	●	●●	●●	●	●●	●●	●	●	●●	●	●			●●	●	●	●●	●	●	●●	●	●	●●	●	●	
<i>Odontella aurita</i>	A																																		
<i>Odontella longicurvis</i>	A	●	●		●●	●●	●	●●	●●	●		●	●	●●	●	●	●	●●		●		●	●●		●	●●		●	●			●	●	●	
<i>Paralia sulcata</i>	A		●		●●	●		●●	●●	●	●●	●●	●	●		●		●				●●	●	●	●	●	●		●	●					
<i>Pleurosigma</i> sp.	A	●●	●●	●	●●	●●		●●	●●	●	●●	●●	●	●●		●	●	●●	●	●	●	●●	●	●	●●	●	●	●●	●	●	●	●	●	●	●
<i>Pseudo-nitzschia americana</i>	A				●●	●●	●	●●	●●	●	●●	●●	●	●●	●●	●	●	●●	●	●●	●	●	●●	●	●	●●	●	●	●	●	●	●	●	●	●
<i>Pseudo-nitzschia</i> sp. (large)	A	●●	●	●	●●	●	●	●●	●	●	●●	●	●	●●	●	●	●	●●	●	●	●	●	●●	●	●	●●	●	●	●	●	●	●	●	●	●
<i>Pseudo-nitzschia</i> sp. (small)	A	●	●●		●●	●●	●	●●	●●		●●	●	●	●●	●●	●		●●				●●	●	●	●	●	●	●	●	●	●	●	●	●	●
<i>Pyrophacus horologium</i>	A	●●	●●	●																															
<i>Rhizosolenia setigera</i>	A	●●	●●	●	●●	●●	●	●●	●●	●	●●	●●	●	●●	●●	●	●	●●	●	●	●	●	●●	●	●	●●	●	●	●●	●	●	●●	●	●	●
<i>Skeletonema costatum</i>	A	●●	●●	●	●●	●●	●	●●	●●	●	●●	●●	●	●●	●●	●	●	●●	●	●	●	●	●●	●	●	●●	●	●	●●	●	●	●●	●	●	●
<i>Stephanopyxis nipponica</i>	A	●	●●		●●	●	●	●●		●	●●	●	●	●●	●	●		●								●	●	●						●	●
<i>Stephanopyxis palmeriana</i>	A	●●	●		●●	●●	●	●●	●●	●	●●	●●		●	●●	●	●	●●				●	●●	●									●		●
<i>Thalassionema frauenfeldii</i>	A																																		
<i>Thalassionema nitzschioides</i>	A	●●	●●	●	●●	●●	●	●●	●●	●	●●	●●	●	●●	●●	●	●	●●	●	●	●	●	●●	●	●	●●	●	●	●●	●	●	●●	●	●	●
<i>Thalassiosira anguste-lineata</i>	A	●●	●●	●	●●	●●		●●	●●	●	●●	●●	●	●●	●●	●	●	●●	●	●	●	●	●●	●	●		●	●	●	●	●	●	●●	●	●
<i>Thalassiosira eccentrica</i>	A			●																															
<i>Thalassiosira nordenskioeldii</i>	A	●			●	●●	●	●●	●●	●	●●	●●	●	●●	●●	●	●	●●	●	●	●	●	●●	●	●	●●	●	●	●	●	●	●	●●	●	●
<i>Thalassiosira pacifica/aestivalis</i>	A						●●	●	●●	●●	●	●●	●●	●	●●	●●	●	●●		●		●	●●		●	●●	●	●	●	●	●	●	●●	●	●
<i>Thalassiosira punctigera</i>	A	●●	●●		●●	●●	●	●●	●●	●	●●	●●	●	●●	●	●		●●	●	●	●	●	●●	●	●	●	●	●	●	●	●	●	●●	●	●
<i>Thalassiosira rotula</i>	A	●●	●●	●	●●	●●	●	●	●	●	●●	●●	●	●●	●●	●	●	●●	●	●	●		●●	●	●	●●	●	●	●●	●	●	●	●	●	●
<i>Thalassiosira</i> sp.	A	●●	●●	●	●●	●●	●	●●	●●	●	●●	●●	●	●●	●●	●	●	●●	●	●●	●	●	●●	●	●	●	●	●	●	●	●	●	●	●	●
<i>Tropidoneis antarctica</i>	A	●●	●●		●●	●●		●●	●					●	●●					●						●									
unidentified centric	A	●●	●●	●	●●	●	●			●●	●●	●	●		●		●								●●		●	●	●	●	●	●	●●	●	●
unidentified pennate	A	●●	●●	●	●●	●	●	●●	●	●	●●	●	●	●●	●	●	●	●●	●	●	●	●	●●	●	●	●	●	●	●	●	●	●	●	●	●

Table A-1 (contd.) p3

DINOFLAGELLATES	Nutrition	2008		2009		2010		2011		2012		2013		2014						2015														
		KSBP01	NSEX01	MSWH01	KSBP01	NSEX01	NSAJ02	KSBP01	NSEX01	NSAJ02	KSBP01	NSEX01	NSAJ02	KSBP01	NSEX01	NSAJ02	JSUR01	KSBP01	KSSK02	LTED04	LSEP01	LSNT01	NSEX01	NSAJ02	JSUR01	KSBP01	KSSK02	LTED04	LSEP01	LSNT01	NSEX01	NSAJ02		
Akashiwo sanguinea	M	••	••		••	••	•	••	••	•	••	•	••	••	•			••			•	•	••	•	•	•	•	•	•	•	••	•		
Alexandrium catenella	M			•					•	•		•		•	•	•						•	•			•	•	•	•	•	•	•		
Alexandrium sp.	M	••	••	•			•			•	•	•		•					•		•		•	•	•	•								
Amphidinium sphenoides	H										•	••	•			•				•							••			•	•			
Amylax triacantha	M			•		••						••												•										
Ceratium furca*	M				•																			•							•	•		
Ceratium fusus*	M	••	••	•	••	••	•	••	••	•	••	••	•	••	••	•	•	••	•	•	•	•	••	•	•	•	••	•	•	•	•	•	•	
Ceratium lineatum*	M																•	•	•	•	•	•	•	•	•	•	•	•	•	•	•	•	•	
Ceratium sp.*	M	•				•		•																							•			
Cochlodinium sp.*	M										•	•	•		•	•							•		•	•							•	
Dinophysis acuminata	M				••	••	•	•	••	•	•	••	•	•	••	•		••	•			•	••	•	•	•	••	•	•	•	•	•	•	
Dinophysis acuta/norvegica	M				••	••	•	••		••	•	•	•	••	••	•			••				•	•				•		•	•	•	•	
Dinophysis fortii	M				•	•	•	••	•	•		•		•	•									•							•	•		
Dinophysis parva	M				••	••		•	•	•	•	••		•	•		•	•						•		•	•	•	•				•	
Dinophysis rotundata	M					••		••	•		•		•			•																		
Dinophysis sp.	M	••	••	•	••	••	•	•		•	•	••			•					•		•			•	•	•	•			•	•		
diplopsalid dinoflagellate	H				•	••	•	•		•	•	••	•	••	•									•		•							•	
Dissodinium pseudolunula	M						••			•					•							•												
Gonyaulax digitale	M						•	•	•	•	••	•	•	•	•																		•	
Gonyaulax sp.	M		•		•	•		•		•		•	•	•	•				•				•	•	•	•	•	•						
gymnodinioid dinoflagellate	H				••	••	•	••	•	•	•	••	•	•	••	•		••			•	•	•	•	•	•	•	•	•		••	•	•	
Gymnodinium gracile	H						•			••	•	•	•	•	•		•	•	•	•		•	•	•	•	•	•	•					•	
Gymnodinium rubrum	H																																	
Gymnodinium sp.	H	•	••	•	•	•	•	•	••			•	•		•		•	•	•	•		•	•	•	•	•	•		•	•		••	•	
Gyrodinium sp.	H	•			••	••	•	•	••	•	••	•	•	•	•			••		•	•		•	•	•	•	•				•		•	
Gyrodinium spirale	H	•	••		••	••		••	•	•	•	••	•	•	•				•			•	•	•	•	•	•	•	•	•	•	•	•	•
Heterocapsa triquetra	M	•		•	••	••	•	•		••	•	•	•	•	•		•	••	•			•	•	•	•	•	•	•	•	•	•	•	•	•
Karlodinium sp.	M										••	••	•	•	•	•	•	••		•	•	•	•	•	•	•	•			•	•			
Katodinium sp.	H										••	••	•	•	•		•	••	•	•	•	•	•	•		•		•	•	•	•	•	•	
Minuscula bipes	M																																•	
Nematodinium armatum	M										•	••			•	•			•						•	•						•	•	
Noctiluca scintillans	H	••	••	•	••	••	•	••	••	•	••	••	•	•	•		•	••		•			••	•	•	•	•			•	•	•	•	
Oxyphysis oxytoxoides	H	•	•	•	••	••	•	•		•	•	•	•	•	•												•							
Oxytoxum sp.	H				•		•																											
Polykrikos schwartzii	H							••			•		•														•			•	•			
Prorocentrum gracile	M	••	••	•	••	••	•	••	•	•	••	••	•	•	•	•	•	••	•	•		•	•	•	•	•	•	•	•	•	•	•	•	•
Prorocentrum micans	M	•																							•	•		•	•					
Protoceratium reticulatum	M				••	••	•	•		•	•	•																				•	•	

[illegible]

DINOFLAGELLATES (contd.)	Nutrition	2008			2009			2010			2011			2012			2013			2014				2015								
		KSBP01	NSEX01	MSWH01	KSBP01	NSEX01	NSAJ02	KSBP01	NSEX01	NSAJ02	KSBP01	NSEX01	NSAJ02	KSBP01	NSEX01	NSAJ02	JSUR01	KSBP01	KSSK02	LTED04	LSEP01	LSNT01	NSEX01	NSAJ02	JSUR01	KSBP01	KSSK02	LTED04	LSEP01	LSNT01	NSEX01	NSAJ02
<i>Protoperidinium brevipes</i>	H		●●	●		●●	●																							●		
<i>Protoperidinium conicum</i>	H	●●	●●	●	●●	●●	●			●●	●●	●	●●	●●	●		●	●●	●				●	●		●●	●					
<i>Protoperidinium depressum</i>	H	●●	●●	●		●				●●	●●	●	●●	●●	●		●	●●	●	●		●	●●	●		●	●		●	●●	●	
<i>Protoperidinium excentricum</i>	H	●																														
<i>Protoperidinium leonis</i>	H		●			●				●						●							●						●	●	●	
<i>Protoperidinium oblongum</i>	H									●●	●			●	●		●					●●	●									
<i>Protoperidinium oceanicum</i>	H		●●			●●	●	●																			●					
<i>Protoperidinium pellucidum</i>	H																															
<i>Protoperidinium sp.</i>	H	●●	●	●	●●	●●	●	●●	●●	●	●●	●●	●	●●	●●	●	●	●●				●	●●	●	●	●	●	●			●	●
<i>Protoperidinium steinii</i>	H	●●	●●	●	●●	●●	●	●●	●●	●	●●	●●	●	●●	●●	●	●	●●	●	●			●	●	●	●●	●		●	●	●●	●
<i>Scrippsiella trochoidea</i>	M	●●	●●	●	●●	●	●	●●	●●	●	●●	●●	●	●●	●●	●	●	●	●			●	●●	●	●	●●	●	●	●	●	●	●
<i>Torodinium sp.</i>	M																						●	●	●	●				●		
unidentified dinoflagellate (<25 um)	M,H	●●	●●	●	●●	●●	●	●●	●●	●	●●	●●	●	●●	●●	●	●	●●	●	●●	●	●	●●	●	●	●●	●	●	●	●	●●	●
unidentified dinoflagellate (>25 um)	M,H	●●	●●	●	●●	●●	●	●●	●●	●	●●	●●	●	●●	●●	●	●	●●	●	●●	●	●	●●	●	●	●●	●	●	●	●	●●	●
OTHER FLAGELLATES																																
<i>Apedinella spinifera</i>	A												●●	●●	●	●	●	●					●	●	●	●●		●	●		●	●
<i>Chrysochromulina sp.</i>	A																									●						
cryptomonad	A												●			●	●	●	●	●	●	●	●	●	●	●●	●	●		●	●●	●
<i>Dictyocha fibula</i>	A	●●	●●	●	●●	●●	●					●				●	●●		●			●	●			●●		●	●	●	●	●
<i>Dictyocha speculum</i>	A	●●	●●	●	●●	●●	●	●●	●	●	●●	●●	●	●●	●●	●		●●				●	●	●	●	●●	●	●	●	●	●●	●
<i>Dinobryon sp.</i>	M																														●	
<i>Ebria tripartita</i>	H	●	●●	●								●	●					●				●	●		●●		●	●		●		
euglenoid	A														●	●	●								●	●●		●	●		●	
<i>Heterosigma akashiwo</i>	M	●●	●	●	●●	●●	●				●●	●●	●	●●		●	●	●●	●	●●	●	●	●●	●	●	●●	●	●	●	●	●●	●
<i>Meringosphaera mediterranea</i>	H			●		●		●	●	●	●	●		●●	●	●	●●	●	●		●		●●		●●	●●	●	●	●	●	●●	●
<i>Phaeocystis sp.</i>	A	●			●			●●		●		●		●											●	●						●
unidentified nanoflagellates	A,H	●●	●●	●	●●	●●	●	●●	●●	●	●●	●●	●	●●	●●	●	●	●●	●	●●	●	●	●●	●	●	●●	●	●	●	●	●●	●
CILATES AND OTHER ZOOPLANKTON																																
<i>Favella sp.</i>	H																														●	
<i>Heliocostomella sp.</i>	H																										●					
<i>Mesodinium rubrum</i>	M															●	●●	●	●	●	●	●	●●	●	●	●	●	●	●	●	●	●
<i>Parafavella sp.</i>	H																						●						●		●	
<i>Strobilidium sp.</i>	H																					●	●●	●	●	●	●	●		●	●	●
<i>Tiarina fusus</i>	H																		●						●				●●	●	●	
unidentified ciliate	H															●	●	●	●●	●	●	●	●●	●	●	●●	●	●	●	●●	●	●
unidentified tintinnid	H															●			●				●		●						●	
copepod	H																	●	●					●	●●				●	●	●	●
nauplius	H															●	●	●	●	●	●			●●	●		●	●	●	●	●	●
unidentified zooplankton	H																			●	●			●	●	●			●	●●	●	●

Table A-1 (contd.) p5

DIATOMS	Nutrition	2016								2017								2018								2019							
		JSUR01	KSBP01	KSSK02	LTED04	LSEP01	LSKQ06	LSNT01	MSJN02	NSEX01	NSAJ02	JSUR01	KSBP01	KSSK02	LTED04	LSEP01	LSKQ06	LSNT01	MSJN02	NSEX01	NSAJ02	JSUR01	KSBP01	KSSK02	LTED04	LSEP01	LSKQ06	LSNT01	MSJN02	NSEX01	NSAJ02		
<i>Actinopterychus senarius</i>	A	•	•	•	•	•	•	•		•	•						•										•	•	•	•	•		
<i>Asterionella formosa</i>	A																																
<i>Asterionellopsis glacialis</i>	A		•									•	•	•	•	•	•	•	•	•	•	•											
<i>Asteromphalus heptactis</i>	A	•	•	•		•	•	•		•							•	•	•	•	•	•	•	•	•	•		•		•	•		
<i>Bacteriastrium delicatulum</i>	A											•			•			•	•	•	•	•	•							•	•		
<i>Cerataulina pelagica</i>	A	•	•	•	•	•	•	•		•	•	•	•	•	•	•	•	•		•	•	•	•	•	•	•	•	•	•	•	•	•	•
<i>Chaetoceros (Hyalochaete) sp.</i>	A	•	•	•	•	•	•	•	•	•	•	•	•	•	•	•	•	•	•	•	•	•	•	•	•	•	•	•	•	•	•	•	•
<i>Chaetoceros (Phaeoceros) sp.</i>	A	•	•	•	•	•	•	•	•	•			•				•				•												
<i>Chaetoceros affinis</i>	A																																
<i>Chaetoceros concavicornis</i>	A																																
<i>Chaetoceros contortus</i>	A	•	•	•	•	•	•	•	•	•	•	•	•	•	•	•	•	•	•	•	•	•	•	•	•	•	•	•	•	•	•	•	•
<i>Chaetoceros convolutus</i>	A																																
<i>Chaetoceros crucifer</i>	A	•	•	•	•	•	•	•	•												•												
<i>Chaetoceros danicus</i>	A	•	•	•	•	•	•	•	•	•	•	•	•	•			•	•	•	•			•	•	•	•	•	•	•	•	•	•	•
<i>Chaetoceros debilis</i>	A	•	•	•	•	•	•	•	•	•	•	•	•	•	•	•	•	•	•	•	•	•	•	•	•	•	•	•	•	•	•	•	•
<i>Chaetoceros decipiens</i>	A	•	•	•	•	•	•	•	•	•	•	•	•	•	•	•	•	•	•	•	•	•	•	•	•	•	•	•	•	•	•	•	•
<i>Chaetoceros diadema</i>	A	•	•	•	•	•	•	•	•	•	•	•	•	•	•	•	•	•	•	•	•	•	•	•	•	•	•	•	•	•	•	•	•
<i>Chaetoceros didymus</i>	A	•	•	•	•	•	•	•	•	•	•	•	•	•	•	•	•	•	•	•	•	•	•	•	•	•	•	•	•	•	•	•	•
<i>Chaetoceros eibenii</i>	A	•	•	•			•		•	•																							
<i>Chaetoceros laciniosus</i>	A	•	•	•	•	•	•	•	•	•	•	•	•	•	•	•	•	•	•	•	•	•	•	•	•	•	•	•	•	•	•	•	•
<i>Chaetoceros lorenzianus</i>	A																																
<i>Chaetoceros radicans</i>	A	•	•	•	•	•	•	•	•	•	•	•	•	•	•	•	•	•	•	•	•	•	•	•	•	•	•	•	•	•	•	•	•
<i>Chaetoceros similis</i>	A	•	•	•	•	•	•	•	•	•	•	•	•	•	•	•	•	•	•	•	•	•	•	•	•	•	•	•	•	•	•	•	•
<i>Chaetoceros socialis</i>	A	•	•	•	•	•	•	•	•	•	•	•	•	•	•	•	•	•	•	•	•	•	•	•	•	•	•	•	•	•	•	•	•
<i>Chaetoceros subtilis</i>	A	•											•								•												
<i>Chaetoceros teres</i>	A	•				•	•	•		•	•	•	•																				
<i>Chaetoceros vanheurckii</i>	A	•	•	•	•	•	•	•	•	•	•	•	•	•	•	•	•	•	•	•	•	•	•	•	•	•	•	•	•	•	•	•	•
<i>Corethron hystrix</i>	A	•	•	•	•	•	•	•	•	•		•																					
<i>Coscinodiscus centralis</i>	A	•																															
<i>Coscinodiscus concinnus</i>	A																																
<i>Coscinodiscus curvatulus</i>	A																																
<i>Coscinodiscus granii</i>	A																																
<i>Coscinodiscus marginatus</i>	A																																
<i>Coscinodiscus oculus-iridis</i>	A					•																											
<i>Coscinodiscus sp.</i>	A		•		•	•		•	•	•	•	•																					
<i>Coscinodiscus walleseii</i>	A	•	•				•		•	•																							
<i>Cylindrotheca closterium</i>	A	•	•	•	•	•	•	•	•	•	•	•	•	•	•	•	•	•	•	•	•	•	•	•	•	•	•	•	•	•	•	•	•

Table A-1 (contd.) p6

DIATOMS (contd.)	Nutrition	2016								2017								2018								2019							
		JSUR01	KSBP01	KSSK02	LTED04	LSEP01	LSKC06	LSNT01	MSJN02	NSEX01	NSAJ02	JSUR01	KSBP01	KSSK02	LTED04	LSEP01	LSKC06	LSNT01	MSJN02	NSEX01	NSAJ02	JSUR01	KSBP01	KSSK02	LTED04	LSEP01	LSKC06	LSNT01	MSJN02	NSEX01	NSAJ02		
<i>Dactyliosolen fragilissimus</i>	A	●	●	●	●	●				●	●	●	●	●	●		●	●			●	●			●				●		●		
<i>Detonula pumila</i>	A	●	●	●	●	●	●		●			●	●	●	●	●						●	●							●			
<i>Ditylum brightwellii</i>	A	●	●	●	●	●	●		●			●	●	●	●	●						●	●			●				●			
<i>Eucampia zodiacus</i>	A	●	●	●	●	●	●		●			●	●	●	●	●						●	●			●				●			
<i>Guinardia delicatula</i>	A	●	●	●	●	●	●		●			●	●	●	●	●						●	●			●				●			
<i>Guinardia striata</i>	A	●	●	●	●	●	●		●			●	●	●	●	●						●	●			●				●			
<i>Hemiaulus hauckii</i>	A	●	●	●	●	●	●		●			●	●	●	●	●														●			
<i>Lauderia annulata</i>	A	●	●	●	●	●	●		●			●	●	●	●	●																	
<i>Leptocylindrus danicus</i>	A	●	●	●	●	●	●		●			●	●	●	●	●						●	●			●				●			
<i>Leptocylindrus minimus</i>	A	●	●	●	●	●	●		●			●	●	●	●	●						●	●			●				●			
<i>Melosira moniliformis</i>	A																																
<i>Navicula</i> sp.	A																																
<i>Nitzschia acicularis</i>	A	●	●	●		●	●	●	●	●	●		●		●		●	●	●	●	●	●	●	●	●	●	●	●	●	●	●		
<i>Odontella aurita</i>	A	●	●																														
<i>Odontella longicruris</i>	A	●	●		●	●	●	●	●	●	●																						
<i>Paralia sulcata</i>	A	●	●		●	●	●	●	●	●	●	●	●	●	●	●						●	●	●	●	●	●	●	●	●	●		
<i>Pleurosigma</i> sp.	A	●	●	●	●	●	●		●			●	●	●	●	●						●	●	●	●	●	●	●	●	●	●		
<i>Pseudo-nitzschia americana</i>	A	●	●	●	●	●	●		●			●	●	●	●	●	●	●	●	●	●	●	●	●	●	●	●	●	●	●	●		
<i>Pseudo-nitzschia</i> sp. (large)	A	●	●	●	●	●	●		●			●	●	●	●	●	●	●	●	●	●	●	●	●	●	●	●	●	●	●	●		
<i>Pseudo-nitzschia</i> sp. (small)	A	●	●	●	●	●	●		●			●	●	●	●	●	●	●	●	●	●	●	●	●	●	●	●	●	●	●	●		
<i>Pyrophacus horologium</i>	A							●																									
<i>Rhizosolenia setigera</i>	A	●	●	●	●	●	●		●			●	●	●	●	●	●	●	●	●	●	●	●	●	●	●	●	●	●	●	●		
<i>Skeletonema costatum</i>	A	●	●	●	●	●	●	●	●	●	●	●	●	●	●	●	●	●	●	●	●	●	●	●	●	●	●	●	●	●	●		
<i>Stephanopyxis nipponica</i>	A	●	●	●		●	●	●					●				●	●	●	●	●												
<i>Stephanopyxis palmeriana</i>	A		●	●	●	●	●	●	●																								
<i>Thalassionema frauenfeldii</i>	A											●	●	●								●							●				
<i>Thalassionema nitzschioides</i>	A	●	●	●	●	●	●	●	●	●	●	●	●	●	●	●	●	●	●	●	●	●	●	●	●	●	●	●	●	●	●		
<i>Thalassiosira anguste-lineata</i>	A	●	●	●	●	●	●	●	●	●	●	●	●	●	●	●	●	●	●	●	●	●	●	●	●	●	●	●	●	●	●		
<i>Thalassiosira eccentrica</i>	A																																
<i>Thalassiosira nordenskiöldii</i>	A	●	●	●	●	●	●		●			●	●	●	●	●	●	●	●	●	●	●	●	●	●	●	●	●	●	●	●		
<i>Thalassiosira pacifica/aestivalis</i>	A	●	●	●	●	●	●		●			●	●	●	●	●	●	●	●	●	●	●	●	●	●	●	●	●	●	●	●		
<i>Thalassiosira punctigera</i>	A			●								●																					
<i>Thalassiosira rotula</i>	A	●	●	●	●	●	●		●			●	●	●	●	●	●	●	●	●	●	●	●	●	●	●	●	●	●	●	●		
<i>Thalassiosira</i> sp.	A	●	●	●	●	●	●		●			●	●	●	●	●	●	●	●	●	●	●	●	●	●	●	●	●	●	●	●		
<i>Tropidoneis antarctica</i>	A																						●										
unidentified centric	A	●	●	●	●	●	●		●	●	●	●	●	●	●	●	●	●	●	●	●	●	●	●	●	●	●	●	●	●	●		
unidentified pennate	A	●	●	●	●	●	●		●	●	●	●	●	●	●	●	●	●	●	●	●	●	●	●	●	●	●	●	●	●	●		

Table A-1 (contd.) p7

DINOFLAGELLATES	Nutrition	2016												2017								2018								2019											
		JSUR01	KSBP01	KSSK02	LTED04	LSEP01	LSKQ06	LSNT01	MSJN02	NSEX01	NSAJ02	JSUR01	KSBP01	KSSK02	LTED04	LSEP01	LSKQ06	LSNT01	MSJN02	NSEX01	NSAJ02	JSUR01	KSBP01	KSSK02	LTED04	LSEP01	LSKQ06	LSNT01	MSJN02	NSEX01	NSAJ02	JSUR01	KSBP01	KSSK02	LTED04	LSEP01	LSKQ06	LSNT01	MSJN02	NSEX01	NSAJ02
Akashiwo sanguinea	M	●	●	●	●	●	●	●	●	●	●	●	●	●	●	●	●	●	●	●	●	●	●	●	●	●	●	●	●	●	●	●	●	●	●	●	●	●	●	●	●
Alexandrium catenella	M	●																																							
Alexandrium sp.	M						●	●		●		●	●		●	●						●	●																		
Amphidinium sphenoides	H				●				●																																
Amylax triacantha	M							●		●	●																														
Ceratium furca*	M								●						●																										
Ceratium fusus*	M		●	●	●	●	●	●	●	●	●	●	●	●	●	●	●	●	●	●	●	●		●		●									●		●	●	●		
Ceratium lineatum*	M										●		●	●	●	●	●	●	●	●	●											●			●		●				
Ceratium sp.*	M																																								
Cochlodinium sp.*	M							●		●			●															●													
Dinophysis acuminata	M	●	●	●			●	●		●	●	●	●	●	●	●	●	●	●	●	●	●	●		●	●	●		●	●										●	
Dinophysis acuta/norvegica	M	●	●	●		●	●	●	●	●	●	●	●						●				●		●																
Dinophysis fortii	M						●		●		●								●		●																				
Dinophysis parva	M			●			●		●		●										●		●					●	●											●	
Dinophysis rotundata	M												●						●																						
Dinophysis sp.	M					●																																			
diplopsalid dinoflagellate	H	●	●	●	●		●	●	●	●	●											●	●	●			●	●	●	●	●	●	●	●	●	●	●	●	●	●	
Dissodinium pseudolunula	M						●					●								●																					
Gonyaulax digitale	M				●																																				
Gonyaulax sp.	M	●	●			●	●	●	●	●	●										●	●		●																	
gymnodinioid dinoflagellate	H	●	●	●	●		●	●	●	●	●				●		●		●	●	●	●	●	●	●	●	●	●	●	●	●	●	●	●	●	●	●	●	●	●	
Gymnodinium gracile	H	●	●	●		●	●		●	●		●											●					●	●												
Gymnodinium rubrum	H																																								
Gymnodinium sp.	H	●	●	●		●				●			●									●						●													
Gyrodinium sp.	H		●						●																																
Gyrodinium spirale	H	●	●	●	●	●	●	●	●	●									●		●	●	●	●	●	●	●	●	●	●	●	●	●	●	●	●	●	●	●	●	
Heterocapsa triquetra	M	●	●	●	●		●	●	●	●	●	●	●	●	●	●	●	●	●	●	●	●	●	●	●	●	●	●	●	●	●	●	●	●	●	●	●	●	●	●	
Karlodinium sp.	M	●	●	●		●	●	●	●	●									●		●	●	●	●	●	●	●	●	●	●	●	●	●	●	●	●	●	●	●	●	
Katodinium sp.	H	●	●			●	●		●			●	●	●	●	●	●	●	●	●	●	●	●	●	●	●	●	●	●	●	●	●	●	●	●	●	●	●	●	●	●
Minuscula bipes	M																																								
Nematodinium armatum	M	●				●		●	●	●										●																●	●	●	●		
Noctiluca scintillans	H					●		●		●	●											●	●	●			●	●	●							●	●	●	●	●	
Oxyphysis oxytoxoides	H		●			●			●	●	●											●																		●	
Oxytoxum sp.	H																																								
Polykrikos schwartzii	H		●			●			●	●	●					●																						●			
Prorocentrum gracile	M	●	●	●		●	●	●		●	●	●	●	●	●	●	●	●	●	●	●	●	●	●	●	●	●	●	●	●	●	●	●	●	●	●	●	●	●	●	
Prorocentrum micans	M	●	●					●	●		●		●	●	●	●	●	●	●	●	●	●	●	●	●	●	●	●	●	●	●	●	●	●	●	●	●	●	●	●	
Protoceratium reticulatum	M					●				●	●	●	●	●	●	●	●	●	●	●	●	●	●	●	●	●	●	●	●	●	●	●	●	●	●	●	●	●	●	●	

Table A-1 (contd.) p8

DINOFLAGELLATES (contd.)	Nutrition	2016								2017								2018								2019													
		JSUR01	KSBP01	KSSK02	LTED04	LSEP01	LSKQ06	LSNT01	MSJN02	NSEX01	NSAJ02	JSUR01	KSBP01	KSSK02	LTED04	LSEP01	LSKQ06	LSNT01	MSJN02	NSEX01	NSAJ02	JSUR01	KSBP01	KSSK02	LTED04	LSEP01	LSKQ06	LSNT01	MSJN02	NSEX01	NSAJ02								
<i>Protoperidinium brevipes</i>	H																																						
<i>Protoperidinium conicum</i>	H																																						
<i>Protoperidinium depressum</i>	H																																						
<i>Protoperidinium excentricum</i>	H																																						
<i>Protoperidinium leonis</i>	H																																						
<i>Protoperidinium oblongum</i>	H																																						
<i>Protoperidinium oceanicum</i>	H																																						
<i>Protoperidinium pellucidum</i>	H																																						
<i>Protoperidinium</i> sp.	H																																						
<i>Protoperidinium steinii</i>	H																																						
<i>Scrippsiella trochoidea</i>	M																																						
<i>Torodinium</i> sp.	M																																						
unidentified dinoflagellate (<25 um)	M,H																																						
unidentified dinoflagellate (>25 um)	M,H																																						
OTHER FLAGELLATES																																							
<i>Apedinella spinifera</i>	A																																						
<i>Chrysochromulina</i> sp.	A																																						
cryptomonad	A																																						
<i>Dictyocha fibula</i>	A																																						
<i>Dictyocha speculum</i>	A																																						
<i>Dinobryon</i> sp.	M																																						
<i>Ebria tripartita</i>	H																																						
euglenoid	A																																						
<i>Heterosigma akashiwo</i>	M																																						
<i>Meringosphaera mediterranea</i>	H																																						
<i>Phaeocystis</i> sp.	A																																						
unidentified nanoflagellates	A,H																																						
CILIALES AND OTHER ZOOPLANKTON																																							
<i>Favella</i> sp.	H																																						
<i>Helicostomella</i> sp.	H																																						
<i>Mesodinium rubrum</i>	M																																						
<i>Parafavella</i> sp.	H																																						
<i>Strobilidium</i> sp.	H																																						
<i>Tiarina fusus</i>	H																																						
unidentified ciliate	H																																						
unidentified tintinnid	H																																						
copepod	H																																						
nauplius	H																																						
unidentified zooplankton	H																																						

Nutrition/Functional Group:

A Autotrophic

M Mixotrophic (tentative assignment)

H Heterotrophic

***Name changes:**

Ceratium is now *Triplos*

Cochlodinium is now *Margalefidinium*

Appendix B: POC Study

Table B-1 Particulate organic C and N results from combustion analysis for particles in fraction A (1.5-100 µm). Also shown are corresponding biovolume results from FlowCAM analysis for particles in fraction A (5-100 µm).

Sample ID	Locator	Fraction	Date Collected	C Amount (µg)	N Amount (µg)	Vol filt'd. (mL)	C/vol (µg/L)	N/vol (µg/L)	Biovolume (mm ³ /L)	C/N (wt/wt)
L62974-1	KSBP01	A	6/15/15	207.05	49.53	250	828.18	198.13	4.9	4.2
L62974-3	JSUR01	A	6/15/15	148.09	30.48	250	592.35	121.94	10.84	4.9
L62974-4	KSSK02	A	6/15/15	111.68	33.41	250	446.72	133.65	7.251	3.3
L62974-5	LTED04	A	6/15/15	115.25	38.77	250	461.02	155.07	15.54	3.0
L62974-6	LSEP01	A	6/16/15	124.74	36.34	250	498.95	145.34	10.08	3.4
L62974-7	LSNT01	A	6/16/15	40.49	8.73	250	161.98	34.91	3.916	4.6
L62974-8	NSEX01	A	6/16/15	116.35	22.76	250	465.42	91.02	3.114	5.1
L62974-10	NSAJ02	A	6/17/15	112.23	22.36	250	448.92	89.45	5.656	5.0
L63060-1	KSBP01	A	7/6/15	57.64	11.71	250	230.56	46.82	4.436	4.9
L63060-3	JSUR01	A	7/6/15	54.79	9.93	250	219.14	39.72	2.383	5.5
L63060-4	KSSK02	A	7/6/15	112.65	23.19	250	450.60	92.78	7.023	4.9
L63060-5	LTED04	A	7/6/15	76.59	14.41	250	306.35	57.65	6.683	5.3
L63060-6	LSEP01	A	7/7/15	33.76	5.50	250	135.02	22.00	0.8243	6.1
L63060-7	LSNT01	A	7/7/15	34.53	5.18	250	138.14	20.71	0.9398	6.7
L63060-8	NSEX01	A	7/7/15	43.62	8.07	250	174.49	32.26	0.9228	5.4
L63060-10	NSAJ02	A	7/8/15	104.87	20.83	250	419.47	83.33	3.723	5.0
L63121-1	KSBP01	A	7/20/15	269.07	48.57	250	1076.29	194.28	35.71	5.5
L63121-3	JSUR01	A	7/20/15	232.02	74.70	250	928.07	298.82	41.68	3.1
L63121-4	KSSK02	A	7/21/15	278.60	76.86	250	1114.42	307.42	44.55	3.6
L63121-5	LTED04	A	7/21/15	170.68	37.42	250	682.72	149.70	22.5	4.6
L63121-6	LSEP01	A	7/23/15	81.88	16.89	250	327.53	67.55	4.725	4.8
L63121-7	LSNT01	A	7/23/15	88.84	29.32	250	355.38	117.29	4.679	3.0
L63121-8	NSEX01	A	7/23/15	174.91	44.67	250	699.63	178.70	8.698	3.9
L63121-10	NSAJ02	A	7/22/15	312.51	52.05	500	625.03	104.11	3.281	6.0
L63268-1	KSBP01	A	8/3/15	369.53	64.73	500	739.07	129.47	36.94	5.7
L63268-3	JSUR01	A	8/3/15	427.28	59.29	500	854.57	118.57	36.57	7.2

Sample ID	Locator	Fraction	Date Collected	C Amount (µg)	N Amount (µg)	Vol filt'd. (mL)	C/vol (µg/L)	N/vol (µg/L)	Biovolume (mm³/L)	C/N (wt/wt)
L63268-4	KSSK02	A	8/3/15	233.56	47.35	500	467.12	94.70	25.07	4.9
L63268-5	LTED04	A	8/3/15	260.61	48.41	500	521.23	96.81	27.5	5.4
L63268-6	LSEP01	A	8/4/15	115.44	22.00	500	230.89	44.00	4.482	5.2
L63268-7	LSNT01	A	8/4/15	87.52	16.12	500	175.04	32.23	2.181	5.4
L63268-8	NSEX01	A	8/4/15	308.47	49.68	500	616.93	99.36	22.64	6.2
L63268-10	NSAJ02	A	8/5/15	95.94	17.96	500	191.88	35.91	11.73	5.3
L63401-1	KSBP01	A	8/17/15	121.25	21.40	1000	121.25	21.40	0.9271	5.7
L63401-3	JSUR01	A	8/17/15	151.08	26.98	1000	151.08	26.98	0.5739	5.6
L63401-4	KSSK02	A	8/17/15	126.68	24.15	1000	126.68	24.15	0.9989	5.2
L63401-5	LTED04	A	8/17/15	116.50	22.12	1000	116.50	22.12	1.033	5.3
L63401-6	LSEP01	A	8/18/15	135.50	24.73	1000	135.50	24.73	0.7362	5.5
L63401-7	LSNT01	A	8/18/15	92.68	26.08	1000	92.68	26.08	0.4456	3.6
L63401-8	NSEX01	A	8/18/15	159.87	31.20	1000	159.87	31.20	1.356	5.1
L63401-10	NSAJ02	A	8/19/15	417.41	68.31	1000	417.41	68.31	5.635	6.1
L63522-1	KSBP01	A	9/8/15	109.23	18.18	1000	109.23	18.18	0.1844	6.0
L63522-3	JSUR01	A	9/8/15	104.52	20.41	1000	104.52	20.41	0.3163	5.1
L63522-4	KSSK02	A	9/8/15	81.94	24.18	1000	81.94	24.18	0.4027	3.4
L63522-5	LTED04	A	9/8/15	101.67	22.81	1000	101.67	22.81	0.7876	4.5
L63522-6	LSEP01	A	9/9/15	81.29	16.96	1000	81.29	16.96	0.6342	4.8
L63522-7	LSNT01	A	9/9/15	71.75	19.09	1000	71.75	19.09	0.3386	3.8
L63522-8	NSEX01	A	9/9/15	90.04	17.30	1000	90.04	17.30	0.5685	5.2
L63522-10	NSAJ02	A	9/9/15	315.31	66.27	1000	315.31	66.27	4.513	4.8
L63669-1	KSBP01	A	9/21/15	142.11	25.50	1000	142.11	25.50	0.959	5.6
L63669-3	JSUR01	A	9/21/15	118.13	21.78	1000	118.13	21.78	1.993	5.4
L63669-4	KSSK02	A	9/21/15	97.16	15.80	1000	97.16	15.80	1.102	6.1
L63669-5	LTED04	A	9/21/15	273.00	48.84	1000	273.00	48.84	3.06	5.6
L63669-6	LSEP01	A	9/22/15	254.04	49.11	1000	254.04	49.11	4.232	5.2
L63669-7	LSNT01	A	9/22/15	396.26	80.16	1000	396.26	80.16	4.899	4.9

Sample ID	Locator	Fraction	Date Collected	C Amount (µg)	N Amount (µg)	Vol filt'd. (mL)	C/vol (µg/L)	N/vol (µg/L)	Biovolume (mm³/L)	C/N (wt/wt)
L63669-8	NSEX01	A	9/22/15	306.79	55.29	500	613.57	110.58	12.29	5.5
L63669-10	NSAJ02	A	9/23/15	415.43	44.04	500	830.86	88.07	24.25	9.4
L63820-1	KSBP01	A	10/5/15	58.87	10.37	1000	58.87	10.37	0.3553	5.7
L63820-3	JSUR01	A	10/5/15	63.50	10.07	1000	63.50	10.07	0.5385	6.3
L63820-4	KSSK02	A	10/5/15	77.53	13.88	1000	77.53	13.88	1.17	5.6
L63820-5	LTED04	A	10/5/15	88.13	16.55	1000	88.13	16.55	0.5539	5.3
L63820-6	LSEP01	A	10/6/15	67.63	11.88	1000	67.63	11.88	0.4974	5.7
L63820-7	LSNT01	A	10/6/15	81.88	13.69	1000	81.88	13.69	0.4387	6.0
L63820-8	NSEX01	A	10/6/15	55.05	8.83	1000	55.05	8.83	0.3907	6.2
L63820-10	NSAJ02	A	10/7/15	495.39	93.51	1000	495.39	93.51	12.61	5.3
L63863-1	KSBP01	A	10/19/15	81.06	13.92	1000	81.06	13.92	0.3913	5.8
L63863-3	JSUR01	A	10/19/15	89.10	12.91	1000	89.10	12.91	0.4635	6.9
L63863-4	KSSK02	A	10/19/15	94.77	16.93	1000	94.77	16.93	1.005	5.6
L63863-5	LTED04	A	10/19/15	81.77	13.61	1000	81.77	13.61	0.3941	6.0
L63863-6	LSEP01	A	10/20/15	88.97	29.86	1000	88.97	29.86	0.6412	3.0
L63863-7	LSNT01	A	10/20/15	70.76	11.08	1000	70.76	11.08	0.7656	6.4
L63863-8	NSEX01	A	10/20/15	103.22	18.27	1000	103.22	18.27	0.6677	5.6
L63863-10	NSAJ02	A	10/21/15	388.15	75.87	1000	388.15	75.87	6.468	5.1
L64027-1	KSBP01	A	11/2/15	55.77	8.56	1000	55.77	8.56	0.3708	6.5
L64027-3	JSUR01	A	11/2/15	56.44	8.87	1000	56.44	8.87	0.2795	6.4
L64027-4	KSSK02	A	11/2/15	164.58	16.57	1000	164.58	16.57	0.8088	9.9
L64027-5	LTED04	A	11/2/15	150.81	19.04	500	301.62	38.08	1.057	7.9
L64027-6	LSEP01	A	11/3/15	74.31	10.33	1000	74.31	10.33	0.3215	7.2
L64027-7	LSNT01	A	11/3/15	60.73	8.91	1000	60.73	8.91	0.2761	6.8
L64027-8	NSEX01	A	11/3/15	82.15	13.33	1000	82.15	13.33	0.6134	6.2
L64027-10	NSAJ02	A	11/4/15	151.19	24.64	1000	151.19	24.64	1.27	6.1
L64127-1	KSBP01	A	11/19/15	60.93	9.44	1000	60.93	9.44	0.5481	6.5
L64127-3	JSUR01	A	11/19/15	99.33	14.60	1000	99.33	14.60	1.115	6.8

Sample ID	Locator	Fraction	Date Collected	C Amount (µg)	N Amount (µg)	Vol filt'd. (mL)	C/vol (µg/L)	N/vol (µg/L)	Biovolume (mm³/L)	C/N (wt/wt)
L64127-4	KSSK02	A	11/19/15	86.03	12.50	1000	86.03	12.50	0.5469	6.9
L64127-5	LTED04	A	11/19/15	176.06	17.43	1000	176.06	17.43	13.17	10.1
L64127-6	LSEP01	A	11/18/15	56.47	8.55	1000	56.47	8.55	0.4875	6.6
L64127-7	LSNT01	A	11/18/15	58.78	7.96	1000	58.78	7.96	0.5379	7.4
L64127-8	NSEX01	A	11/18/15	87.61	10.55	1000	87.61	10.55	1.802	8.3
L64127-10	NSAJ02	A	11/18/15	198.00	29.66	1000	198.00	29.66	2.45	6.7
L64191-1	KSBP01	A	12/14/15	62.08	9.41	1000	62.08	9.41	0.6785	6.6
L64191-3	JSUR01	A	12/14/15	54.67	7.91	1000	54.67	7.91	0.6196	6.9
L64191-4	KSSK02	A	12/14/15	91.24	15.77	1000	91.24	15.77	1.729	5.8
L64191-5	LTED04	A	12/14/15	129.21	14.58	1000	129.21	14.58	2.368	8.9
L64191-6	LSEP01	A	12/15/15	60.85	7.22	1000	60.85	7.22	0.7885	8.4
L64191-7	LSNT01	A	12/15/15	74.11	8.40	900	82.35	9.33	0.7389	8.8
L64191-8	NSEX01	A	12/15/15	88.08	13.29	1000	88.08	13.29	2.12	6.6
L64191-10	NSAJ02	A	12/16/15	138.56	17.25	1000	138.56	17.25	1.374	8.0
L65057-1	KSBP01	A	3/21/16	nd ⁽¹⁾	nd ⁽¹⁾	1000	-	-	4.784	-
L65057-2	JSUR01	A	3/21/16	340.22	65.82	1000	340.22	65.82	7.783	5.2
L65057-3	KSSK02	A	3/21/16	331.99	58.07	1000	331.99	58.07	5.795	5.7
L65057-4	LTED04	A	3/21/16	312.79	68.40	1000	312.79	68.40	3.389	4.6
L65057-5	LSEP01	A	3/21/16	148.71	26.54	1000	148.71	26.54	2.533	5.6
L65057-7	LSNT01	A	3/21/16	111.12	18.63	1000	111.12	18.63	2.931	6.0
L65057-9	NSEX01	A	3/21/16	198.10	38.80	1000	198.10	38.80	3.56	5.1
L65057-10	NSAJ02	A	3/21/16	362.17	66.25	1000	362.17	66.25	2.561	5.5
L64988-1	KSBP01	A	4/6/16	293.56	62.41	1000	293.56	62.41	4.059	4.7
L64988-2	JSUR01	A	4/6/16	305.02	72.44	1000	305.02	72.44	2.405	4.2
L64988-3	KSSK02	A	4/6/16	360.60	72.68	1000	360.60	72.68	7.462	5.0
L64988-4	LTED04	A	4/6/16	252.32	48.77	1000	252.32	48.77	3.707	5.2
L64988-5	LSEP01	A	4/5/16	627.07	105.51	1000	627.07	105.51	5.674	5.9
L64988-7	LSNT01	A	4/5/16	477.27	91.90	1000	477.27	91.90	3.405	5.2

Sample ID	Locator	Fraction	Date Collected	C Amount (µg)	N Amount (µg)	Vol filt'd. (mL)	C/vol (µg/L)	N/vol (µg/L)	Biovolume (mm³/L)	C/N (wt/wt)
L64988-9	NSEX01	A	4/5/16	470.22	87.89	1000	470.22	87.89	7.989	5.4
L64988-10	NSAJ02	A	4/5/16	191.51	34.25	1000	191.51	34.25	4.361	5.6
L65045-1	KSBP01	A	4/18/16	667.12	140.13	1000	667.12	140.13	22.3	4.8
L65045-2	JSUR01	A	4/18/16	781.33	194.98	1000	781.33	194.98	28.99	4.0
L65045-3	KSSK02	A	4/18/16	443.42	99.35	1000	443.42	99.35	10.52	4.5
L65045-4	LTED04	A	4/18/16	329.31	65.27	1000	329.31	65.27	7.228	5.0
L65045-5	LSEP01	A	4/19/16	503.97	79.96	1000	503.97	79.96	30.69	6.3
L65045-7	LSNT01	A	4/19/16	257.54	51.14	1000	257.54	51.14	10.93	5.0
L65045-9	NSEX01	A	4/19/16	1222.04	139.67	1000	1222.04	139.67	73.83	8.7
L65045-10	NSAJ02	A	4/20/16	749.26	85.32	1000	749.26	85.32	13.67	8.8
L65150-1	KSBP01	A	5/2/2016	454.16	54.27	1000	454.16	54.27	23.24	8.4
L65150-2	JSUR01	A	5/2/2016	662.99	77.47	1000	662.99	77.47	16.68	8.6
L65150-3	KSSK02	A	5/2/2016	692.81	98.36	1000	692.81	98.36	24.73	7.0
L65150-4	LTED04	A	5/2/2016	491.12	62.03	1000	491.12	62.03	29.42	7.9
L65150-5	LSEP01	A	5/3/2016	452.43	82.54	1000	452.43	82.54	14.42	5.5
L65150-7	LSNT01	A	5/3/2016	522.14	94.91	1000	522.14	94.91	31.19	5.5
L65150-9	NSEX01	A	5/3/2016	634.60	80.40	1000	634.60	80.40	40.43	7.9
L65150-10	NSAJ02	A	5/4/2016	315.74	48.20	1000	315.74	48.20	14.53	6.6
L65302-1	KSBP01	A	5/16/2016	122.41	30.69	1000	122.41	30.69	2.021	4.0
L65302-2	JSUR01	A	5/16/2016	131.72	24.09	1000	131.72	24.09	1.193	5.5
L65302-3	KSSK02	A	5/16/2016	104.83	26.39	1000	104.83	26.39	1.632	4.0
L65302-4	LTED04	A	5/16/2016	70.24	14.99	1000	70.24	14.99	0.3895	4.7
L65302-5	LSEP01	A	5/17/2016	523.75	106.75	1000	523.75	106.75	12.78	4.9
L65302-7	LSNT01	A	5/17/2016	566.91	118.37	1000	566.91	118.37	20.27	4.8
L65302-9	NSEX01	A	5/17/2016	672.63	126.65	1000	672.63	126.65	30.36	5.3
L65302-10	NSAJ02	A	5/18/2016	498.10	58.83	1000	498.10	58.83	32.69	8.5
L65360-1	KSBP01	A	6/6/2016	276.45	57.89	1000	276.45	57.89	8.563	4.8
L65360-2	JSUR01	A	6/6/2016	426.79	75.62	1000	426.79	75.62	7.24	5.6

Sample ID	Locator	Fraction	Date Collected	C Amount (µg)	N Amount (µg)	Vol filt'd. (mL)	C/vol (µg/L)	N/vol (µg/L)	Biovolume (mm³/L)	C/N (wt/wt)
L65360-3	KSSK02	A	6/6/2016	503.50	91.24	1000	503.50	91.24	5.121	5.5
L65360-4	LTED04	A	6/6/2016	366.18	74.99	1000	366.18	74.99	4.099	4.9
L65360-5	LSEP01	A	6/7/2016	300.64	66.74	1000	300.64	66.74	3.655	4.5
L65360-7	LSNT01	A	6/7/2016	236.03	73.92	1000	236.03	73.92	2.809	3.2
L65360-9	NSEX01	A	6/7/2016	207.78	40.12	1000	207.78	40.12	2.027	5.2
L65360-10	NSAJ02	A	6/10/2016	308.82	68.57	1000	308.82	68.57	6.628	4.5
L65486-1	KSBP01	A	6/20/2016	523.70	77.72	1000	523.70	77.72	7.098	6.7
L65486-2	JSUR01	A	6/20/2016	430.43	67.20	1000	430.43	67.20	6.348	6.4
L65486-3	KSSK02	A	6/20/2016	464.75	81.47	1000	464.75	81.47	5.29	5.7
L65486-4	LTED04	A	6/20/2016	390.32	73.10	1000	390.32	73.10	3.514	5.3
L65486-5	LSEP01	A	6/21/2016	382.24	70.99	1000	382.24	70.99	8.073	5.4
L65486-7	LSNT01	A	6/21/2016	384.87	82.82	1000	384.87	82.82	3.86	4.6
L65486-9	NSEX01	A	6/21/2016	533.30	67.21	1000	533.30	67.21	7.5	7.9
L65486-10	NSAJ02	A	6/22/2016	469.06	92.68	1000	469.06	92.68	5.62	5.1
L65565-1	KSBP01	A	7/5/2016	412.29	83.37	1000	412.29	83.37	3.2	4.9
L65565-2	JSUR01	A	7/5/2016	399.25	74.89	1000	399.25	74.89	5.551	5.3
L65565-3	KSSK02	A	7/5/2016	233.71	44.33	1000	233.71	44.33	3.511	5.3
L65565-4	LTED04	A	7/5/2016	262.31	48.08	1000	262.31	48.08	2.929	5.5
L65565-5	LSEP01	A	7/6/2016	177.72	39.03	1000	177.72	39.03	1.504	4.6
L65565-7	LSNT01	A	7/6/2016	199.27	38.23	1000	199.27	38.23	1.682	5.2
L65565-9	NSEX01	A	7/6/2016	285.90	50.92	1000	285.90	50.92	6.217	5.6
L65565-10	NSAJ02	A	7/6/2016	223.73	49.12	864	258.95	56.85	1.414	4.6
L65692-1	KSBP01	A	7/18/2016	668.71	98.64	1000	668.71	98.64	13.09	6.8
L65692-2	JSUR01	A	7/18/2016	623.43	92.62	1000	623.43	92.62	14.86	6.7
L65692-3	KSSK02	A	7/18/2016	765.38	135.61	1000	765.38	135.61	17.26	5.6
L65692-4	LTED04	A	7/18/2016	502.56	92.40	1000	502.56	92.40	8.402	5.4
L65692-5	LSEP01	A	7/19/2016	391.85	74.22	1000	391.85	74.22	9.82	5.3
L65692-7	LSNT01	A	7/19/2016	366.92	68.55	1000	366.92	68.55	7.047	5.4

Sample ID	Locator	Fraction	Date Collected	C Amount (µg)	N Amount (µg)	Vol filt'd. (mL)	C/vol (µg/L)	N/vol (µg/L)	Biovolume (mm³/L)	C/N (wt/wt)
L65692-9	NSEX01	A	7/19/2016	542.71	72.40	1000	542.71	72.40	17.91	7.5
L65692-10	NSAJ02	A	7/19/2016	333.71	61.05	1000	333.71	61.05	2.93	5.5
L65834-1	KSBP01	A	8/1/2016	374.08	76.44	1000	374.08	76.44	5.436	4.9
L65834-2	JSUR01	A	8/1/2016	563.24	110.77	1000	563.24	110.77	9.985	5.1
L65834-3	KSSK02	A	8/1/2016	185.05	35.26	1000	185.05	35.26	3.331	5.2
L65834-4	LTED04	A	8/1/2016	225.93	44.35	1000	225.93	44.35	1.59	5.1
L65834-5	LSEP01	A	8/2/2016	154.28	30.39	1000	154.28	30.39	1.79	5.1
L65834-7	LSNT01	A	8/2/2016	246.30	44.81	1000	246.30	44.81	6.585	5.5
L65834-9	NSEX01	A	8/2/2016	840.84	143.19	1000	840.84	143.19	37.11	5.9
L65834-10	NSAJ02	A	8/3/2016	403.93	63.33	1000	403.93	63.33	8.157	6.4
L65917-1	KSBP01	A	8/15/2016	494.27	98.86	1000	494.27	98.86	8.104	5.0
L65917-2	JSUR01	A	8/15/2016	548.28	120.79	1000	548.28	120.79	12.41	4.5
L65917-3	KSSK02	A	8/15/2016	513.56	101.77	1000	513.56	101.77	11.52	5.0
L65917-4	LTED04	A	8/15/2016	384.73	86.79	910	422.78	95.38	2.602	4.4
L65917-5	LSEP01	A	8/16/2016	424.84	83.10	832	510.62	99.88	5.308	5.1
L65917-7	LSNT01	A	8/16/2016	164.30	28.75	1000	164.30	28.75	4.887	5.7
L65917-9	NSEX01	A	8/16/2016	898.64	118.82	548	1639.85	216.82	38.6	7.6
L65917-10	NSAJ02	A	8/17/2016	486.78	67.95	1000	486.78	67.95	10.79	7.2
L65973-1	KSBP01	A	9/6/2016	107.18	26.07	1000	107.18	26.07	0.3852	4.1
L65973-2	JSUR01	A	9/6/2016	134.47	24.63	1000	134.47	24.63	0.3462	5.5
L65973-3	KSSK02	A	9/6/2016	134.14	27.03	1000	134.14	27.03	0.515	5.0
L65973-4	LTED04	A	9/6/2016	110.06	23.62	1000	110.06	23.62	0.4024	4.7
L65973-5	LSEP01	A	9/7/2016	117.06	22.93	1000	117.06	22.93	0.5208	5.1
L65973-7	LSNT01	A	9/7/2016	81.36	13.57	1000	81.36	13.57	0.5039	6.0
L65973-9	NSEX01	A	9/7/2016	201.30	38.26	1000	201.30	38.26	0.5002	5.3
L65973-10	NSAJ02	A	9/7/2016	996.98	132.77	1000	996.98	132.77	20.17	7.5
L66032-1	KSBP01	A	9/19/2016	68.45	23.45	1000	68.45	23.45	0.3092	2.9
L66032-2	JSUR01	A	9/19/2016	74.70	12.73	1000	74.70	12.73	0.5691	5.9

Sample ID	Locator	Fraction	Date Collected	C Amount (µg)	N Amount (µg)	Vol filt'd. (mL)	C/vol (µg/L)	N/vol (µg/L)	Biovolume (mm³/L)	C/N (wt/wt)
L66032-3	KSSK02	A	9/19/2016	74.48	16.33	1000	74.48	16.33	0.4561	4.6
L66032-4	LTED04	A	9/19/2016	90.91	19.74	1000	90.91	19.74	0.7332	4.6
L66032-5	LSEP01	A	9/20/2016	70.17	12.20	1000	70.17	12.20	1.021	5.8
L66032-7	LSNT01	A	9/20/2016	95.93	19.20	1000	95.93	19.20	0.8065	5.0
L66032-9	NSEX01	A	9/20/2016	117.72	21.58	1000	117.72	21.58	0.4736	5.5
L66032-10	NSAJ02	A	9/21/2016	515.32	96.67	1000	515.32	96.67	14.6	5.3
									mean:	5.6
									SD:	1.3
									N:	199
									min	0.1844
									max	73.83
									mean	7.693
									SD	10.795
									mean+2SD	29.283
									mean-2SD	-13.896

⁽¹⁾ No data reported from UC Davis lab (sample fell in with standard)

Table B-2 Particulate organic C and N results from combustion analysis for particles in fraction B (100-300 µm). Also shown are corresponding biovolume results from FlowCAM analysis for particles in fraction B.

Sample ID	Locator	Fraction	Date Collected	C Amount	N Amount	Vol filt'd.	C/vol	N/vol	Biovolume	C/N
				(µg)	(µg)	(mL)	(µg/L)	(µg/L)	(mm³/L)	(wt/wt)
L62974-1	KSBP01	B	6/15/15	95.59	15.29	250	382.35	61.16	65.74	6.3
L62974-3	JSUR01	B	6/15/15	77.42	29.80	250	309.68	119.20	39.66	2.6
L62974-4	KSSK02	B	6/15/15	85.54	32.63	250	342.17	130.53	35.43	2.6
L62974-5	LTED04	B	6/15/15	115.80	24.72	250	463.22	98.86	34.48	4.7
L62974-6	LSEP01	B	6/16/15	111.82	22.46	250	447.27	89.84	60.46	5.0
L62974-7	LSNT01	B	6/16/15	45.73	9.30	250	182.93	37.20	10.92	4.9
L62974-8	NSEX01	B	6/16/15	187.87	31.27	250	751.46	125.06	78.48	6.0
L62974-10	NSAJ02	B	6/17/15	56.48	26.67	250	225.94	106.69	31.35	2.1
L63060-1	KSBP01	B	7/6/15	45.70	7.45	250	182.80	29.79	15.17	6.1
L63060-3	JSUR01	B	7/6/15	49.59	8.40	250	198.37	33.62	28.37	5.9
L63060-4	KSSK02	B	7/6/15	79.96	47.07	250	319.84	188.28	44.52	1.7
L63060-5	LTED04	B	7/6/15	73.99	34.14	250	295.97	136.57	17.80	2.2
L63060-6	LSEP01	B	7/7/15	49.59	6.26	250	198.37	25.05	1.99	7.9
L63060-7	LSNT01	B	7/7/15	26.74	3.85	250	106.98	15.42	0.95	6.9
L63060-8	NSEX01	B	7/7/15	35.31	5.44	250	141.25	21.76	2.56	6.5
L63060-10	NSAJ02	B	7/8/15	28.04	3.97	250	112.17	15.89	8.41	7.1
L63121-1	KSBP01	B	7/20/15	90.85	40.20	250	363.40	160.79	40.79	2.3
L63121-3	JSUR01	B	7/20/15	129.48	40.03	250	517.92	160.14	74.95	3.2
L63121-4	KSSK02	B	7/21/15	117.87	55.61	250	471.47	222.43	59.30	2.1
L63121-5	LTED04	B	7/21/15	47.08	43.45	250	188.34	173.82	6.14	1.1
L63121-6	LSEP01	B	7/23/15	35.17	37.34	250	140.70	149.37	1.43	0.9
L63121-7	LSNT01	B	7/23/15	33.59	6.32	250	134.38	25.30	1.56	5.3
L63121-8	NSEX01	B	7/23/15	33.59	6.00	250	134.38	24.00	3.15	5.6
L63121-10	NSAJ02	B	7/22/15	84.52	22.66	500	169.04	45.33	10.65	3.7
L63268-1	KSBP01	B	8/3/15	174.02	38.80	1000	174.02	38.80	53.35	4.5
L63268-3	JSUR01	B	8/3/15	281.26	49.95	1000	281.26	49.95	92.94	5.6

Sample ID	Locator	Fraction	Date Collected	C Amount (µg)	N Amount (µg)	Vol filtd. (mL)	C/vol (µg/L)	N/vol (µg/L)	Biovolume (mm³/L)	C/N (wt/wt)
L63268-4	KSSK02	B	8/3/15	151.46	27.09	1000	151.46	27.09	32.69	5.6
L63268-5	LTED04	B	8/3/15	132.85	23.58	1000	132.85	23.58	21.32	5.6
L63268-6	LSEP01	B	8/4/15	98.52	20.97	1000	98.52	20.97	6.51	4.7
L63268-7	LSNT01	B	8/4/15	78.82	13.84	1000	78.82	13.84	6.76	5.7
L63268-8	NSEX01	B	8/4/15	161.64	27.34	1000	161.64	27.34	57.75	5.9
L63268-10	NSAJ02	B	8/5/15	137.57	28.80	1000	137.57	28.80	5.34	4.8
L63401-1	KSBP01	B	8/17/15	26.47	4.72	1000	26.47	4.72	0.77	5.6
L63401-3	JSUR01	B	8/17/15	27.16	16.77	1000	27.16	16.77	0.07	1.6
L63401-4	KSSK02	B	8/17/15	51.57	8.83	1000	51.57	8.83	0.02	5.8
L63401-5	LTED04	B	8/17/15	50.68	7.93	1000	50.68	7.93	0.02	6.4
L63401-6	LSEP01	B	8/18/15	79.04	19.33	1000	79.04	19.33	0.23	4.1
L63401-7	LSNT01	B	8/18/15	46.29	8.42	1000	46.29	8.42	0.05	5.5
L63401-8	NSEX01	B	8/18/15	48.83	10.27	1000	48.83	10.27	0.21	4.8
L63401-10	NSAJ02	B	8/19/15	57.52	8.56	1000	57.52	8.56	2.08	6.7
L63522-1	KSBP01	B	9/8/15	72.72	11.78	1000	72.72	11.78	3.28	6.2
L63522-3	JSUR01	B	9/8/15	70.40	14.27	1000	70.40	14.27	3.33	4.9
L63522-4	KSSK02	B	9/8/15	47.69	8.02	1000	47.69	8.02	3.47	5.9
L63522-5	LTED04	B	9/8/15	30.60	5.39	1000	30.60	5.39	0.51	5.7
L63522-6	LSEP01	B	9/9/15	78.19	14.67	1000	78.19	14.67	3.55	5.3
L63522-7	LSNT01	B	9/9/15	60.89	17.64	1000	60.89	17.64	1.77	3.5
L63522-8	NSEX01	B	9/9/15	66.29	15.77	1000	66.29	15.77	8.52	4.2
L63522-10	NSAJ02	B	9/9/15	85.15	20.03	1000	85.15	20.03	10.36	4.3
L63669-1	KSBP01	B	9/21/15	27.09	4.41	1000	27.09	4.41	0.77	6.1
L63669-3	JSUR01	B	9/21/15	42.64	8.64	1000	42.64	8.64	4.71	4.9
L63669-4	KSSK02	B	9/21/15	26.48	6.52	1000	26.48	6.52	1.07	4.1
L63669-5	LTED04	B	9/21/15	109.24	22.84	1000	109.24	22.84	12.59	4.8
L63669-6	LSEP01	B	9/22/15	99.69	26.06	1000	99.69	26.06	17.53	3.8
L63669-7	LSNT01	B	9/22/15	140.17	26.24	1000	140.17	26.24	23.54	5.3

Sample ID	Locator	Fraction	Date Collected	C Amount (µg)	N Amount (µg)	Vol filt'd. (mL)	C/vol (µg/L)	N/vol (µg/L)	Biovolume (mm³/L)	C/N (wt/wt)
L63669-8	NSEX01	B	9/22/15	293.59	51.95	1000	293.59	51.95	68.97	5.7
L63669-10	NSAJ02	B	9/23/15	379.19	32.94	500	758.38	65.89	174.20	11.5
L63820-1	KSBP01	B	10/5/15	16.60	2.55	1000	16.60	2.55	0.13	6.5
L63820-3	JSUR01	B	10/5/15	14.76	2.37	1000	14.76	2.37	0.11	6.2
L63820-4	KSSK02	B	10/5/15	29.16	4.52	1000	29.16	4.52	0.19	6.5
L63820-5	LTED04	B	10/5/15	29.51	5.23	1000	29.51	5.23	0.79	5.6
L63820-6	LSEP01	B	10/6/15	102.19	18.33	1000	102.19	18.33	0.53	5.6
L63820-7	LSNT01	B	10/6/15	35.33	5.08	1000	35.33	5.08	0.31	7.0
L63820-8	NSEX01	B	10/6/15	38.85	5.33	1000	38.85	5.33	0.33	7.3
L63820-10	NSAJ02	B	10/7/15	395.31	63.34	1000	395.31	63.34	39.84	6.2
L63863-1	KSBP01	B	10/19/15	13.09	1.41	1000	13.09	1.41	0.33	9.3
L63863-3	JSUR01	B	10/19/15	17.33	1.41	1000	17.33	1.41	0.22	12.3
L63863-4	KSSK02	B	10/19/15	16.51	1.75	1000	16.51	1.75	0.13	9.4
L63863-5	LTED04	B	10/19/15	14.68	1.40	1000	14.68	1.40	0.05	10.5
L63863-6	LSEP01	B	10/20/15	16.62	2.08	1000	16.62	2.08	0.47	8.0
L63863-7	LSNT01	B	10/20/15	25.48	1.74	1000	25.48	1.74	0.53	14.6
L63863-8	NSEX01	B	10/20/15	16.45	1.91	1000	16.45	1.91	0.21	8.6
L63863-10	NSAJ02	B	10/21/15	34.59	5.86	1000	34.59	5.86	4.16	5.9
L64027-1	KSBP01	B	11/2/15	18.83	3.65	1000	18.83	3.65	0.12	5.2
L64027-3	JSUR01	B	11/2/15	36.08	6.56	1000	36.08	6.56	0.46	5.5
L64027-4	KSSK02	B	11/2/15	24.00	4.11	1000	24.00	4.11	0.09	5.8
L64027-5	LTED04	B	11/2/15	14.31	nd ⁽¹⁾	1000	14.31	-	0.06	-
L64027-6	LSEP01	B	11/3/15	14.48	nd ⁽¹⁾	1000	14.48	-	0.17	-
L64027-7	LSNT01	B	11/3/15	31.64	9.58	1000	31.64	9.58	0.05	3.3
L64027-8	NSEX01	B	11/3/15	31.52	6.47	1000	31.52	6.47	0.02	4.9
L64027-10	NSAJ02	B	11/4/15	35.22	6.58	1000	35.22	6.58	0.54	5.3
L64127-1	KSBP01	B	11/19/15	8.84	nd ⁽¹⁾	1000	8.84	-	0.11	-
L64127-3	JSUR01	B	11/19/15	31.33	nd ⁽¹⁾	1000	31.33	-	0.06	-

Sample ID	Locator	Fraction	Date Collected	C Amount (µg)	N Amount (µg)	Vol filt'd. (mL)	C/vol (µg/L)	N/vol (µg/L)	Biovolume (mm³/L)	C/N (wt/wt)
L64127-4	KSSK02	B	11/19/15	11.68	nd ⁽¹⁾	1000	11.68	-	0.61	-
L64127-5	LTED04	B	11/19/15	15.21	nd ⁽¹⁾	1000	15.21	-	0.07	-
L64127-6	LSEP01	B	11/18/15	13.76	nd ⁽¹⁾	1000	13.76	-	0.15	-
L64127-7	LSNT01	B	11/18/15	18.75	3.59	1000	18.75	3.59	0.02	5.2
L64127-8	NSEX01	B	11/18/15	14.43	nd ⁽¹⁾	1000	14.43	-	0.08	-
L64127-10	NSAJ02	B	11/18/15	12.62	nd ⁽¹⁾	1000	12.62	-	0.11	-
L64191-1	KSBP01	B	12/14/15	24.09	4.71	1000	24.09	4.71	0.05	5.1
L64191-3	JSUR01	B	12/14/15	18.76	2.87	1000	18.76	2.87	0.09	6.5
L64191-4	KSSK02	B	12/14/15	26.55	10.74	1000	26.55	10.74	0.05	2.5
L64191-5	LTED04	B	12/14/15	21.34	8.70	1000	21.34	8.70	0.04	2.5
L64191-6	LSEP01	B	12/15/15	18.03	7.40	1000	18.03	7.40	0.01	2.4
L64191-7	LSNT01	B	12/15/15	24.90	4.58	1000	24.90	4.58	0.02	5.4
L64191-8	NSEX01	B	12/15/15	32.45	4.33	1000	32.45	4.33	0.02	7.5
L64191-10	NSAJ02	B	12/16/15	22.78	6.84	1000	22.78	6.84	0.03	3.3
L65057-1	KSBP01	B	3/21/16	82.04	15.79	1000	82.04	15.79	2.34	5.2
L65057-2	JSUR01	B	3/21/16	108.65	21.55	1000	108.65	21.55	5.01	5.0
L65057-3	KSSK02	B	3/21/16	59.54	11.40	1000	59.54	11.40	2.63	5.2
L65057-4	LTED04	B	3/21/16	38.96	5.98	1000	38.96	5.98	1.23	6.5
L65057-5	LSEP01	B	3/21/16	50.76	9.55	1000	50.76	9.55	0.75	5.3
L65057-7	LSNT01	B	3/21/16	39.51	7.05	1000	39.51	7.05	0.44	5.6
L65057-9	NSEX01	B	3/21/16	48.84	8.39	1000	48.84	8.39	2.10	5.8
L65057-10	NSAJ02	B	3/21/16	61.73	9.81	1000	61.73	9.81	0.24	6.3
L64988-1	KSBP01	B	4/6/16	44.63	6.75	1000	44.63	6.75	4.14	6.6
L64988-2	JSUR01	B	4/6/16	49.10	9.74	1000	49.10	9.74	3.12	5.0
L64988-3	KSSK02	B	4/6/16	61.40	10.88	1000	61.40	10.88	4.58	5.6
L64988-4	LTED04	B	4/6/16	28.54	24.69	1000	28.54	24.69	0.60	1.2
L64988-5	LSEP01	B	4/5/16	106.89	20.22	1000	106.89	20.22	2.36	5.3
L64988-7	LSNT01	B	4/5/16	106.63	26.26	1000	106.63	26.26	2.76	4.1

Sample ID	Locator	Fraction	Date Collected	C Amount (µg)	N Amount (µg)	Vol filtd. (mL)	C/vol (µg/L)	N/vol (µg/L)	Biovolume (mm³/L)	C/N (wt/wt)
L64988-9	NSEX01	B	4/5/16	87.95	47.83	1000	87.95	47.83	2.44	1.8
L64988-10	NSAJ02	B	4/5/16	66.38	26.98	1000	66.38	26.98	1.37	2.5
L65045-1	KSBP01	B	4/18/16	137.85	52.42	1000	137.85	52.42	13.38	2.6
L65045-2	JSUR01	B	4/18/16	149.32	31.67	1000	149.32	31.67	23.05	4.7
L65045-3	KSSK02	B	4/18/16	119.07	23.36	1000	119.07	23.36	8.18	5.1
L65045-4	LTED04	B	4/18/16	45.24	7.31	1000	45.24	7.31	4.62	6.2
L65045-5	LSEP01	B	4/19/16	98.28	21.62	1000	98.28	21.62	19.69	4.5
L65045-7	LSNT01	B	4/19/16	76.96	15.72	1000	76.96	15.72	11.64	4.9
L65045-9	NSEX01	B	4/19/16	467.17	76.08	1000	467.17	76.08	92.47	6.1
L65045-10	NSAJ02	B	4/20/16	90.49	10.68	1000	90.49	10.68	8.90	8.5
L65150-1	KSBP01	B	5/2/2016	512.43	63.33	1000	512.43	63.33	70.24	8.1
L65150-2	JSUR01	B	5/2/2016	556.90	68.47	1000	556.90	68.47	69.54	8.1
L65150-3	KSSK02	B	5/2/2016	445.01	66.63	1000	445.01	66.63	62.02	6.7
L65150-4	LTED04	B	5/2/2016	898.47	88.97	1000	898.47	88.97	67.57	10.1
L65150-5	LSEP01	B	5/3/2016	265.22	51.94	1000	265.22	51.94	19.13	5.1
L65150-7	LSNT01	B	5/3/2016	428.57	79.04	1000	428.57	79.04	58.21	5.4
L65150-9	NSEX01	B	5/3/2016	932.45	90.52	1000	932.45	90.52	131.80	10.3
L65150-10	NSAJ02	B	5/4/2016	136.23	38.07	1000	136.23	38.07	28.33	3.6
L65302-1	KSBP01	B	5/16/2016	56.56	10.92	1000	56.56	10.92	5.69	5.2
L65302-2	JSUR01	B	5/16/2016	38.75	8.47	1000	38.75	8.47	2.75	4.6
L65302-3	KSSK02	B	5/16/2016	32.80	10.51	1000	32.80	10.51	1.50	3.1
L65302-4	LTED04	B	5/16/2016	35.86	13.34	1000	35.86	13.34	1.40	2.7
L65302-5	LSEP01	B	5/17/2016	129.63	27.47	1000	129.63	27.47	12.25	4.7
L65302-7	LSNT01	B	5/17/2016	186.63	34.79	1000	186.63	34.79	16.29	5.4
L65302-9	NSEX01	B	5/17/2016	135.11	30.07	1000	135.11	30.07	29.72	4.5
L65302-10	NSAJ02	B	5/18/2016	214.32	36.03	1000	214.32	36.03	24.75	5.9
L65360-1	KSBP01	B	6/6/2016	539.03	64.44	1000	539.03	64.44	74.42	8.4
L65360-2	JSUR01	B	6/6/2016	281.89	62.86	1000	281.89	62.86	54.18	4.5

Sample ID	Locator	Fraction	Date Collected	C Amount (µg)	N Amount (µg)	Vol filt'd. (mL)	C/vol (µg/L)	N/vol (µg/L)	Biovolume (mm³/L)	C/N (wt/wt)
L65360-3	KSSK02	B	6/6/2016	360.17	67.82	1000	360.17	67.82	60.26	5.3
L65360-4	LTED04	B	6/6/2016	191.80	60.62	1000	191.80	60.62	33.00	3.2
L65360-5	LSEP01	B	6/7/2016	123.71	44.12	1000	123.71	44.12	27.74	2.8
L65360-7	LSNT01	B	6/7/2016	129.34	28.91	1000	129.34	28.91	17.66	4.5
L65360-9	NSEX01	B	6/7/2016	138.08	17.80	1000	138.08	17.80	25.03	7.8
L65360-10	NSAJ02	B	6/10/2016	101.20	39.58	1000	101.20	39.58	16.83	2.6
L65486-1	KSBP01	B	6/20/2016	344.41	61.08	1000	344.41	61.08	96.82	5.6
L65486-2	JSUR01	B	6/20/2016	529.47	84.93	1000	529.47	84.93	82.43	6.2
L65486-3	KSSK02	B	6/20/2016	422.82	71.55	1000	422.82	71.55	77.28	5.9
L65486-4	LTED04	B	6/20/2016	219.31	40.93	1000	219.31	40.93	37.41	5.4
L65486-5	LSEP01	B	6/21/2016	394.85	63.76	1000	394.85	63.76	100.50	6.2
L65486-7	LSNT01	B	6/21/2016	218.11	45.68	1000	218.11	45.68	61.52	4.8
L65486-9	NSEX01	B	6/21/2016	383.42	42.00	1000	383.42	42.00	97.46	9.1
L65486-10	NSAJ02	B	6/21/2016	282.71	39.84	1000	282.71	39.84	77.09	7.1
L65565-1	KSBP01	B	7/5/2016	149.96	30.78	1000	149.96	30.78	21.80	4.9
L65565-2	JSUR01	B	7/5/2016	132.63	25.55	1000	132.63	25.55	26.96	5.2
L65565-3	KSSK02	B	7/5/2016	82.98	16.40	1000	82.98	16.40	10.18	5.1
L65565-4	LTED04	B	7/5/2016	64.77	11.90	1000	64.77	11.90	11.91	5.4
L65565-5	LSEP01	B	7/6/2016	52.28	23.75	1000	52.28	23.75	6.36	2.2
L65565-7	LSNT01	B	7/6/2016	91.36	16.07	1000	91.36	16.07	9.12	5.7
L65565-9	NSEX01	B	7/6/2016	292.09	51.41	1000	292.09	51.41	64.13	5.7
L65565-10	NSAJ02	B	7/6/2016	77.00	24.30	1000	77.00	24.30	9.98	3.2
L65692-1	KSBP01	B	7/18/2016	182.88	38.58	1000	182.88	38.58	63.32	4.7
L65692-2	JSUR01	B	7/18/2016	161.40	25.08	1000	161.40	25.08	35.02	6.4
L65692-3	KSSK02	B	7/18/2016	108.26	19.05	1000	108.26	19.05	31.91	5.7
L65692-4	LTED04	B	7/18/2016	64.27	11.51	1000	64.27	11.51	13.08	5.6
L65692-5	LSEP01	B	7/19/2016	76.69	23.52	1000	76.69	23.52	15.85	3.3
L65692-7	LSNT01	B	7/19/2016	60.39	10.26	1000	60.39	10.26	11.30	5.9

Sample ID	Locator	Fraction	Date Collected	C Amount (µg)	N Amount (µg)	Vol filt'd. (mL)	C/vol (µg/L)	N/vol (µg/L)	Biovolume (mm³/L)	C/N (wt/wt)
L65692-9	NSEX01	B	7/19/2016	167.25	15.80	1000	167.25	15.80	31.89	10.6
L65692-10	NSAJ02	B	7/19/2016	85.86	14.77	1000	85.86	14.77	21.22	5.8
L65834-1	KSBP01	B	8/1/2016	30.72	8.41	200	153.62	42.05	11.99	3.7
L65834-2	JSUR01	B	8/1/2016	67.98	13.67	200	339.90	68.37	24.03	5.0
L65834-3	KSSK02	B	8/1/2016	28.30	5.11	200	141.49	25.55	4.65	5.5
L65834-4	LTED04	B	8/1/2016	12.58	1.62	200	62.89	8.09	1.62	7.8
L65834-5	LSEP01	B	8/2/2016	15.97	2.85	200	79.83	14.25	7.09	5.6
L65834-7	LSNT01	B	8/2/2016	22.60	3.39	200	112.98	16.96	10.80	6.7
L65834-9	NSEX01	B	8/2/2016	53.57	8.79	200	267.83	43.93	107.10	6.1
L65834-10	NSAJ02	B	8/3/2016	56.98	14.23	200	284.91	71.15	29.53	4.0
L65917-1	KSBP01	B	8/15/2016	48.87	10.51	1000	48.87	10.51	12.15	4.6
L65917-2	JSUR01	B	8/15/2016	47.12	12.53	1000	47.12	12.53	14.86	3.8
L65917-3	KSSK02	B	8/15/2016	49.64	6.72	1000	49.64	6.72	8.31	7.4
L65917-4	LTED04	B	8/15/2016	15.85	7.23	1000	15.85	7.23	0.08	2.2
L65917-5	LSEP01	B	8/16/2016	43.14	6.84	1000	43.14	6.84	14.48	6.3
L65917-7	LSNT01	B	8/16/2016	35.77	6.22	1000	35.77	6.22	1.58	5.7
L65917-9	NSEX01	B	8/16/2016	114.08	13.83	1000	114.08	13.83	48.60	8.3
L65917-10	NSAJ02	B	8/17/2016	57.67	7.87	1000	57.67	7.87	10.36	7.3
L65973-1	KSBP01	B	9/6/2016	21.93	7.98	1000	21.93	7.98	0.02	2.7
L65973-2	JSUR01	B	9/6/2016	33.25	4.37	1000	33.25	4.37	0.00	7.6
L65973-3	KSSK02	B	9/6/2016	31.66	6.44	1000	31.66	6.44	0.03	4.9
L65973-4	LTED04	B	9/6/2016	19.30	5.45	1000	19.30	5.45	0.00	3.5
L65973-5	LSEP01	B	9/7/2016	17.05	4.10	1000	17.05	4.10	0.00	4.2
L65973-7	LSNT01	B	9/7/2016	18.24	3.07	1000	18.24	3.07	0.00	5.9
L65973-9	NSEX01	B	9/7/2016	18.35	11.69	1000	18.35	11.69	0.00	1.6
L65973-10	NSAJ02	B	9/7/2016	62.50	11.38	1000	62.50	11.38	10.96	5.5
L66032-1	KSBP01	B	9/19/2016	22.41	4.13	1000	22.41	4.13	0.02	5.4
L66032-2	JSUR01	B	9/19/2016	24.42	5.25	1000	24.42	5.25	0.42	4.7

Sample ID	Locator	Fraction	Date Collected	C Amount	N Amount	Vol filt'd.	C/vol	N/vol	Biovolume	C/N
				(µg)	(µg)	(mL)	(µg/L)	(µg/L)	(mm³/L)	(wt/wt)
L66032-3	KSSK02	B	9/19/2016	20.55	6.77	1000	20.55	6.77	0.24	3.0
L66032-4	LTED04	B	9/19/2016	14.73	1.94	1000	14.73	1.94	0.10	7.6
L66032-5	LSEP01	B	9/20/2016	16.95	5.83	1000	16.95	5.83	0.05	2.9
L66032-7	LSNT01	B	9/20/2016	13.28	2.29	1000	13.28	2.29	0.87	5.8
L66032-9	NSEX01	B	9/20/2016	16.52	2.93	1000	16.52	2.93	0.16	5.6
L66032-10	NSAJ02	B	9/21/2016	54.56	9.68	1000	54.56	9.68	0.90	5.6
									mean:	5.4
(i) No data reported from UC Davis lab (too small)									SD:	2.1
									N:	191
									min	0.001856
									max	174.2

⁽¹⁾ No data reported from UC Davis lab (too small)

Table B-3 Calculation of carbon density for each FlowCAM category using published cell volume-dependent equations, and published or FlowCAM measured median cell volume.

FlowCAM category	Commonly recognized species in FlowCAM category	Species substituted as in (1)	Cell Diam. Median (μm)	Cell Vol Median (μm ³)	Reference	Carbon equation	C content (pgC cell ⁻¹)	C density (pgC μm ⁻³)
Diatoms								
<i>Actinoptychus</i>	<i>Actinoptychus senarius</i>		34.10	20,700	(1)	LD	742.26	0.0359
<i>Asterionellopsis</i>	<i>Asterionellopsis glacialis</i>		10.00	524	(1)	SD	46.21	0.0882
<i>Asteromphalus</i>	<i>Asteromphalus heptactis</i>		46.30	52,052	(2)	LD	1,672.50	0.0321
<i>Bacteriastrum</i>	<i>Bacteriastrum delicatulum</i>	<i>B. hyalinum</i>	27.40	10,800	(1)	LD	418.44	0.0387
<i>Cerataulina</i>	<i>Cerataulina pelagica</i>		25.50	8,720	(1)	LD	346.56	0.0397
<i>Chaetoceros</i>	<i>Chaetoceros debilis</i>		14.50	1,600	(1)	SD	114.27	0.0714
	<i>Chaetoceros decipiens</i>		25.80	9,020	(1)	LD	357.04	0.0396
	<i>Chaetoceros diadema</i>		19.90	4,130	(1)	LD	179.41	0.0434
	<i>Chaetoceros didymus</i>		15.70	2,030	(1)	SD	138.60	0.0683
	<i>Chaetoceros eibonii</i>		29.30	13,200	(1)	LD	499.36	0.0378
	<i>Chaetoceros laciniosus</i>		17.40	2,740	(1)	SD	176.77	0.0645
	<i>Chaetoceros radicans</i>		12.30	984	(1)	SD	77.04	0.0783
	<i>Chaetoceros similis</i>		11.30	764	(1)	SD	62.75	0.0821
	<i>Chaetoceros socialis</i>		7.56	226	(1)	SD	23.37	0.1034
	Mean			3,855	(3)			0.0654
<i>Coscinodiscus</i>	<i>Coscinodiscus centralis</i>		130.00	1,160,000	(1)	LD	25,761.63	0.0222
	<i>Coscinodiscus oculus-iris</i>		78.70	255,000	(1)	LD	6,781.84	0.0266
	Mean			707,500	(3)			0.0244
<i>Cylindrotheca</i>	<i>Cylindrotheca closterium</i>		8.20	289	(1)	SD	28.52	0.0987
<i>Ditylum</i>	<i>Ditylum brightwelli</i>		50.20	66,400	(1)	LD	2,072.60	0.0312
<i>Eucampia</i>	<i>Eucampia zodiacus</i>		25.30	8,460	(1)	LD	337.44	0.0399
<i>Guinardia et al</i>	<i>Guinardia delicatula</i>		20.60	4,580	(1)	LD	196.52	0.0429
	<i>Leptocylindrus danicus</i>		15.00	1,750	(1)	SD	122.88	0.0702
	Mean			3,165	(3)			0.0566

FlowCAM category	Commonly recognized species in FlowCAM category	Species substituted as in (1)	Cell Diam. Median (μm)	Cell Vol Median (μm ³)	Reference	Carbon equation	C content (pgC cell ⁻¹)	C density (pgC μm ⁻³)
<i>Hemiaulus</i>	<i>Hemiaulus hauckii</i>		27.30	10,700	(1)	LD	415.02	0.0388
<i>Lauderia/Detonula</i>	<i>Lauderia annulata</i>		35.50	23,500	(1)	LD	830.04	0.0353
	<i>Detonula pumila</i>		29.30	13,100	(1)	LD	496.02	0.0379
	Mean			18,300	(3)			0.0366
<i>Nitzschia</i>	<i>Nitzschia acicularis</i>		8.42	312	(1)	SD	30.35	0.0973
<i>Odontella</i>	<i>Odontella longicruris</i>	<i>O. aurita</i>	32.60	18,200	(1)	LD	662.69	0.0364
<i>Paralia</i>	<i>Paralia sulcata</i>		21.30	5,030	(1)	LD	213.44	0.0424
<i>Pleurosigma</i>	<i>Pleurosigma</i> sp.		49.30	62,776	(2)	LD	1,972.62	0.0314
<i>Pseudo-nitzschia</i>	<i>P. delicatissima</i>		7.25	200	(1)	SD	21.16	0.1058
	<i>P. pseudodelicatissima</i>		7.26	200	(1)	SD	21.16	0.1058
	<i>P. pungens</i>		13.00	1,140	(1)	SD	86.80	0.0761
	<i>P. seriata</i>		13.50	1,290	(1)	SD	95.96	0.0744
	Mean			708	(3)			0.0905
<i>Rhizosolenia</i>	<i>Rhizosolenia setigera</i>		27.40	10,800	(1)	LD	418.44	0.0387
<i>Skeletonema</i>	<i>Skeletonema costatum</i>		7.44	215	(1)	SD	22.44	0.1044
	<i>Stephanopyxis palmeriana</i>	<i>S. turris</i>	31.60	16,500	(1)	LD	607.84	0.0368
	<i>Thalassionema nitzschioides</i>		11.40	774	(1)	SD	63.41	0.0819
<i>Thalassiosira</i>	<i>Thalassiosira anguste-lineata</i>		34.20	21,000	(1)	LD	751.73	0.0358
	<i>Thalassiosira nordenskiöldii</i>		24.10	7,330	(1)	LD	297.40	0.0406
	<i>Thalassiosira rotula</i>		28.60	12,200	(1)	LD	465.87	0.0382
	Mean			13,510	(3)			0.0382
<i>Tropidoneis</i>	<i>Tropidoneis antarctica</i>		153.40	2,210,000	(2)	LD	45,456.44	0.0206
misc diatoms	Mean, all diatom categories		25.40	8,580	(1)		341.66	0.0532

Dinoflagellates

FlowCAM category	Commonly recognized species in FlowCAM category	Species substituted as in (1)	Cell Diam. Median (μm)	Cell Vol Median (μm ³)	Reference	Carbon equation	C content (pgC cell ⁻¹)	C density (pgC μm ⁻³)
<i>Akashiwo</i>	<i>Akashiwo sanguinea</i>		40.00	33,500	(1)	F	3,605.97	0.1076
<i>Alexandrium</i>	<i>Alexandrium catenella</i>	<i>A. tamarense</i>	29.70	13,700	(1)	F	1,665.37	0.1216
<i>Amphidinium</i>	<i>Amphidinium sphenoides</i>	<i>A. longum</i>	14.00	1,440	(1)	F	237.80	0.1651
<i>Amylax</i>	<i>Amylax triacantha</i>		27.80	11,300	(1)	F	1,410.08	0.1248
<i>Ceratium</i>	<i>Ceratium fusus</i>	<i>Tripus fusus</i>	33.40	19,400	(1)	F	2,249.28	0.1159
	<i>Ceratium lineatum</i>		29.70	13,700	(1)	F	1,665.37	0.1216
	Mean			16,550	(3)			0.1188
<i>Cochlodinium</i>	<i>Cochlodinium</i>		25.10	8,300	(2)	F	1,080.11	0.1301
<i>Dinophysis</i>	<i>Dinophysis acuminata</i>		27.30	10,700	(1)	F	1,345.15	0.1257
	<i>Dinophysis acuta</i>		47.00	54,300	(1)	F	5,473.31	0.1008
	<i>Dinophysis norvegica</i>		39.40	32,000	(1)	F	3,466.03	0.1083
	Mean			32,333	(3)			0.1116
<i>Gonyaulax</i>	<i>Gonyaulax digitale</i>		32.40	17,800	(1)	F	2,088.07	0.1173
<i>Heterocapsa</i>	<i>Heterocapsa triquetra</i>		16.60	2,400	(1)	F	369.73	0.1541
<i>Karlodinium</i>	<i>Karlodinium</i> sp.	<i>K. veneficum</i>	11.40	772	(1)	F	138.77	0.1797
<i>Katodinium</i>	<i>Katodinium glaucum</i>		15.60	1,980	(1)	F	313.11	0.1581
<i>Nematodinium</i>	<i>Nematodinium</i>		30.62	15,036	(2)	F	1,804.76	0.1200
<i>Noctiluca</i>	<i>Noctiluca scintillans</i> (<300 μm)		347.90	22,050,000	(2)	F	981,946.88	0.0445
<i>Oxyphysis</i>	<i>Oxyphysis</i>		29.34	13,331	(2)	F	1,626.55	0.1220
<i>Polykrikos</i>	<i>Polykrikos schwartzii</i>		66.60	155,000	(1)	F	13,546.58	0.0874
<i>Prorocentrum</i>	<i>Prorocentrum gracile</i>		19.10	3,650	(1)	F	531.13	0.1455
	<i>Prorocentrum micans</i>		26.50	9,700	(1)	F	1,235.82	0.1274
	Mean			6,675	(3)			0.1365
<i>Protoceratium</i>	<i>Protoceratium reticulatum</i>		30.90	15,400	(1)	F	1,842.47	0.1196
<i>Protoperidinium</i>	<i>Protoperidinium conicum</i>		57.40	99,000	(1)	F	9,196.27	0.0929
	<i>Protoperidinium depressum</i>		95.40	454,000	(1)	F	34,283.03	0.0755
	<i>Protoperidinium steinii</i>		31.20	16,000	(1)	F	1,904.33	0.1190

FlowCAM category	Commonly recognized species in FlowCAM category	Species substituted as in (1)	Cell Diam. Median (µm)	Cell Vol Median (µm ³)	Reference	Carbon equation	C content (pgC cell ⁻¹)	C density (pgC µm ⁻³)
	Mean			189,667	(3)			0.0958
<i>Scrippsiella</i>	<i>Scrippsiella trochoidea</i>		20.70	4,630	(1)	F	652.30	0.1409
<i>Torodinium</i>	<i>Torodinium</i> sp.	<i>T. robustum</i>	18.00	3,070	(1)	F	457.37	0.1490
<i>gymnodinioids</i>	<i>Gymnodinium gracile</i>		56.80	95,764	(2)	F	8,935.96	0.0933
	<i>Gyrodinium spirale</i>		34.10	20,700	(1)	F	2,378.93	0.1149
	Mean			58,232	(3)			0.1041
misc small dinos	10-25 µm ABD		17.50	2,806	(5)	F	423.19	0.1508
misc med/large dinos	25-100 µm ABD		62.50	128,000	(5)	F	11,481.86	0.0897
Other Phytoplankton								
<i>Dictyocha</i>	<i>Dictyocha fibula</i>		21.40	5,130	(1)	P	658.04	0.1283
<i>Ebria</i>	<i>Ebria tripartita</i>		26.90	10,200	(1)	P	1,254.67	0.1230
<i>Heterosigma</i>	<i>Heterosigma akashiwo</i>		15.40	1,910	(1)	P	260.22	0.1362
<i>Meringosphaera</i>	<i>Meringosphaera mediterranea</i>		7.00	180	(4)	P	28.32	0.1574
<i>Phaeocystis</i>	<i>Phaeocystis</i> sp.		5.50	87	(4)	P	14.31	0.1645
Ciliates and other Zoo								
<i>Mesodinium</i>	<i>Mesodinium rubrum</i>		18.75	3,453	(2)	C	697.13	0.2019
misc ciliates	mostly ciliates 12-75 µm		44.00	44,600	(5)	C	8,643.18	0.1938
misc zoo	misc micrograzers				(6)	NA		0.04
Other - misc								
misc 10-25 µm	misc biol. particles 10-25 µm		17.50	2,806	(5)	P	373.43	0.1331
misc 25-100 µm	misc biol. particles 25-100 µm		62.50	128,000	(5)	P	13,493.48	0.1054
misc >100 µm	misc biol. particles 100-300 µm		200.00	33,500,000	(5)	P	2,514,611.08	0.0751

(1) Harrison et al, 2015; using medians

(2) KCEL FlowCAM data (library); medians, as
ABD

(3) Calculated mean for FlowCAM taxon

(4) Horner, 2002

(5) Size class average, spherical volume (no
data)

(6) Estimate, see Methods (density = 1, DW/WW = 0.1, C/DW = 0.4)

Carbon equations (Menden-Deuer & Lessard, 2000):

Small Diatoms

(SD) <3,000 μm^3 $\text{pgC cell}^{-1} = 0.288 \times \text{CellVol}^{0.811}$

Large Diatoms

(LD) >3,000 μm^3 $\text{pgC cell}^{-1} = 0.117 \times \text{CellVol}^{0.881}$

Dinoflagellates (F)

$\text{pgC cell}^{-1} = 0.444 \times \text{CellVol}^{0.864}$

Other phyto (P)

$\text{pgC cell}^{-1} = 0.216 \times \text{CellVol}^{0.939}$

Ciliates (aloricate) (C)

$\text{pgC cell}^{-1} = 0.230 \times \text{CellVol}^{0.984}$

Table B-4 Particulate organic C and N results for A) blanks prepared once per month and for B) dry combusted and non-combusted filters. Filtered seawater (0.45 µm) was used as the monthly blank and processed in the same manner. * No data (sample sheared in autosampler). ** reported by UC Davis lab as below detection

	Date Prepared	C Amount (µg)	N Amount (µg)	Vol. filtered (mL)	C/vol (µg/L)	N/vol (µg/L)
A) monthly samples						
L62974	6/15/15	0.07	0.60	250	0.29	2.39
L63121	7/21/15	19.27	3.75	250	77.06	15.01
L63401	8/18/15	28.81	26.13	500	57.62	52.25
L63669	9/23/15	19.95	5.02	500	39.90	10.03
L63863	10/19/15	11.30	1.12	1000	11.30	1.12
L64127	11/18/15	12.99	0**	1000	12.99	0.00
L65045	4/18/16	13.56	18.06	200	67.82	90.29
L65302	5/16/16	79.79	22.58	200	398.96	112.88
L65486	6/20/16	31.19	5.58	200	155.93	27.92
L65692	7/19/16	nd*	nd	200	nd	nd
L65917	8/17/16	13.35	1.85	200	66.73	9.26
L66032	9/20/16	10.91	0.81	200	54.56	4.04
	Mean	12.67	2.34		41.33	8.72
	SD	6.11	2.15		29.74	0.30
	N	8	8		8	8
B) Dry filters						
Non-combusted	2/27/18	8.53	29.52			
Non-combusted	2/27/18	9.03	49.74			
Non-combusted	2/27/18	8.70	38.63			
Non-combusted	2/27/18	6.58	40.62			
Non-combusted	2/27/18	9.47	49.53			
Non-combusted	2/27/18	9.31	36.75			
Non-combusted	2/27/18	5.38	43.66			
Non-combusted	2/27/18	4.99	55.52			
Non-combusted	2/27/18	7.66	28.55			
Non-combusted	2/27/18	8.02	56.38			
	Mean	7.77	42.89			
	SD	1.61	9.88			
	N	10	10			
Combusted	2/27/18	2.12	38.50			
Combusted	2/27/18	3.90	36.68			
Combusted	2/27/18	2.49	13.28			
Combusted	2/27/18	3.75	29.24			
Combusted	2/27/18	1.99	26.72			
Combusted	2/27/18	2.27	33.03			
Combusted	2/27/18	2.02	40.58			
Combusted	2/27/18	3.52	16.61			
Combusted	2/27/18	3.42	40.93			
Combusted	2/27/18	2.81	25.17			
	Mean	2.83	30.07			
	SD	0.75	9.73			
	N	10	10			

Table B-5 Particulate organic C and N results for samples and their corresponding lab duplicates collected once per month on a station rotation schedule. Fractions A and B contain particles in the 1.5-100 µm and 100-300 µm range, respectively.

Sample ID	Date Collected	Fraction	Sample					Lab Duplicate					RPD (%) ⁽¹⁾	
			C Amount (µg)	N Amount (µg)	Vol filt'd. (mL)	C/vol (µg/L)	N/vol (µg/L)	C Amount (µg)	N Amount (µg)	Vol filt'd. (mL)	C/vol (µg/L)	N/vol (µg/L)	C	N
L62974-3	6/15/15	A	148.09	30.48	250	592.35	121.94	179.64	34.58	250	718.56	138.33	19.3	12.6
L62974-3	6/15/15	B	77.42	29.80	250	309.68	119.20	86.78	16.27	250	347.13	65.10	11.4	58.7
L63121-5	7/21/15	A	170.68	37.42	250	682.72	149.70	150.60	37.02	250	602.42	148.07	12.5	1.1
L63121-5	7/21/15	B	47.08	43.45	250	188.34	173.82	31.17	5.14	250	124.68	20.57	40.7	157.7
L63401-7	8/18/15	A	92.68	26.08	1000	92.68	26.08	82.46	15.69	1000	82.46	15.69	11.7	49.8
L63401-7	8/18/15	B	46.29	8.42	1000	46.29	8.42	49.10	8.47	1000	49.10	8.47	5.9	0.5
L63669-10	9/23/15	A	415.43	44.04	500	830.86	88.07	342.65	39.34	500	685.31	78.67	19.2	11.3
L63669-10	9/23/15	B	379.19	32.94	500	758.38	65.89	452.21	38.87	500	904.41	77.75	17.6	16.5
L63863-3	10/19/15	A	89.10	12.91	1000	89.10	12.91	82.39	14.08	1000	82.39	14.08	7.8	8.7
L63863-3	10/19/15	B	17.33	1.41	1000	17.33	1.41	12.41	1.22	1000	12.41	1.22	33.1	14.1
L64127-8	11/18/15	A	87.61	10.55	1000	87.61	10.55	85.16	11.28	1000	85.16	11.28	2.8	6.7
L64127-8	11/18/15	B	14.43	0 ⁽²⁾	1000	14.43	0.00	9.09	0 ⁽²⁾	1000	9.09	0.00	45.4	⁽³⁾
L65045-1	4/18/16	A	667.12	140.13	1000	667.12	140.13	814.33	153.98	1000	814.33	153.98	19.9	9.4
L65045-1	4/18/16	B	137.85	52.42	1000	137.85	52.42	118.97	27.36	1000	118.97	27.36	14.7	62.8
L65302-4	5/16/2016	A	70.24	14.99	1000	70.24	14.99	43.22	17.09	1000	43.22	17.09	47.6	13.1
L65302-4	5/16/2016	B	35.86	13.34	1000	35.86	13.34	13.81	10.96	1000	13.81	10.96	88.8	19.6
L65486-4	6/20/2016	A	390.32	73.10	1000	390.32	73.10	584.17	94.73	1000	584.17	94.73	39.8	25.8
L65486-4	6/20/2016	B	219.31	40.93	1000	219.31	40.93	397.68	56.34	1000	397.68	56.34	57.8	31.7
L65692-9	7/19/2016	A	542.71	72.40	1000	542.71	72.40	626.95	83.54	1000	626.95	83.54	14.4	14.3
L65692-9	7/19/2016	B	167.25	15.80	1000	167.25	15.80	131.33	16.92	1000	131.33	16.92	24.1	6.9
L65917-10	8/17/2016	A	486.78	67.95	1000	486.78	67.95	448.35	67.09	1000	448.35	67.09	8.2	1.3
L65917-10	8/17/2016	B	57.67	7.87	1000	57.67	7.87	51.51	8.05	1000	51.51	8.05	11.3	2.2
L66032-9	9/20/2016	A	117.72	21.58	1000	117.72	21.58	103.50	20.16	1000	103.50	20.16	12.9	6.8
L66032-9	9/20/2016	B	16.52	2.93	1000	16.52	2.93	20.02	6.33	1000	20.02	6.33	19.2	73.6

⁽¹⁾ RPD is the Relative Percent Difference and is calculated as the absolute value of:
(concentration in sample - concentration in duplicate)/(mean concentration of sample and duplicate) x 100

⁽²⁾ reported by UC Davis lab as "below detection"

⁽³⁾ cannot be calculated

Mean A:	18.0	13.4
SD A:	13.1	13.2
Mean B:	30.8	40.4
SD B:	24.1	46.5

Table B-6 Particulate organic C and N results for whole samples collected at LSNT01. Summed fractions results are added for comparison. Whole samples contain all particles >1.5 µm. Fractionated samples contain particles in the 1.5-100 µm (A) and 100-300 µm (B) range.

Sample ID	Date Collected	Whole					Fractions (A+B)	
		C amount (µg)	N amount (µg)	Vol. filtered (mL)	C/vol (µg/L)	N/vol (µg/L)	C/vol (µg/L)	N/vol (µg/L)
L62974-7	6/16/15	37.74	13.81	125	301.89	110.51	344.91	72.10
L63060-7	7/7/15	28.82	5.78	125	230.58	46.23	245.12	36.13
L63121-7	7/23/15	48.24	8.60	250	192.98	34.41	489.76	142.59
L63268-7	8/4/15	106.48	21.34	360	295.77	59.28	253.86	46.07
L63401-7	8/18/15	61.49	13.21	1000	61.49	13.21	138.97	34.50
L63522-7	9/9/15	108.01	18.19	1000	108.01	18.19	132.64	36.73
L63669-7	9/22/15	332.89	63.01	500	665.79	126.01	536.42	106.40
L63820-7	10/6/15	93.83	17.15	1000	93.83	17.15	117.21	18.77
L63863-7	10/20/15	68.91	12.39	1000	68.91	12.39	96.24	12.82
L64027-7	11/3/15	53.37	7.97	1000	53.37	7.97	92.37	18.49
L64127-7	11/18/15	50.81	7.81	1000	50.81	7.81	77.54	11.55
L64191-7	12/15/15	66.60	8.71	1000	66.60	8.71	107.24	13.91
L65057-7	3/21/16	124.57	22.11	1000	124.57	22.11	150.63	25.68
L64988-7	4/5/16	153.04	31.38	318	481.26	98.69	583.90	118.16
L65045-7	4/19/16	346.06	72.52	1000	346.06	72.52	334.50	66.86
L65150-7	5/3/2016	572.61	105.73	670	854.64	157.80	950.71	173.95
L65302-7	5/17/2016	483.85	93.80	1000	483.85	93.80	753.54	153.17
L65360-7	6/7/2016	306.24	67.45	1000	306.24	67.45	365.38	102.82
L65486-7	6/21/2016	681.53	147.78	1000	681.53	147.78	602.99	128.50
L65565-7	7/6/2016	244.61	47.27	1000	244.61	47.27	290.63	54.30
L65692-7	7/19/2016	408.72	76.61	1000	408.72	76.61	427.32	78.81
L65834-7	8/2/2016	280.64	59.86	1000	280.64	59.86	359.28	61.78
L65917-7	8/16/2016	201.36	36.72	1000	201.36	36.72	200.07	34.98
L65973-7	9/7/2016	81.98	16.31	1000	81.98	16.31	99.60	16.64
L66032-7	9/20/2016	99.83	17.60	1000	99.83	17.60	109.21	21.50